

POLITECNICO DI TORINO

Collegio di Ingegneria Chimica e dei Materiali

**Corso di Laurea Magistrale
in Ingegneria Chimica e dei Processi Sostenibili**

Tesi di Laurea Magistrale

**Use of amino acids as stabilizers in
lyophilization of biopharmaceuticals**



Relatori

Prof. Dr. Davide Fissore

Candidato

Alessandro Enrico Bregolin

Marzo 2018

Acknowledgements

The Thesis was produced in the Department of Pharmaceuticcal Technology and Biopharmaceutics at the Ludwig-Maximilians Universität of Munich, in the research team supervised by Prof. Dr. Wolfgang Frieß.

I'm thankful to Prof. Dr. Wolfgang Frieß for his welcome in his team and for having provided me this interesting topic of work. His constant and precious suggestions helped me to achieve the aimed objectives throughout the whole Thesis.

I would thank my tutor Ivonne Seifert for her important and relevant support in stimulating me to improve my skills through an intense and collaborative work together.

A huge thanks to all the team members of Prof. Dr. Frieß, Prof. Dr. Winter, and Prof. Dr. Merkel research groups for having created an informal, friendly atmosphere and for having invited me in the enjoyable social activities, especially I would thank both my office colleagues Christian Haase and Martin Domnowski. All of them made this experience unforgettable for me.

I am thankful to Prof. Dr. Davide Fissore for having offered me the opportunity to make this valuable experience and to for his support with his constant presence.

The last but not the least, I would to thank my parents, and friends for being always on my side in every decision I took and for having helped me constantly to achieve my goals.

Table of Contents

| | | |
|----------|--|----|
| 1 | Introduction | 1 |
| 1.1 | Lyophilization process..... | 1 |
| 1.1.1 | Freeze-Dryer equipment..... | 2 |
| 1.2 | Design of rational lyophilized formulation for biopharmaceuticals..... | 3 |
| 1.2.1 | Introduction to protein protection mechanisms during freeze-drying..... | 3 |
| 1.2.2 | Complementary physical characteristics of lyophilized cakes and role of bulking agents and surfactants in formulations | 4 |
| 1.3 | Novel employment of L-Arginine salts as stabilizer in lyophilized formulations and impact of its counterion | 5 |
| 2 | Objective of the Thesis | 6 |
| 3 | Materials and Methods | 7 |
| 3.1 | Materials | 7 |
| 3.2 | Preparation of the solutions for the investigation of protein stability | 7 |
| 3.3 | Freeze-Thawing cycle..... | 9 |
| 3.4 | Freeze-Drying cycle..... | 10 |
| 3.5 | Light obscuration measurement..... | 10 |
| 3.6 | Turbidity | 11 |
| 3.7 | Differential Scanning Calorimetry (DSC)..... | 11 |
| 3.7.1 | Evaluation of the T_g' in the solutions..... | 11 |
| 3.7.2 | Evaluation of the T_g in the freeze-dried cakes..... | 11 |
| 3.8 | Karl-Fisher titration | 12 |
| 3.9 | Reconstitution time..... | 12 |
| 3.10 | Visual inspection..... | 12 |
| 3.11 | X-ray diffraction | 13 |
| 3.12 | Statistical analysis of the results | 13 |
| 3.12.1 | Investigation of protein stability in sucrose-based formulation throughout repeated freeze-thawing cycle | 13 |
| 3.12.2 | Investigation of protein stability in L-arginine-based formulations at different values of pH | 14 |
| 3.12.3 | Statistical model development | 14 |
| 4 | Results | 17 |
| 4.1 | Cryoprotection of L-arginine-based formulations and comparison with sucrose | 17 |
| 4.1.1 | Impact of the number of freeze-thawing cycles on the protein agglomeration in sucrose-based formulations | 17 |
| 4.1.2 | Protein stability of sucrose-based formulations | 23 |
| 4.1.3 | Protein stability at pH 7 in L-arginine-based formulations at different counterions | 25 |

| | | |
|-------|---|----|
| 4.1.4 | Protein stability at pH 6 in L-arginine-based formulations at different counterions | 30 |
| 4.1.5 | Protein stability at pH 5 in L-arginine-based formulations at different counterions | 35 |
| 4.2 | Lyophilization of L-arginine-based formulations and investigation on lyoprotection abilities..... | 39 |
| 4.2.1 | Physical characteristics of lyophilized arginine formulations..... | 40 |
| 4.2.2 | Protein stability at pH 7 in L-arginine-based formulations at different counterions | 47 |
| 4.2.3 | Protein stability at pH 6 in L-arginine-based formulations at different counterions | 51 |
| 4.2.4 | Protein stability at pH 5 in L-arginine-based formulations at different counterions | 55 |
| 5 | Conclusions | 59 |
| 6 | Outlook | 63 |
| | References | 64 |

List of Abbreviations

| | |
|------------------|--|
| A | Arginine |
| C | Citric acid |
| DSC | Differential scanning calorimetry |
| FD | Freeze-drying cycle |
| FT | Freeze-thawing cycles |
| H | Hydrochloride acid |
| HPW | Highly purified water |
| L | Lactobionic Acid |
| LO | Light obscuration |
| LRM | Linear regression model |
| m / mAb | Monoclonal antibody |
| P | Phosphoric acid |
| PS80 | Polysorbate 80 |
| Q ² | Precision of further predictions |
| R ² | Coefficient of determination |
| RM | Residual moisture |
| S | Succinic acid |
| Suc | Sucrose |
| T _c | Collapse temperature |
| T _g | Glass transition temperature of freeze-dried formulations |
| T _g ' | Glass transition temperature of the maximally freeze concentrated solution |
| T _m | Melting temperature |

Sommario

Introduzione

La liofilizzazione viene largamente impiegata nell'industria farmaceutica data la sua capacità di allungare la shelf-life dei prodotti e ridurre i loro costi di trasporto ed immagazzinamento [1].

Il processo di liofilizzazione consiste nel congelamento del prodotto liquido e successivamente nella sublimazione dell'acqua congelata, al di sotto del suo punto triplo ($T=0.01^{\circ}\text{C}$ and $P=4.58\text{ mmHg}$ [2]). La deidratazione consente di inibire la maggior parte delle reazioni chimiche di denaturazione del farmaco [1], mentre una progettazione adeguata della formulazione garantisce il mantenimento dell'attività, evitando possibili reazioni immunologiche sui pazienti [3].

La formulazione consiste nel corretto abbinamento del principio attivo con una serie di eccipienti atti a garantire risultati soddisfacenti durante tutto il processo [1].

Il packaging del prodotto avviene tramite fiale di vetro chiuse con tappi di gomma, al fine di rispettare i requisiti di sterilità e sicurezza del prodotto [4] stabiliti nelle norme GMP.

Il processo di liofilizzazione è composto da tre passaggi: il congelamento, l'essiccamento primario e quello secondario. Durante la fase di congelamento l'abbassamento della temperatura induce la nucleazione e l'accrescimento dei cristalli di solvente, molto spesso acqua, all'interno della miscela [5]. La parte della soluzione non congelata viene quindi ad essere concentrata fino al raggiungimento della propria massima concentrazione [6] alla temperatura di transizione vetrosa (T_g') [7]. La forma e la grandezza dei cristalli è influenzata dal programma di congelamento e dall'uso di tecniche per il controllo della nucleazione [5]; inoltre, la compattezza della struttura ottenuta determina la resistenza al passaggio di materia durante il processo di essiccamento [7].

Prima dell'inizio della fase di essiccamento primario avviene la formazione del vuoto all'interno della camera ed in taluni casi la pressione viene regolata tramite un flusso minimo di gas inerte [8]. La temperatura del piatto sul quale giacciono le fiale viene innalzata per fornire il calore necessario alla sublimazione del solvente [4]. La temperatura all'interno del prodotto deve però rimanere al di sotto della T_g' , al fine di evitare cedimenti durante la formazione nella struttura essiccata [1]. Minimi difetti nel liofilizzato sono accettati a patto che non influenzino la qualità del prodotto [9]. L'essiccamento primario finisce quando tutto il ghiaccio è sublimato.

L'essiccamento secondario è finalizzato alla rimozione dell'acqua adsorbita all'interno della torta di liofilizzato e, quindi, all'abbassamento ulteriore dell'umidità residua nel prodotto. La temperatura del ripiano viene quindi nuovamente innalzata, ma sempre in modo tale per cui la temperatura del prodotto sia mantenuta al di sotto della temperatura di transizione vetrosa (T_g) del solido essiccato [9]. Le condizioni di vuoto vengono mantenute fino al termine del processo e successivamente interrotte, dopo la completa chiusura delle fiale tramite i tappi di gomma.

Il liofilizzatore è composto da una camera di essiccamento collegata tramite un giunto ad un condensatore e ad una pompa a vuoto. All'interno della camera sono presenti diversi ripiani su cui vengono disposte le fiale contenenti la formulazione da liofilizzare. La modifica della temperatura del ripiano e della pressione interna alla camera permette di controllare la temperatura del prodotto [1].

La formulazione farmaceutica liquida contiene solubilizzati al suo interno diversi eccipienti, in aggiunta al principio attivo, al fine di preservare le caratteristiche del prodotto al termine del processo di liofilizzazione [10]. La resa di processo in termini di stabilità ed attività del principio attivo è garantita da agenti stabilizzanti. Gli stabilizzatori si dividono quindi in crioprotettori, i quali contrastano lo stress dovuto al congelamento del solvente, e lioprotettori, che provvedono a proteggere il principio attivo durante la fase di essiccamento [3].

Il congelamento graduale del solvente produce infatti un innalzamento della concentrazione dei soluti all'interno della soluzione e di conseguenza l'aumento della velocità di reazione dei processi degradativi [11], come l'agglomerazione [12]. Il meccanismo di protezione proposto comprende l'esclusione preferenziale dei co-soluti dalla superficie della molecola attiva e la formazione di un guscio di idratazione composto dal solvente [13]. Sono considerati crioprotettori gli zuccheri, polioli, amminoacidi, polimeri, sali organici e inorganici [14]. Inoltre, una concentrazione elevata della molecola attiva (> 50 mg/ml) riduce apparentemente la denaturazione [15], in aggiunta ad una scelta accurata della soluzione tampone e quindi del pH [15,16].

Due diversi meccanismi di protezione sono proposti in letteratura per spiegare l'azione dei lioprotettori. Il primo assume che la stabilizzazione sia data dalla sostituzione del guscio di idratazione con una rete di ponti idrogeno tra gli eccipienti e la molecola attiva [15]. Il secondo approccio assume che la formazione della matrice vetrosa sia direttamente implicata nella stabilizzazione, poiché riduce drasticamente la diffusione e quindi la velocità delle reazioni degradative. [13]. È stato però dimostrato che lo stato vetroso è una condizione necessaria, ma non sufficiente all'ottenimento di molecole stabili ed attive [15].

Largamente impiegati come stabilizzanti contro entrambi i tipi di stress, sia di congelamento che di essiccamento, sono i disaccaridi non riducenti come saccarosio e trealosio, poiché instaurano una matrice vetrosa ad una $T_g' = -32^\circ\text{C}$ [17].

Il liofilizzato deve presentare alcune caratteristiche fisiche imprescindibili al fine di essere considerato accettabile. La struttura della torta deve essere compatta ed uniforme per assicurare la forza meccanica necessaria a preservare il prodotto. La temperatura di conservazione durante l'immagazzinamento deve essere minore della T_g per un mantenimento della struttura vetrosa [13]. Il collasso del liofilizzato, che può verificarsi durante la fase di essiccamento, porta ad un innalzamento dell'umidità residua all'interno della torta [3]. L'umidità residua crea ad un decremento della T_g a causa dell'effetto plasticizzante dell'acqua, usata come solvente. Diventa quindi fondamentale evitare il collasso della torta durante l'intero processo. A tal fine si deve operare l'essiccamento al di sotto della T_g' per evitare una drastica diminuzione di viscosità nella struttura, che non sarà più in grado di resistere agli stress prodotti dal processo [3].

Agenti di bulk come glicina e mannitolo vengono aggiunti alla formulazione per permettere l'instaurazione di strutture rigide, grazie alla loro cristallizzazione durante la fase di congelamento [3]. Il saccarosio ed il trealosio oltre ad essere utilizzati come lioprotettori, svolgono anche la funzione di agenti di bulk [15]. Molti amino acidi possiedono capacità di bulk data la loro capacità di cristallizzare a basse temperature [12].

I tensioattivi, come il polisorbato 80 e polisorbato 20, sono impiegati all'interno delle formulazioni poiché ne inibiscono l'agglomerazione [12].

L'uso degli amminoacidi come eccipienti farmacologici è legato al comportamento che presentano alle basse temperature. Per esempio, la glicina tende a cristallizzare ed è considerata un agente di bulk [18], mentre l'arginina, come gli altri amino acidi basici, genera una struttura principalmente amorfa, seppur è stato osservato un leggero grado di cristallizzazione con la diffrazione di raggi X [19].

All'interno delle formulazioni proteiche liquide l'arginina, e specialmente i suoi sali, aumentano la solubilità del principio attivo; inoltre, essi inibiscono il processo di agglomerazione, pur non impedendo le ragioni di unfolding [12]. Le caratteristiche termiche della soluzione, come T_g e T_g' , dipendono dalla tipologia di acido utilizzato per la titolazione dell'amminoacido [20]. Acidi dicarbossilici causano un aumento della T_g' , rispetto al valore delle singole componenti [21]. Si suppone che questo comportamento sia conseguenza della creazione di una fitta rete di interazioni intermolecolari tra i gruppi funzionali delle diverse molecole [21]. Al contrario, acidi monovalenti inorganici, come l'acido cloridrico, causano un abbassamento della T_g' , mentre l'acido fosforico causa un effetto stabilizzante solamente a certe frazioni con l'arginina [22].

Stärtzel et al. [23] studiarono l'impatto di diversi controioni dell'arginina sulla stabilizzazione degli anticorpi monoclonali durante il processo di liofilizzazione, in formulazioni contenenti anche saccarosio. Si concluse che i cloruri fossero l'alternativa migliore, perché davano una maggiore stabilità del prodotto durante lo stoccaggio. Comunque, la bassa T_g' della formulazione rendeva il processo molto impegnativo e la maggior parte dei prodotti furono affetti da difetti. Per questo motivo gli autori consigliarono di aggiungere basse percentuali dell'amminoacido a formulazioni di saccarosio ed evitare le alte concentrazioni di arginina [24].

Obiettivi

L'obiettivo di questo lavoro è valutare come il controione dell'arginina influenzasse la stabilità proteica in formulazioni farmaceutiche da liofilizzare. Nella prima parte della Tesi si è studiato come il tipo di eccipiente andasse a modificare il processo di aggregazione proteica in atto durante la fase di congelamento della formulazione. I risultati sono stati comparati con formulazioni contenenti saccarosio e polisorbato 80 (PS80) al fine di evidenziare se si avessero benefici significativi per la stabilizzazione del prodotto nell'impiegare le formulazioni a base di arginina. Infine, si è individuato quale acido avesse capacità crioprotettrici migliori e se il pH della formulazione fosse un fattore rilevante per la stabilizzazione. Nella seconda parte della Tesi le medesime formulazioni sono state liofilizzate tramite un ciclo di prova e successivamente analizzate per valutarne le caratteristiche chimico-fisiche. Si voleva, quindi, determinare quali preparati portassero a liofilizzati di ottima fattura, come il processo incentivasse l'aggregazione delle proteine e se i risultati ottenuti fossero confrontabili con i precedenti.

Materiali e metodologie utilizzate

Lo studio si basa sull'analisi di cinque diversi acidi usati come controioni dell'arginina: acido citrico, cloridrico, lactobionico, fosforico e succinico. Le formulazioni analizzate comprendono le soluzioni placebo ed una concentrazione proteica di 3.2 mg/ml. La concentrazione di arginina è stata mantenuta costante al 5% in peso, tranne nel caso dell'acido lactobionico, dove si è registrata una concentrazione del 3.6% in peso. In Tabella 1.1 sono riportate tutte le concentrazioni delle formulazioni a base arginina.

Lo studio dell'impatto dei cicli consecutivi di congelamento-scongelo sull'aggregazione proteica è stato svolto tramite l'impiego di formulazioni a base saccarosio al 7% in peso e con l'aggiunta del tensioattivo PS80. Le formulazioni sono state processate nuovamente, riducendo il volume da 2 ml a 1.5 ml per fiale ed innalzando la concentrazione dell'anticorpo monoclonale a 3.2 mg/ml, per renderle confrontabili con le formulazioni di arginina (Tabella 1.2).

Tabella 1.1 Componenti e concentrazioni delle soluzioni a base arginina. (A) L-arginina; acido (C) citrico; (H) cloridrico; (L) lactobionico; (P) fosforico; (S) succinico ed (m) anticorpo monoclonale.

| Formulazione | pH | L-arginina (% in perso) | Acido (% in peso) | mAb (mg/ml) |
|---------------------|-----------|------------------------------------|------------------------------|------------------------|
| AC5 | 5,1 | 5,0% | 2,6% | 0,00 |
| AC6 | 6,2 | 5,0% | 2,0% | 0,00 |
| AC7 | 7,0 | 5,0% | 1,8% | 0,00 |
| ACm5 | 5,1 | 4,9% | 2,5% | 3,23 |
| ACm6 | 6,1 | 4,9% | 1,9% | 3,27 |
| ACm7 | 7,0 | 4,9% | 1,8% | 3,04 |
| AH5 | 5,2 | 5,0% | 1,0% | 0,00 |
| AH6 | 5,8 | 5,0% | 1,5% | 0,00 |
| AH7 | 7,0 | 5,0% | 1,0% | 0,00 |
| AHm5 | 5,2 | 4,9% | 1,0% | 3,38 |
| AHm6 | 5,7 | 4,9% | 1,4% | 3,12 |
| AHm7 | 7,0 | 4,9% | 1,0% | 3,32 |
| AL5 | 5,1 | 3,5% | 7,2% | 0,00 |
| AL6 | 6,3 | 3,7% | 7,4% | 0,00 |
| AL7 | 7,2 | 3,7% | 7,4% | 0,00 |
| ALm5 | 5,1 | 3,4% | 7,0% | 3,21 |
| ALm6 | 6,2 | 3,6% | 7,2% | 3,28 |
| ALm7 | 7,0 | 3,6% | 7,2% | 3,25 |
| AP5 | 5,3 | 5,0% | 2,6% | 0,00 |
| AP6 | 6,1 | 5,0% | 0,8% | 0,00 |
| AP7 | 7,0 | 5,0% | 1,5% | 0,00 |
| APm5 | 5,3 | 4,9% | 2,5% | 3,22 |
| APm6 | 6,3 | 4,9% | 0,8% | 3,23 |
| APm7 | 7,0 | 4,9% | 1,5% | 3,26 |
| AS5 | 5,0 | 5,0% | 2,1% | 0,00 |
| AS6 | 6,0 | 6,8% | 2,1% | 0,00 |
| AS7 | 6,9 | 5,0% | 1,4% | 0,00 |
| ASm5 | 5,0 | 4,8% | 2,1% | 3,21 |
| ASm6 | 6,0 | 6,6% | 2,0% | 3,19 |
| ASm7 | 6,9 | 4,9% | 1,4% | 3,15 |

Tabella 1.2 Composizioni e concentrazioni delle formulazioni a base saccarosio. (Su) Saccarosio; (PS80) Polisorbato 80; (m) anticorpo monoclonale; (FT) soluzioni utilizzate durante lo studio dell'impatto dei cicli di congelamento e scongelamento.

| Formulazione | Saccarosio (%wt.) | PS80 (%wt.) | mAb (mg/ml) |
|------------------------------------|------------------------------|------------------------|------------------------|
| Su | 7.0% | 0.0% | 0.00 |
| Sum | 6.8% | 0.0% | n.m. |
| SuPS80 | 7.0% | 0.16% | 0.00 |
| SumPS80 | 7.0% | 0.10% | n.m. |
| Su_FT | 6,67% | - | - |
| SuPS80_FT | 6,67% | 0,02% | - |
| Sum_FT | 6,54% | - | 2.91 |
| SumPS80_FT | 6,54% | 0,007% | 2.91 |
| n.m. = Valore non misurato. | | | |

Il programma di cicli di congelamento-scongelamento riportato in Tabella 1.3 è stato impiegato per lo studio delle abilità crioprotettrici delle formulazioni a base di arginina e saccarosio.

Tabella 1.3 Programma ciclico di congelamento-scongelamento impiegato per lo studio della crioprotezione.

| Step | Temperatura (°C) | Pressione (mbar) | Rampa (°C/min) | Tempo di mantenimento (1/min) |
|--|-----------------------------|-----------------------------|---------------------------|--|
| 1 | 20 | ambiente | -- | 20 |
| 2^a | -50 | ambiente | 1 | 180 |
| 3^a | 20 | ambiente | 1 | 180 |
| ^a step ripetuti durante i diversi cicli. | | | | |

La lioprotezione è stata studiata tramite l'impiego di un ciclo di liofilizzazione di prova con lo scopo di evidenziare quali formulazioni a base arginina potessero risultare liofilizzabili e come il processo di aggregazione cambiasse in base al contrione. La fase iniziale di congelamento raggiunge una temperatura minima di -50°C con una rampa di 1°C al minuto; tale temperatura viene mantenuta per un tempo di 90 minuti. L'essiccamento primario avviene ad una pressione di 0.06 mbar con una temperatura di ripiano costante a -20°C, fino al raggiungimento di una differenza di 0.007 mbar tra le misure di pressione ottenute col manometro capacitivo e con quello a termocoducibilità (Pirani). Il successivo essiccamento secondario è effettuato per 450 minuti ad una temperatura costante di 40°C. In Figura 1.1 è riportato il ciclo di liofilizzazione precedentemente descritto.

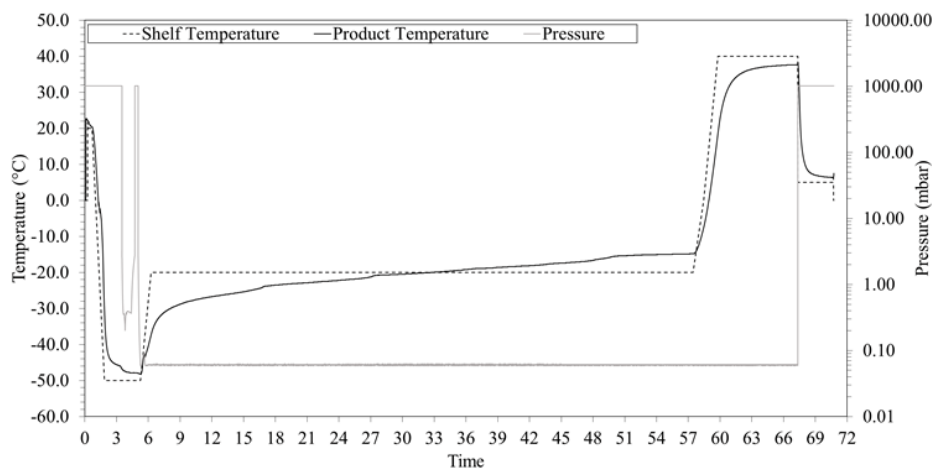


Figura 1.1 Ciclo di liofilizzazione impiegato durante lo studio. La fase di congelamento porta ad una temperatura minima di -50°C . La pressione della camera di liofilizzazione durante la fase di essiccamento è di 0.06 mbar, mentre la temperatura del ripiano è stata impostata a -20°C . L'essiccamento secondario è condotto a 40°C per 450 min.

Lo studio della stabilità proteica prevedeva la misura della torbidità e del numero cumulativo di particelle all'interno delle formulazioni. Inoltre, per i cicli di congelamento e scongelamento sono state condotte delle valutazioni di aspetto macroscopico. Il conto delle particelle per millilitro di soluzione è stato effettuato tramite la tecnica analitica della light obscuration. Oltre al numero di particelle aventi diametro maggiore di $1\ \mu\text{m}$, sono stati valutati i valori per le particelle maggiori di $10\ \mu\text{m}$ e $25\ \mu\text{m}$, poiché le farmacopee (USP <788> and Ph. Eur. 2.9.19) ne delimitano il valore limite a 6000 e 600 unità per fiala (29, 30). Entrambe le tecniche di analisi dovrebbero condurre a risultati analoghi, perché la misura della torbidità si basa sullo scattering della luce causato dalle particelle presenti nel campione [27].

I campioni liofilizzati sono stati sottoposti ad un'analisi fisica delle loro proprietà. Inizialmente, si è provveduto a una valutazione degli aspetti macroscopici con il fine di individuare eventuali criticità, difetti ed collasso del prodotto. In seguito, è stata misurata la quantità di umidità residua tramite la titolazione di Karl-Fisher e la temperatura di transizione vetrosa T_g mediante la tecnica di analisi della DSC modulata. I campioni sottoposti allo studio della stabilità proteica sono stati precedentemente ricostituiti tramite acqua ultra pura (HPW) e si è misurato il tempo necessario alla ricostituzione. La DSC è stata anche impiegata per l'identificazione della T_g delle diverse formulazioni.

L'effetto di anticorpo, processo tecnologico e controione è stato investigato a differenti valori di pH. I dati ottenuti dall'analisi di stabilità proteica sono quindi stati analizzati tramite il software statistico MODDE Pro (12.0 – Trial version) con un intervallo di confidenza al 95% (equivalente a $\alpha = 0.05$) ed il test statistico di Fisher sulla media aritmetica al fine di valutare l'impatto di ogni fattore sui risultati. Il software ha valutato i dati sulla base del modello statistico a regressione lineare multipla (MLR) per poi valutarne successivamente gli effetti e le interazioni legate ad ogni fattore. Sono stati sviluppati dei modelli statistici per ogni tecnica analitica, ma solo il risultato più adeguato, secondo quattro parametri di valutazione, è stato riportato all'interno dei risultati. Si sono tenuti in considerazione il fitting dei dati (R^2), la precisione di previsione future (Q^2), la presenza di lack-of-fit e la riproducibilità.

Crioprotezione delle formulazioni a base di L-arginina e confronto con il saccarosio

Lo scopo di questa sezione è quello di mettere in risalto lo stress da congelamento che viene a verificarsi durante la prima fase della liofilizzazione al fine di evidenziare il comportamento di ogni formulazione studiata. Il saccarosio è un'importante crioprotettore ed è ampiamente usato per la stabilizzazione proteica, anche in combinazione con dei tensioattivi [17]. L'obiettivo della prima parte del lavoro è individuare se all'aumentare del numero di cicli ripetitivi di congelamento-scongelo si abbia un evidente aumento della torbidità e del numero di particelle all'interno delle formulazioni a base saccarosio. I risultati sono stati successivamente confrontati con quelli ottenuti in cinque diverse formulazioni a base arginina. Nello studio sono stati considerati diversi controioni dell'amminoacido, al fine di dimostrare se l'impatto del pH e del specifico eccipiente portasse ad una efficace stabilizzazione proteica. L'obiettivo finale era quello di provare quale formulazione apportasse la migliore crioprotezione e se gli eccipienti utilizzati al suo interno possano essere una valida alternativa al saccarosio.

Il numero totale delle particelle con dimensioni maggiori di 1 μm all'interno delle formulazioni a base saccarosio varia in maniera significativa solamente con l'aggiunta della proteina (mAb), mentre rimane pressochè costante nei placebo, all'aumentare del numero di cicli di congelamento-scongelo (FT). L'aggiunta di PS80 alla formulazione proteica consente di mantenere all'incirca costanti le dimensioni delle particelle misurate. Risultati analoghi sono stati rilevati tramite le misure di torbidità e light obscuration per particelle con dimensioni maggiori di 10 μm . Al contrario, l'aumento delle dimensioni delle particelle a 25 μm non permette di definire alcun andamento preciso. Dall'analisi statistica sia la torbidità che la light obscuration a 10 μm sono interpretabili con modelli statistici sufficientemente precisi ed in assenza di lack-of-fit. Dall'analisi è possibile concludere che sia mAb che FT sono le principali cause dell'aumento del numero di particelle, mentre il PS80 ne produce una diminuzione in combinazione con mAb e FT. Queste conclusioni sono analoghe a quanto osservato nelle misurazioni sperimentali.

L'ispezione macroscopica delle formulazioni a pH 7 ha rilevato un aumento significativo delle particelle visibili, a causa di FT, all'interno delle formulazioni proteiche di citrato (C) e fosfato (P). La torbidità e la light obscuration confermano una distinzione netta tra placebo e formulazioni proteiche, come nelle preparazioni a base saccarosio. I placebo mostrano misure simili tra loro e costanti, mentre i valori delle formulazioni proteiche presentano alcune differenze in base al tipo di acido utilizzato. L'acido lactobionico (L) e C forniscono il numero maggiore di particelle totali nella light obscuration a 1 μm prima di FT, mentre le restanti formulazioni mostrano risultati simili tra loro. FT causa l'aumento significativo del numero di particelle totali solo di alcuni campioni, analogamente a quanto osservato durante l'ispezione macroscopica. Il maggior numero di particelle si è misurato in P, seguito in ordine da L e C. Al contrario, il cloruro (H) ed il succinato (S) rimangono pressochè costanti e presentano i valori minori rispetto agli ioni precedenti. La light obscuration a diametri di particelle maggiori mostra risultati simili, sebbene meno distinguibili. H ed S assicurano meno particelle rispetto alle formulazioni contenenti solo saccarosio. È possibile una descrizione quantitativa dei risultati tramite l'analisi statistica. Il migliore modello statistico in termini di R^2 , Q^2 , riproducibilità ed in assenza di lack-of-fit è stato sviluppato usando le misure della light obscuration a 1 μm . Dall'analisi si conclude che la causa maggiore di particelle è mAb, anche se FT provoca un aumento delle misure, verosimilmente a quanto osservato per le formulazioni in base saccarosio. Entrambi S ed H mostrarono una diminuzione rilevante del numero di particelle totali rispetto a C, al contrario, P ed L ne provocano un aumento altrettanto significativo. In conclusione, si afferma che il migliore controione dell'arginina a pH 7 è H, poiché causa, in maniera significativa, il minor numero di particelle.

Le medesime formulazioni sono studiate a pH 6, al fine di comprendere se l'acidità modifichi la stabilizzazione proteica. L'ispezione visiva non evidenzia alcuna distinzione nell'aspetto dei placebo, mentre le formulazioni proteiche contenenti P o C aumentano, in maniera rilevante, il numero di particelle visibili al loro interno. I valori di torbidità e light obscuration mostrano una

netta distinzione tra placebo e formulazioni proteiche, come nello studio a pH 7. Le misure dei placebo rimangono pressoché costanti e significativamente minori rispetto alle formulazioni proteiche. La light obscuration a 1 μm non permette di distinguere tra di loro le formulazioni prima di FT, ma vengono osservate alcune differenze in seguito. FT causa un aumento del numero di particelle in tutti i campioni proteici, in particolare all'interno di P ed in maniera minore nelle formulazioni contenenti C o H. Al contrario, L e S non mostrano alcun aumento significativo, a seguito di FT e forniscono il minore numero di particelle. In generale, a pH 6, si ottengono misure di torbidità e light obscuration maggiori, rispetto al pH 7. Si è svolta un'analisi statistica dei risultati atta a quantificare ogni fattore. Il migliore modello statistico per precisione, riproducibilità ed assenza di lack-of-fit è stato sviluppato usando la light obscuration ad 1 μm . Analogamente al precedente pH, mAb è la causa principale di particelle all'interno dei campioni; sebbene il processo FT ne aumenti le misure, ma in maniera minore rispetto alla proteina. Entrambi gli ioni P ed H procurano un aumento significativo delle particelle in confronto a C, mentre L e S ne causano una riduzione altrettanto rilevante. In conclusione, il più promettente controione a pH 6 è L, il quale procura il numero minore di particelle rispetto agli altri ioni ed al saccarosio, sebbene mostri risultati simili a quelli ottenuti da H a pH 7.

Lo studio delle formulazioni a base arginina è ripetuto a pH 5, al fine di confermare l'aumento della torbidità e del numero di particelle al diminuire del pH. L'ispezione visiva dei campioni rileva un aumento significativo delle particelle visibili, a seguito di FT, nelle formulazioni proteiche contenenti C, L o P. Rispetto agli studi precedenti, si osserva un aumento delle misure causato dalla diminuzione del pH. Entrambe le tecniche di misura rilevano una sostanziale differenza tra formulazioni proteiche ed i placebo, come nei precedenti studi. I placebo causano misure significativamente minori rispetto alle proteine, mentre FT aumenta i valori delle sole formulazioni proteiche. La light obscuration ad 1 μm mostra che il numero maggiore di particelle è fornito da P, seguito nell'ordine da C, H, L ed S. Risultati analoghi sono ottenuti ai diametri maggiori, sebbene le differenze tra gli ioni siano meno evidenti. L'analisi statistica non è stata completata, sebbene abbia l'obiettivo di confermare i risultati, poiché tutti i modelli statistici presentano lack-of-fit.

I valori minori di torbidità e numero di particelle all'interno dei placebo, rispetto alle formulazioni proteiche, indicano, con rilevanza statistica, che la causa principale dell'aumento delle misure è la presenza dell'anticorpo. Si può affermare correttamente che l'aumento delle misurazioni sia causato dall'aggregazione proteica. La crioprotezione delle formulazioni a base di arginina dipende sia dal pH, che dal tipo di contro-ione utilizzato. Infine, le analisi statistiche indicano come migliori contro-ioni per l'arginina H a pH 7 e L a pH 6.

Liofilizzazione e lioprotezione di formulazioni a base di L-arginina

I liofilizzati devono soddisfare alcune caratteristiche fisiche per essere considerati accettabili. È necessario che la torta si presenti visibilmente uniforme ed in assenza di danni ingenti alla propria struttura, poiché sono richiesti livelli minimi di umidità relativa ed una T_g elevata. Le formulazioni sottoposte a liofilizzazione vengono sollecitate sia durante la fase di congelamento, che durante quella di essiccamento. Gli eccipienti stabilizzanti devono prevenire la denaturazione del principio attivo durante entrambe le fasi del processo, inoltre forniscono le caratteristiche fisiche desiderate. In questa sezione si è provveduto a liofilizzare le formulazioni a base di arginina al fine di valutarne le proprietà e la stabilizzazione proteica nei prodotti ricostituiti.

L'ispezione visiva dei liofilizzati mostra il collasso totale delle formulazioni contenenti H e parziale per S. La variazione di pH non influenza l'aspetto visivo dei prodotti, tranne nel caso di P, dove si verifica un inizio di collasso a pH 5. Al contrario, le formulazioni contenenti C, oppure L presentano torte uniformi e dall'aspetto elegante. Il collasso del liofilizzato causa un aumento dell'umidità residua (RM), per cui si registrarono valori di circa 1% per il C ed il 3% per H. L'effetto plasticizzante dell'acqua porta ad un drastico calo della T_g . Quest'ultima oscilla tra i 40°C ed i 65°C per le torte collassate, come H e S; mentre nei prodotti uniformi si attesta tra i 90°C ed i 105°C. I termogrammi ottenuti dalla DSC modulata mostrano un picco di cristallizzazione a temperature maggiori di quella ambiente, per tutti i liofilizzati collassati. Al contrario, la diffrazione di raggi X (XRD) conferma la natura amorfa dei campioni nei liofilizzati proteici a pH 7. I risultati ottenuti sono simili a quelli riportati da Mattern et al. [19] e da Stärtzel et al. [23]. I tempi di ricostituzione dei liofilizzati non superarono i due minuti e mezzo e vengono considerati accettabili. Il collasso del prodotto è dovuto al superamento della T_g' , durante la fase di essiccamento primario del ciclo di liofilizzazione. Le formulazioni collassate, mostrarono i valori di T_g' compresi tra -46°C e -37,5°C; mentre C ed L hanno T_g' decisamente maggiori e comprese tra i -28°C per C ed i -22°C per L. La variazione del pH non influenza il valore di T_g' , tranne nel caso di P. Infatti, P mostra un aumento della T_g' all'aumentare del pH. I risultati ottenuti sono in accordo con le conclusioni espresse da Izutsu et al., i quali dimostrarono che la T_g' fosse proporzionale al numero di gruppi carbossilici all'interno dell'acido usato come controione dell'arginina [21]. In conclusione, le formulazioni considerate accettabili per le loro caratteristiche fisiche devono contenere come controione dell'arginina C, L, o P.

La stabilizzazione proteica delle formulazioni ricostituite differisce dai risultati precedenti sulla crioprotezione. A pH 7 il controione con la maggiore torbidità e numero di particelle è L, mentre P ed S mostrano valori decisamente minori e simili tra di loro, sebbene le misure minori siano causate da C ed H. La light obscuration a 10 μm ed a 25 μm mostra risultati meno distinguibili e pertanto non conferma le differenze tra i diversi ioni. Al fine di quantificare ogni fattore, si è sviluppata un'analisi statistica dei risultati. Nello studio è stato preso in considerazione il modello statistico della light obscuration ad 1 μm per di mantenere la coerenza con le passate analisi e data la sua buona capacità predittiva ed assenza di lack-of-fit. La presenza dell'anticorpo si conferma essere la prima causa di aumento delle misurazioni, analogamente ai passati esperimenti. Un'altra causa decisiva di aumento delle particelle è il processo di liofilizzazione; mentre gli unici ioni che differiscono significativamente da C sono L e P. L provoca un'aumento delle misure, mentre P ne causa una diminuzione, al contrario di quanto osservato per la crioprotezione. In conclusione, la migliore lioprotezione a pH 7 è data dal P.

La diminuzione del pH provoca un aumento della torbidità e del numero di particelle nelle formulazioni ricostituite. Durante la light obscuration ad 1 μm si registra un aumento del numero di particelle per H, rispetto al pH precedente, mentre C, P ed S mostrano valori preccoshé invariati. Al contrario, L diminuisce, sebbene rimane lo ione con il maggior numero di particelle al suo interno. La torbidità e la light obscuration a diametri maggiori confermano solo parzialmente i risultati, poiché le misure risultano meno distinguibili tra loro. L'analisi statistica permette di quantificare ogni fattore. Si è analizzato il modello statistico per la light obscuration ad 1 μm , poiché

risulta il più preciso, riproducibile ed in assenza di lack-of-fit. L'anticorpo è la causa principale di particelle, analogamente a quanto osservato negli studi precedenti, sebbene il processo di liofilizzazione generi un aumento significativo delle misure. Gli ioni P e L aumentano le misure in maniera significativa rispetto a C, mentre non si mostra alcuna differenza rilevante rispetto a H e S. In conclusione, la migliore stabilizzazione proteica a pH 6 avviene usando C, H o S come contrione.

La minore stabilizzazione dell'anticorpo causata dalla diminuzione del pH è stata confermata con l'analisi a pH 5. Sia la torbidità che la light obscuration delle formulazioni ricostituite mostrano un aumento al diminuire del pH. La light obscuration ad 1 μm procura risultati facilmente distinguibili tra loro. Il numero maggiore di particelle è causato da L, mentre H mostra il valore minore. La torbidità conferma i risultati, sebbene le misure siano meno distinguibili. Non è stato possibile concludere l'analisi statistica poiché tutti i modelli mostrarono presenza di lack-of-fit al loro interno.

Conclusioni

La distinzione netta tra soluzioni placebo e formulazioni proteiche permette di concludere che l'aumento della torbidità e light obscuration è legata alla presenza dell'anticorpo all'interno delle formulazioni. H ed L svolgono un'efficiente crioprotezione del principio attivo a pH 7 e 6, ma H produce liofilizzati collassati, a causa della sua bassa T_g , mentre L produce una scarsa lioprotezione delle formulazioni. Al contrario, C e P non mostrano alcuna azione crioprotettrice rilevante, ma producono liofilizzati dall'aspetto uniforme, con bassi livelli di umidità residua ed alte T_g . Inoltre, la stabilizzazione proteica sulle formulazioni ricostituite indica che la migliore lioprotezione si ottiene usando P a pH 7.

La prosecuzione del lavoro potrebbe focalizzarsi sull'impiego di un eccipiente di bulk aggiuntivo atto ad evitare il collasso delle formulazioni a base di H durante la fase di essiccamento primario, al fine di sfruttare interamente le abilità crioprotettrici dello ione, secondo l'esempio di Stärtzel et al. [23,24]. In alternativa, si potrebbe cercare di formulare una soluzione di L con al suo interno una concentrazione di arginina al 5% in peso, invece del 3,6%, al fine di studiare se l'aumento di concentrazione dell'aminoacido possa indurre un aumento del potere lioprotettivo della formulazione.

1 Introduction

1.1 Lyophilization process

Lyophilization is a crucial manufacturing process in drugs pharmaceutical industry since it guarantees long shelf life of sensitive pharmaceuticals and a reduction in long-term storage cost and shipping costs [1].

Freeze-drying consists of the water sublimation inside the product, which is previously frozen until either its glassy or crystalline state is reached, depending on the ingredients inside the formulation. Ice sublimation is feasible only at working conditions below the water triple point ($T=0.01^{\circ}\text{C}$ and $P=4.58\text{ mmHg}$ [2]). As a consequence of the dehydration, most of the degradative chemical reactions and physical transformations are inhibited [1]. A well-designed lyophilized formulation of biopharmaceuticals maintains biological activity, whereas immunological reactions to patient are avoided. Moreover, the weight loss permits to deliver the product easily and the dehydration allows to get long-term storage even at ambient temperature [3].

Formulations of pharmaceuticals that have to be freeze-dried are composed by various excipients to guarantee satisfactory behavior throughout the process [1], beside, obviously, the active pharmaceutical ingredient. Containers must ensure fundamental requirements of sterility, stability, and safety of the product to the patients [4]. Commonly used containers are glass vials, with rubber stoppers [4].

The lyophilization process is divided into three stages: freezing, primary drying and secondary drying (Figure 1.1).

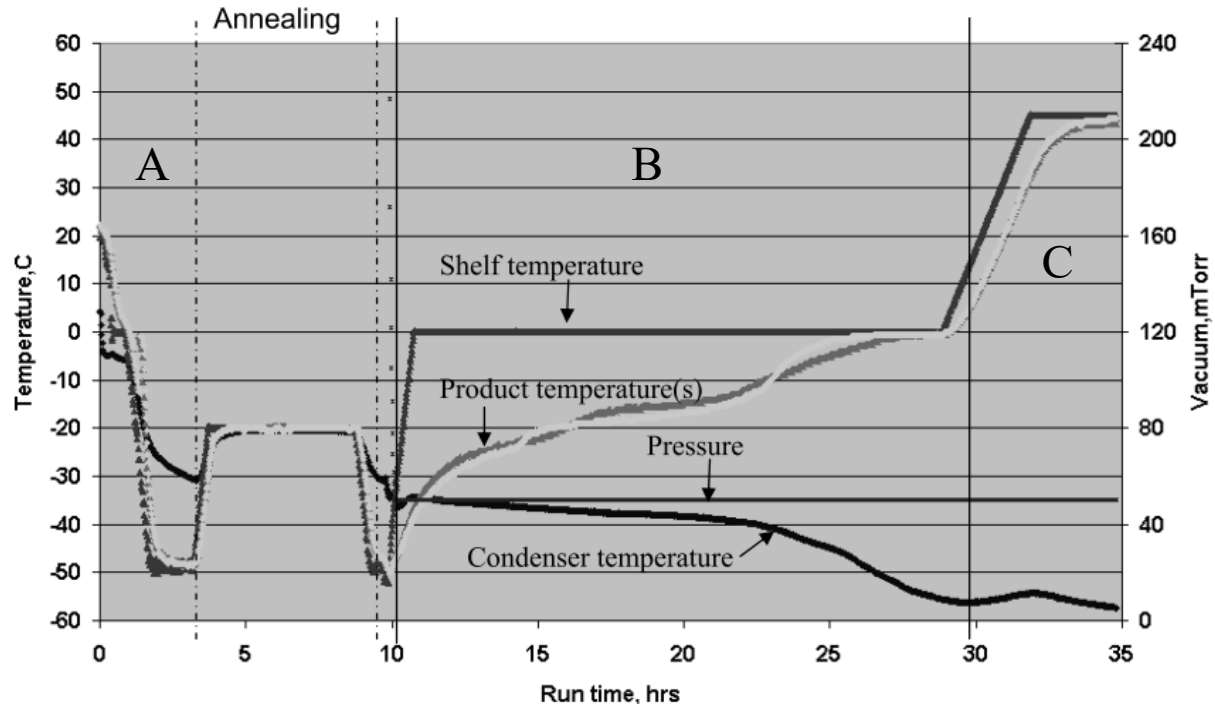


Figure 1.1 Example of freeze-drying cycle diagram. It shows the chamber pressure and the temperature of shelf, products, and condenser. Freeze concentration (A) with annealing step, primary drying (B) and secondary drying (C) are highlighted in the diagram. Picture was taken from [4] with modifications.

The freezing step is necessary to freeze the solvent, generally water, inside the solutions in order to obtain the maximally freeze-concentration in the remaining liquid phase [6]. The temperature of the

shelves is decreased with a ramp. Below the melting temperature of the formulation (T_m), liquid and solid phases coexist as nucleation and growth of small crystalline clusters of free solvent occur inside the product [5]. Sharpe and size of the crystals are influenced by the cooling rate and the possible use of methods to induce and control the nucleation [5]. The resistance to mass transfer during the drying steps is dependent on the porosity of the obtained cake [7]. Consequently, a strewed grid of large crystals facilitates the transport of water vapor from the interface of sublimation to the drying chamber [7]. Nevertheless, the remaining structure will be extremely fragile, and breaks can occur due to the mechanical stress during the process. The temperature during the freezing stage decreases at least until the glass transition temperature (T_g') is reached inside the product. With a change in heat capacity the glassy state is formed below the T_g' and the viscosity rises [28]. A small fraction of water does not crystallize and remains bounded to the solutes molecules [29]. It is called unfrozen water.

Primary drying starts afterwards, by creating vacuum inside the drying chamber. A small flux of inert gas is supplied, in certain cases, to the freeze-dryer in order to control the pressure inside [8]. The shelves are warmed up to allow the sublimation of the ice crystals [4]. The drying process starts to the top of the product in the vial and it proceeds until the bottom [1]. The temperature of the forming cake has to remain below the T_g' otherwise the structure will lose its mechanical strength and it will consequently collapse [1]. The cake collapse inhibits mass transfer and more residual moisture remains at the end of the process. The appearance of collapsed cakes is characterized by the presence of cracks and even “meltback”. Anyway, small damages are usually accepted, as long as the product quality is not affected [9]. The primary drying ends when all the frozen water has been removed from the product. When this occurs, the partial pressure of the vapor inside the chamber decreases and, finally, it reaches the target value.

Secondary drying aims to remove the remaining solvent, thus obtaining the target residual moisture level [1]. The shelf temperature is raised up to increase the kinetics of the endothermic process of water desorption, whereas it must be below the glass transition temperature (T_g), otherwise the cake will lose its glassy state [9]. The chamber is held in vacuum conditions throughout the whole drying process, and its release occurs afterward the vials are completely closed by the stoppers.

1.1.1 Freeze-Dryer equipment

The freeze-dryer is composed by a drying chamber connected with a duct to a vapor condenser (Figure 1.2). Several shelves are placed inside the chamber to load the products. The shelves also provide the heat required to the product by means of technological fluids. The vacuum is generated by a pump, downstream to the condenser. The vapor passes through the chamber and it sublimates on the condenser surface.

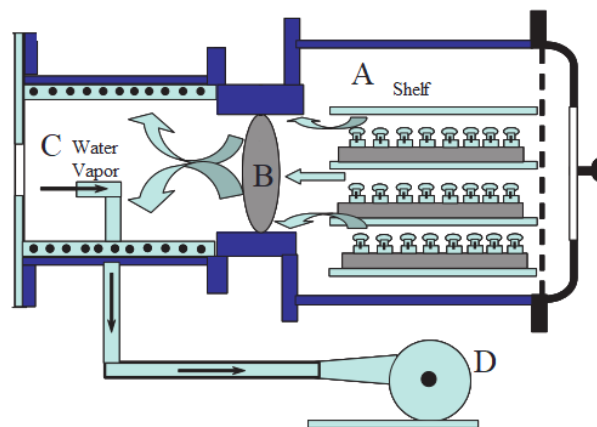


Figure 1.2 Scheme of a lyophilizer during the drying step. It is possible to distinguish the drying chamber (A) connected by a duct (B) to the condenser (C). The vacuum is obtained through a vacuum pump (D). The picture was taken from [4] with modifications.

The process temperature is controlled by modifying the flow and the temperature of technological fluid passing through the shelves [1]. Nevertheless, the pressure of the chamber impacts on the product temperature at same shelves conditions [11]. A decrease in the pressure causes a decrease in the temperature inside the product [11]. The pressure can be modified either acting on the vacuum pump or adjusting the flux of inert gas (N₂) when it is introduced in the drying chamber [8].

1.2 *Design of rational lyophilized formulation for biopharmaceuticals*

A rational design of biopharmaceuticals is governed by essential constraints. Using a mixture of excipients means to add inert substances to the pharmaceutical ingredient in order to ensure biological activity, uniformity, dose of active pharmaceutical ingredients (APIs) throughout the technological process [10] and in the final product. Coping with freezing and drying stresses in lyophilization is necessary to gain real benefits from the process. Labile proteins are protected from freezing damages by excipients called cryoprotectants, whereas lyoprotectants provide stabilizing effect during the dehydration

1.2.1 Introduction to protein protection mechanisms during freeze-drying

During the freezing step water is almost completely removed from the liquid phase and, therefore a rapid increase in solute concentration occurs and reactions rates are suddenly accelerated in the aqueous solution, whereas temperature decreases [11]. The proposed stabilization mechanism during freeze-concentration is comparable to the stabilization in aqueous solutions. On the contrary, the drying protection mechanism is completely different. Cryoprotectants encompass a wide variety of diverse molecules such as sugars, polyols, amino acids, polymers, inorganic and organic salts [14]. The common characteristic shared by all aforementioned compounds is the preferential exclusion of those co-solutes from the surface of native proteins, which are surrounded by a hydration shell of water [13]. The altered structure of proteins causes aggregation and, therefore co-solutes also inhibit self-association [12]. A relatively high protein concentration (> 50 mg/ml) apparently reduces freeze-denaturation and, therefore, it is frequently suggested to begin the design of the formulation with a high concentration of protein, aiming to increase the “intrinsic” resistance [15]. An optimal stabilization requires the selection of the right pH and buffer system to minimize pH shifts throughout the freeze-concentration. Crystallization and phase precipitation of buffer occurs with certain salts, and it promotes drastic undesired pH changes. For example, the dibasic form of sodium phosphate crystallizes and shifts the pH up to 4 units [15,16]. Either inorganic or organic salts are employed as buffer, typically in a range of pH from 4 to 8.

Protection mechanism from dehydration is different and more specific than the freeze-stabilization, since many cryoprotectants do not show any effect after drying process [13]. Two mechanisms are usually proposed to describe the stabilization throughout the dehydration process. Several investigations pointed out the substitution of the water hydration shell with sugars through hydrogen bonds with the polar sites of proteins in order to maintain the native configuration and to avoid aggregation [13]. The protection is directly correlated with the weight ratio of excipients to protein, although an excessive bulk concentration of co-solutes causes their crystallization and, consequentially, a reduction in hydrogen bonds availability, with a loss in protein stabilization [15]. The second approach assumes that protein protection by lyoprotectants is directly related to the glassy state formation, since the reduction of chemical degradation reactions rates is due to the sudden decrease of molecular diffusion in the amorphous phase. An increase in protein stabilization is expected due to higher T_g and molecular weight of excipients. However, a negative correlation between excipients molecular weight and protein stability [13] was demonstrated. It can be concluded that glassy state is not a sufficient condition to provide active proteins during drying, whereas it is necessary to permit hydrogen bonding.

The preservation of labile products during lyophilization requires both cryoprotection and drying protection. Stabilizing agents encompass saccharides and amino acids, as they minimize aggregates

formation and inhibit unfolding reactions. Disaccharides, especially the non-reducing sugars sucrose and trehalose, are popular lyoprotectants since they provide a glassy matrix below the glass transition temperature of the maximally freeze-concentrated solution (T_g') of around -32°C [17]. The hydrolysis of both sugars occurs unless the pH shifts below 4 during the freezing step. Reducing species must be avoided otherwise proteins are damaged by Millard reactions [4] in the solid state during long-term storage, with a change in color of the cake [9]. Reducing saccharides, such as maltose and lactose, should thus be avoided.

1.2.2 Complementary physical characteristics of lyophilized cakes and role of bulking agents and surfactants in formulations

An elegant cake appearance is essential to preserve mechanical strength in the amorphous phase. Low percentage of residual moisture in cakes is required to keep long-term protein stability due to plasticizing properties of water in dried structures. Preservation of freeze-dried pharmaceuticals during shipping and storage needs high glass transition temperature (T_g). The looseness in structure strength increases molecular mobility and, consequentially, the degradation processes, which are caused by temperatures higher than T_g [13]. Collapsed cakes are affected by excessively high residual moisture and T_g moves therefore towards lower values [3]. Correct tonicity and pH must be preserved throughout the reconstitution stage. The reconstitution process depends on the cake morphology, and the required time to obtain a completely liquid solution decreases when increasing the porosity of the solid. High protein concentrations provide more dense cakes and, thus, the reconstitution time increases due to more compact structures [4].

The aforementioned characteristics are obtained whether product temperature during the primary drying process is kept below T_g' . If crystalline excipients are added to the formulation, it will be necessary to maintain the temperature also below their eutectic melting temperature (T_e) in order to avoid melting-back events [3]. The cake collapse occurs as the solid is softened above the T_g' , with a sudden loss in viscosity, and it becomes unable to preserve the structure during water sublimation [3]. An accurate investigation is therefore required to determinate the T_g' of the formulation. Differential scanning calorimetry (DSC) is the most common analytical technique used for that purpose [4]. The T_g' is a function of the composition and small molecules provide a lower value than high molecular weight molecules.

Bulking excipients such as glycine and mannitol provide stable structures by means of crystallization during freeze-concentration, and they are tonicity modifiers [3]. An ideal formulation has to provide a ratio of stabilizer to bulking agents of approximately 1:2 to 1:4 to maintain an optimal protein stability, especially in protein formulation with a concentration lower than 50 mg/ml [15]. Sucrose and trehalose are also used as bulking agents. Trehalose has a higher T_g than sucrose, although this advantage might be minimized with high protein concentration, which increases the T_g [15]. On the contrary, sucrose shows a more effective lyoprotection due to the higher tendency of trehalose to crystallize and to show phase separation [15]. Amino acids are also used as bulking agents due to their capacity to crystallize [12]. The reconstitution time and protein aggregation are reduced by adding a small amount of nonionic surfactant (0.0003 – 0.3 %wt.) such as polysorbate 80 and 20. Surfactants also protect proteins from heating and stirring stresses, which occur during preparation, and prevent non-specific adsorption on the container surface [14]. Protein aggregation is suppressed because the tendency of the surfactant to bind at the hydrophobic sites of protein. Moreover, cryogenic protection is caused by its presence at the interfaces, although its impact is not as effective as that of disaccharides [12]. The addition of a surfactant might generate auto-oxidation reactions and increase the kinetics of denaturation processes [12].

1.3 Novel employment of L-Arginine salts as stabilizer in lyophilized formulations and impact of its counterion

The development of formulations based on amino acids instead of sugars as stabilizers and bulking agents requires much more effort due to their different physical behaviors in frozen state. Certain amino acids, for instance glycine and its salts, are used as bulking agents because they crystallize during the process [18]. On the contrary, amorphous phase in freeze-dried cakes is provided only by basic amino acids (Lys, Arg, His and Cit), although a weak crystallization was observed in x-rays diffraction patterns [19].

Among other amino acids, L-arginine has a rather significant importance as cryoprotectant, since it inhibits protein aggregation in liquid phase, even though it does not suppress protein unfolding reactions [12]. Moreover, it has been proven that arginine, and especially its salts, rises the solubility of proteins and reduces the viscosity in high concentrated antibody solutions [12]. Thermal proprieties like T_g and T_g' of lyophilized formulation are rather depended on the employed L-arginine counterion and the mixing state in the solution [20]. Aqueous solutions of arginine base show a $T_g' = -41.4^\circ\text{C}$ in an amorphous structure [22]. Di- and tricarboxylic acids, such as citric and L-tartaric acids in combination with L-arginine provide a bell-shaped profile of T_g' at different pHs, with values higher than those derived from pure arginine base. It is supposed that the rise of glass transitions temperatures (T_g , T_g') is caused by the formation of a wide interaction network of multifunctional molecules [21]. On the contrary, monovalent acids (HCl and formic acid) do not increase the T_g' , but they can decrease it slightly [22]. Either destabilizing or stabilizing effect of protein with phosphoric acid is achieved in different ratios with arginine. It is therefore important to optimize the process, and even more, their concentrations [22]. Stärtzel et al. [23] investigated the antibody stabilization with different counterions of L-arginine and concluded that the best long-term stability is achieved when employing arginine chloride in formulations with sucrose. However, the rather low T_g' provided major defects in the cakes throughout the lyophilization process. Therefore, a further investigation was focused on process and formulation concentrations. Anyway, it was not possible to avoid major defects at high concentrations of arginine salts. Thus, the author suggests to use the amino acid salts in low concentration in sucrose-based formulations [24].

2 Objective of the Thesis

The work is aimed to investigate the impact of the type of counterion in L-arginine-based biopharmaceutical formulations throughout the processes of freeze-thawing and lyophilization. Disaccharides are well described in the literature and commonly employed as protein stabilizers in freeze-drying, especially sucrose [3]. Anyway, amino acids are deeply investigated as excipients and classified basically on their behavior in solution as bulking agents, buffers, or stabilizers [30]. It has been proved that L-arginine, as the other basic amino acids, provides stable amorphous states in both freeze-dried and vacuum-dried products. Moreover, it is also used to stabilize liquid protein solutions due to its characteristic of reducing agglomeration [12]. Thermal proprieties (T_g , T_g') are widely dependent on the composition; however, only few investigations are focused on L-arginine-based protein products [21]. Antibody stability, and physical features of lyophilized cakes, has been investigated using different arginine salts with sucrose [23]. It would be therefore remarkable to focus on protection abilities of arginine salts in the freezing stage in order to claim a feasible alternative to sucrose as stabilizer in lyophilization. Furthermore, it is essential to obtain freeze-dried products that respect key features such as low residual moisture, relatively high T_g , acceptable reconstitution time and elegant appearance.

The comparison among five counterions (citric acid, hydrochloric acid, phosphate acid, succinate acid and lactobionic acid) was carried out to highlight differences and advantages. Due to the impact of pH in protein stability, the investigation included a range from 5 to 7. Antibody stability was investigated in terms of subvisible particles number by light obscuration and turbidity. A comparison between placebo and protein solutions allow distinguishing the number of protein agglomerations. The impact of the freeze-thawing process on particle formation was analyzed after 5 cycles. The repetitions aimed to overstress the formulation in order to obtain distinguishable differences between the counterions. All formulations were processed through a tested cycle of lyophilization to acquire information about their suitability in freeze-drying.

3 Materials and Methods

3.1 Materials

All excipients were provided with a laboratory grade. Therefore, further purifications were not considered. L-Arginine and Citric Acid were supplied by JT Baker[®] (Countries of origins: Japan and USA); hydrochloric acid at concentration of 1 molar was supplied by Bernd Kraft GmbH (Duisburg, Germany); lactobionic acid was purchased from Acros Organic with a purity of 97 %wt. (India); highly concentrated orthophosphoric acid was delivered from FCP (Faculty of Chemistry and Pharmacy – LMU, Germany); succinic acid was supplied by Merck-Schuchardt (Hohenbrunn, Germany) with a purity at least of 99 %wt. and sucrose pure at 99 %wt. was supplied by Fluka Analytical[®] (Japan). The studied active principle is a monoclonal antibody (mAb), which was solubilized in a 50 mmolar buffer of histidine at pH of 5.3. The declared concentration of the protein stock solution was 94 mg/ml. All formulations were obtained with highly purified water (HPW). HPW was produced through a reverse osmosis purification system (USF EGLA, UK).

3.2 Preparation of the solutions for the investigation of protein stability

Some hundreds of milliliters of stock solutions were prepared for each chemical. A weighted volume of L-arginine solution was titrated with previously mentioned acid in order to get the wished pH. During the titrations, the pH was monitored by a pH-meter (METTLER TOLEDO[®], Germany). Afterwards, the solutions were diluted with HPW until the concentration of 5 %wt. of L-Arginine was reached. The pH was checked again at the end.

The mAb was pipetted in the labeled “protein formulation” and, afterwards, the pH was checked. The protein concentration was accurately measured in triplicate with an UV-visible spectrophotometer (Nanodrop 2000, Thermo Fisher) at the wavelength of 280 nm. The name of “placebo solutions” was given to the solutions without mAb. All formulations were filtered with a 0.2 μm VWR[®] syringe filter. The required amount of FIOLAX[®] injection vials type 2R per formulation were washed at 93°C for 30 minutes to get rid of particles and, then, they were rinsed three times with HPW and dried at 40°C for 24 hours. The stoppers were also cleaned with HPW and then dried as well. A volume of 1.5 ml of formulation per vial was pipetted. The samples used for the freeze-thawing tests were completely closed with a stopper, whereas the vials with the product to be freeze-dried were just partially stopped.

It has to be pointed out that the sucrose solution was directly prepared at the desired concentration, and the surfactant PS80 was added in the filtered solution.

Table 1.1 and Table 3.2 show the composition of all L-arginine and sucrose-based formulations. All solutions, except those containing lactobionic acid, were obtained by following the same constraints. The first target was the arginine concentration, which was defined at 5.0 ± 0.3 %wt., whereas every protein formulations had to show an antibody concentration of 3.23 ± 0.08 mg/ml. The investigation was performed at pH ranging from 5.0 ± 0.3 to 7.0 ± 0.3 and, therefore, the total solid concentration was not considered during the design of formulations. However, it was a function of the amount of acid needed to reach the desired pH. The investigation was therefore based on three different variables: pH, presence of antibody, and kind of counterion employed.

Table 3.1 The components and final concentrations of L-arginine-based formulations considered in this study. (A) L-arginine; (C) Citric acid; (H) Hydrochloric acid; (L) Lactobionic acid; (P) Phosphoric acid; (S) Succinic acid; (m) Monoclonal antibody.

| Formulation | pH | L-arginine (%wt.) | Acid (%wt.) | mAb (mg/ml) |
|--------------------|-----------|------------------------------|------------------------|------------------------|
| AC5 | 5.1 | 5.0% | 2.6% | 0.00 |
| AC6 | 6.2 | 5.0% | 2.0% | 0.00 |
| AC7 | 7.0 | 5.0% | 1.8% | 0.00 |
| ACm5 | 5.1 | 4.9% | 2.5% | 3.23 |
| ACm6 | 6.1 | 4.9% | 1.9% | 3.27 |
| ACm7 | 7.0 | 4.9% | 1.8% | 3.04 |
| AH5 | 5.2 | 5.0% | 1.0% | 0.00 |
| AH6 | 5.8 | 5.0% | 1.5% | 0.00 |
| AH7 | 7.0 | 5.0% | 1.0% | 0.00 |
| AHm5 | 5.2 | 4.9% | 1.0% | 3.38 |
| AHm6 | 5.7 | 4.9% | 1.4% | 3.12 |
| AHm7 | 7.0 | 4.9% | 1.0% | 3.32 |
| AL5 | 5.1 | 3.5% | 7.2% | 0.00 |
| AL6 | 6.3 | 3.7% | 7.4% | 0.00 |
| AL7 | 7.2 | 3.7% | 7.4% | 0.00 |
| ALm5 | 5.1 | 3.4% | 7.0% | 3.21 |
| ALm6 | 6.2 | 3.6% | 7.2% | 3.28 |
| ALm7 | 7.0 | 3.6% | 7.2% | 3.25 |
| AP5 | 5.3 | 5.0% | 2.6% | 0.00 |
| AP6 | 6.1 | 5.0% | 0.8% | 0.00 |
| AP7 | 7.0 | 5.0% | 1.5% | 0.00 |
| APm5 | 5.3 | 4.9% | 2.5% | 3.22 |
| APm6 | 6.3 | 4.9% | 0.8% | 3.23 |
| APm7 | 7.0 | 4.9% | 1.5% | 3.26 |
| AS5 | 5.0 | 5.0% | 2.1% | 0.00 |
| AS6 | 6.0 | 6.8% | 2.1% | 0.00 |
| AS7 | 6.9 | 5.0% | 1.4% | 0.00 |
| ASm5 | 5.0 | 4.8% | 2.1% | 3.21 |
| ASm6 | 6.0 | 6.6% | 2.0% | 3.19 |
| ASm7 | 6.9 | 4.9% | 1.4% | 3.15 |

The lactobionic acid was prepared at the same pH values; however, its arginine concentration (around 3.6 ± 0.1 %wt.) is not directly comparable with the other counterion formulations. This is due to the fact that the low solubility of the lactobionic acid did not permit to achieve the same concentration of the L-arginine during the titration to the desired pH. At a room temperature, it was not possible to reach a stable value of the pH and, therefore, the solutions were warmed up at 35°C to accelerate the acid-base reaction rate. Moreover, the temperature was kept below 37°C , when the first thermal degradations begins, as reported by Bisinella et al. [31].

The sucrose-based formulations (Table 3.2) had a concentration of sucrose of 6.95 ± 0.09 %wt., whereas they differed with respect to the presence of antibody and surfactant (PS80).

Table 3.2 Compositions and final concentrations of sucrose-based formulations considered in this study. (Su) Sucrose; (PS80) Polysorbate 80; (m) Monoclonal antibody; (FT) solution used to investigate the impact of different number of freeze-thawing cycles.

| Formulation | Sucrose (%wt.) | PS80 (%wt.) | mAb (mg/ml) |
|-----------------------------------|---------------------------|------------------------|------------------------|
| Su | 7.0% | 0.0% | 0.00 |
| Sum | 6.8% | 0.0% | n.m. |
| SuPS80 | 7.0% | 0.16% | 0.00 |
| SumPS80 | 7.0% | 0.10% | n.m. |
| Su_FT | 6.67% | - | - |
| SuPS80_FT | 6.67% | 0.02% | - |
| Sum_FT | 6.54% | - | 2.91 |
| SumPS80_FT | 6.54% | 0.007% | 2.91 |
| n.m. = value not measured. | | | |

3.3 Freeze-Thawing cycle

The freeze-thawing process was performed in the SP Scientific FTS Systems freeze dryer and repeated for 5 cycles to emphasize the protein stress inside the formulation and the different impact of L-arginine counterions in the protein stabilization. The Table 1.4 shows the cycle used for this test. 4 vials per formulation were placed in the center of the tray, and surrounded by dummy vials filled with 1.5ml of HPW. The temperature of the process was monitored with 3 thermocouples placed around the product vials.

Table 3.3 Repetitive freeze-thawing cycle carried out for the protein stability study.

| Step | Temperature (°C) | Pressure (mbar) | Ramp (°C/min) | Hold Time (1/min) |
|----------------------|-----------------------------|----------------------------|--------------------------|------------------------------|
| 1 | 20 | ambient | -- | 20 |
| 2^a | -50 | ambient | 1 | 180 |
| 3^a | 20 | ambient | 1 | 180 |

^a Repeated steps in the following cycles

3.4 Freeze-Drying cycle

The freeze-drying cycle illustrated in Table 1.3 is performed in the SP Scientific FTS Systems lyophilizer. 7 vials per formulation were placed in the center of the tray and surrounded by dummy vials filled with 1.5ml of HPW. The process was monitored with 3 thermocouples placed around the product vials. The freeze-drying run was performed as shown in Table 3.4. The end of the primary drying was identified when a difference of 8 mbar between capacitive manometer and Pirani manometer was measured. After the drying, a storage temperature of 5°C and pressure of 8 mbar were imposed to encourage the closure of the vials. The stoppers were then pushed inside the vials before stopping the cycle and extracting the product.

Table 3.4 Freeze-drying protocol carried out in case of the L-arginine-based formulations.

| Step (-) | Temperature (°C) | Pressure (mbar) | Ramp (°C/min) | Hold Time (min) |
|---------------------|-----------------------------|----------------------------|--------------------------|--|
| 1 | 20 | ambient | -- | 20 |
| 2 | -50 | ambient | 1 | 90 |
| 3 | -50 | 0.06 | -- | -- |
| 4 | -20 | 0.06 | 0.5 | until pressure difference below 0.007 mbar |
| 5 | 0 | 0.06 | 0.33 | -- |
| 6 | 40 | 0.06 | 0.5 | 450 |

3.5 Light obscuration measurement

The particle counter is an analytical instrument that counts particles in low-viscosity liquid suspensions. Few hundred microliters of sample are drawn with a syringe by means of a stepper motor pump and injected in a lighted chamber. The sample passes through a laser-diode sensor, which uses the light extinction technique to identify the particles [26] in a range between 1 µm to 200 µm.

The PAMAS SVSS-C instrument (PAMAS, Rutesheim, Germany) was used for particles counting. A volume of 1.0 ml of solution was analyzed in 4 aliquots of 0.2 ml and a pre-run volume of 0.2 ml. The measures were performed in 4 replicates. The method of analysis followed the mandatory monograph of USP<787> [26]. The average and the standard deviations were reported.

The pharmacopeias (USP <788> and Ph. Eur. 2.9.19) delimits the total number of particles larger than 10 μm and 25 μm permitted in pharmaceuticals (less than 6000 and 600 units per container) (29, 30). The analysis considered both these limits and also the total number of particles larger than 1 μm .

3.6 Turbidity

The measured turbidity is based on light scattering of solid particles suspended in the solution. The interactions among particles and light depend on the dimension, concentration, and shape of the particles and on the wavelength of the light. The instrument includes a lamp, a lens to focus the light on the sample, and a light detector at 90° to measure the scattered light [27].

A 1.5 ml of solution was smoothly dispersed in a tube and then measured. The measured turbidity is expressed in the Formazin Nephelometric Unit (FNU). NEPHLA Turbidimeter (Dr. Lange, Duesseldorf, Germany) has a single detector tilted at 90° ($\lambda = 860 \text{ nm}$) with respect to the incident beam.

The method of analysis used was slightly different when it was used to study how the number of sequential freeze-thawing cycles impact on the protein aggregation in sucrose-based solutions. In this case a volume of 2.0 ml was used to perform the measurements, instead of 1.5 ml.

3.7 Differential Scanning Calorimetry (DSC)

The DSC is a calorimetric technique of analysis used to measure thermal proprieties of materials. A few milligrams of sample are sealed in a pan and placed with an empty-reference inside the oven. Both pans are monitored during a temperature protocol. In the meantime, a sensor measures the difference of heat flux needed to keep the pans at the same temperature. A controlled gas flow rate was fluxed through the chamber. During the analysis, physical and chemical transformations take place in the sample pan. A thermogram is produced and all transformations occurred in the samples are plotted on it. For instance, crystallization and melting are identified by a peak and the glass transition (T_g or T_g') can be figured out according to a change in the slope of the curve.

The investigation of the T_g' in the liquid phase and of the T_g in the freeze-dried cakes were performed using the differential scanning calorimetry (DSC821^e, METTLER TOLEDO[®], Germany) equipped with a cooling system control software ASTAR[®]. The instrument was previously calibrated with Indium and it used an empty pan as reference. Aluminum pans of 40 μl volume (DSC821^e, METTLER TOLEDO[®], Germany) were used in all experiments.

3.7.1 Evaluation of the T_g' in the solutions

15 μl of solution were sealed in the previously mentioned pans. The samples were balanced at 20°C for 3 minutes; then, they were cooled down with a rate of 10°C/min to -60°C and kept for 5 minutes in those conditions. Afterwards, the pans were heated up at 5°C/min to 20°C.

The T_g' was evaluated as midpoint of the second order transition occurring in the thermogram during the heating step. The average and the standard deviation were calculated from 3 measurements.

3.7.2 Evaluation of the T_g in the freeze-dried cakes

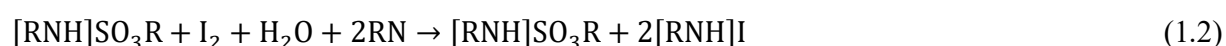
The preparation of the samples was completely performed with a humidity lower than 10 % in the environment to avoid water absorption in the powders and, consequently, the decrease of T_g . This purpose was achieved by using a glovebox fluxed with dried air. An amount of about 3-5 mg of powder was dispersed in the pans. The measurements involved a modulated protocol known as

modulated Differential Scanning Calorimetry (mDSC). The heating rate was set to 2°C/min with an amplitude of ±1°C and a period of 2 minutes starting from 25°C up to 140°C.

The T_g is obtained from the reversible phase. The wished value of the temperature is evaluated at the midpoint of the second order transition. The result was evaluated in triplicate.

3.8 Karl-Fisher titration

The Karl-Fischer titration is a well-known analytical method to determine the water amount in various samples. It is based on the oxidation reaction of the sulfur dioxide (SO₂) by iodine (I₂) in an aqueous environment. In the first reaction, SO₂ is dissolved in alcohol (ROH), generally methanol, and it reacts with a base (RN) (e.g. imidazole or diethanolamine) to form alkyl sulfite ([RNH]SO₃R) (1.1). Afterwards, the alkyl sulfite is oxidized with water (H₂O) by the I₂ (1.2) [32]:



The KF titration is highly selective to water, as it can cover a wide range of concentrations and the analysis is performed in few minutes. Two different techniques are available, depending on the concentration range investigated: the volumetric and the coulometric titration [33]. The volumetric method uses a joint solution of solvent base SO₂ and I₂ as titrant. On the contrary, the coulometric method generates the I₂ from an electrode of platinum inserted in the analyte solution. The endpoint of the titration is evaluated by a pair of platinum electrodes through a strong decrease of the resistance in the solution. With a well-designed reactant solution, the reaction has a molar ratio 1:1 of I₂ and H₂O. The amount of water in the sample is thus easily evaluated.

The instrument used in this study is an Aqua 40.0 titrator (Analytik Jena AG, Halle). Some milligrams of sample were fed in a FIOLAX[®] injection vial type 2R and closed with an injection stopper. The water absorption from the freeze-dried powders was avoided by preparing the samples in a glovebox, which was fluxed with dried air. The moisture inside the glovebox was kept below 10 %. The instrument was equipped with a headspace oven able to warm up the samples to 100°C. to evaporate all water inside the vials. Before starting the measurements three empty vials were measured as blank and the endpoint drift was set to 8 µg/min. The result was reported as average of three replicates.

3.9 Reconstitution time

The reconstitution time was investigated by adding 1.5 ml of water in the vial; the timer was then started and the vial was smoothly turned around. The time was stopped when there were no visible particles inside the vial (and, thus, the solution appeared transparent). The reconstitution time was investigated in 3 replicates. Both the average and the standard deviation were calculated and reported.

3.10 Visual inspection

The visual inspection of the samples was performed with a professional camera. It was aimed to see and report any defects in the lyophilized cakes and the changes after the freeze-thawing cycles in the solution.

3.11 X-ray diffraction

X-ray diffraction is an important technique used to investigate qualitatively and quantitatively the crystalline structure of materials. It is based on the evaluation of the diffraction patterns of crystals, which were beat from a focused x-ray beam (with wavelength ranging between 10^{-3} and 10^1 nm). The physics phenomena occur during the experiment are explained by the Bragg's law (1.3):

$$n\lambda = 2d_{hkl} \sin(\theta) \quad (1.3)$$

where n is the refractive index of the material, d is the interplane distance, “ hkl ” are the Miller indexes to label the plane I refer to, θ is the incidence angle.

A constructive interference among diffracted rays occurs when their energy is equal to the gap and direction between the repetitive planes of crystals. The signal coming out from the instrument is analyzed through the Fourier formalism. The hardware is composed of few devices. Firstly, the X-rays are generated by a source (e.g. a sealed tube or a rotating anodes). Some wavelengths with high intensity are highlighted. Therefore, some optical devices are placed afterwards to isolate and reduce the divergence of the monochromatic peak ($K_{\alpha 1}$). The core of the instrument is the goniometer. It allows to move the source, the sample, and the detector, in order to scan every angle. The Bragg-Bretano geometry is the most used one. The diffracted photons are also manipulated optically, before they are converted to another type of signal by a detector, that can be analyzed [34]. The data are represented as intensity of the signal with respect to twice the θ angle. The qualitative analysis is given from the peaks positions in the graph, whereas the intensity provides some information about the crystal structure. The absence of peak highlights the amorphous structure of the sample.

Diffraction was used to confirm the crystalline structure shown during the DSC analysis of some freeze-dried cakes. Some grams of powder were dispersed on a copper disc plate and pressed with a glass until a compact layer was formed. Instrument Seifert 3000TT diffractometer was programmed to investigate angles between 5° to 45° with a step width of 0.05° and a Cu K_{α} radiation (40 kV, 30 mA). The data were shown until 37° , although the copper peak at 43.2° was used as references.

3.12 Statistical analysis of the results

The statistical analysis was performed by using MODDE Pro (12.0 – Trial version): a confidence interval of 95% (equivalent to $\alpha = 0.05$) was used with Fisher test on the arithmetic means.

3.12.1 Investigation of protein stability in sucrose-based formulation throughout repeated freeze-thawing cycle

The impact of freeze-thawing cycles on protein stability was investigated before and after 1, 3 and 5 cycles in solutions that were composed by 7 % wt. of sucrose. The investigation was performed on both placebo and protein formulations (3.2 mg/ml), meanwhile it was studied the effect of polysorbate 80 (PS80) at low concentration (0.001 % wt.) on protein aggregation.

The design of experiment was therefore performed considering 2 qualitative factors: presence of PS80 (Factor PS80) in 2 levels (Yes or No) and presence of antibody (Factor PT) in 2 levels (Placebo – Placebo and Antibody – mAb). Moreover, the impact of the technological process (Factor FT) in 4 levels (before process – FT0 and after 1 – FT1, 3 – FT3 and 5 processes – FT5). It was used a full design of experiment with two levels two factors and one factor in four levels. The experiments were performed on 3 replicates ($n = 3$) to evaluate mean values and standard deviations. The experiments were quantified in terms of turbidity (TB) and total particles counting at 3 diameters: 1 μm (LO1), 10 μm (LO10) and 25 μm (LO25).

3.12.2 Investigation of protein stability in L-arginine-based formulations at different values of pH

The impact of the L-arginine counterions on protein stability at 3 different values of pH was investigated by employing 4 different acids (citric, hydrochloride, phosphoric and succinic) in comparable solutions with a constant concentration of arginine (5%wt.). The investigation was performed on both placebo and protein formulations with a concentration of antibody of 3.2 mg/ml. Moreover, all solutions were analyzed before and after the technological process of freeze-thawing or freeze-drying.

The design of experiment was therefore performed throughout 3 qualitative factors: type of acid (Factor IO) in 5 levels (Citrate – C, Chloride – H, Lactobionate – L, Phosphate – P and Succinate – S), presence of antibody (Factor PT) in 2 levels (Placebo – Placebo and Antibody – mAb) and impact of the technological process (Factor FT) in 2 levels (before the process – FT0 and after freeze-thawing – FT5 or freeze-drying – FD). It was used a full factorial design of experiments with one factor more than two levels. The objective of this statistical analysis was to find crucial factors that mostly affect the results of the experiments. The design space was recognizable as 5×2^2 factorial design with 20 different interactions among factors. The experiments were performed on 4 replicates ($n = 4$) to evaluate mean values and standard deviations. The experiments were quantified in terms of turbidity (TB) and total particles counting at 3 diameters: 1 μm (LO1), 10 μm (LO10) and 25 μm (LO25).

3.12.3 Statistical model development

The statistical analysis was aimed to develop a useful empirical model to define quantitatively the results and to identify a relationship between input and output parameters [35].

In detail, a multiple linear regression model (MLR) was employed, which was described in general by the relationship (1.4):

$$y = \beta_0 + \beta_1 x_1 + \beta_2 x_2 + \dots + \beta_k x_k + \varepsilon \quad (1.4)$$

The dependent variable (y), that was also called response, depends on k predictor variables (x_i), whereas ε was the error of the model. The parameters ($\beta_i, i = 0, 1, \dots, k$) were called regression coefficients and they were estimated by using the method of least square minimization (1.5):

$$\min_{\forall \beta_i \in \mathbb{R}} \left\{ \sum_{i=0}^n (y_i - \beta_0 + \sum_{j=1}^k \beta_j x_{ij})^2 \right\} \quad (1.5)$$

Residuals (e_i) were evaluated as difference between the observations (y_i) and the fitted model values (\hat{y}_i) (1.6):

$$e_i = y_i - \hat{y}_i \quad (1.6)$$

The essential assumption on which the analysis was based is the random origin of the error (ε), i.e. the normal distribution of the data or constant variance. The probability plot of normalized residuals was a useful procedure to check this assumption, in addition to the plot of residuals versus fitted values. Deviations from the normal distribution and patterns in residuals plots were clear defects on the hypothesis, and they suggested nonconstant variance. Moreover, possible outliers could be detected through the normal probability plot, since they were recognizable as wide scattered points standing outside the interval of ± 4 standard deviation (σ). Skewed data distribution provided a nonconstant variance that tended to be dependent on the mean. Anyway, the variance sometimes was dependent on the observations magnitude as the observations error was a percentage of the measurements. A usual approach to correct the observations distribution was to apply an appropriate transformation on the data depending on their initial distribution [35]. In the case studies, it was possible to use a logarithmic transformation (3.1) to normalize the observed lognormal distributions:

$$y^* = \ln y \quad (1.7)$$

where y^* is the transformed measurement and y is the initial measurement. It was possible to get a measure of the distribution skewness through the computation of skewness parameter. Finally, it had to be considered that when a transformation is used the final model is developed according to the transformed data.

Additional information about the significance of every model were provided by some statistical parameters. R^2 was the fraction of the data variability “explained” by the model and it was defined as (1.8):

$$R^2 = \frac{SS_{model}}{SS_{tot}} = 1 - \frac{SS_{residual}}{SS_{tot}} = 1 - \frac{\sum_{i=1}^n (y_i - \hat{y}_i)^2}{\sum_{i=1}^n (y_i - \bar{y})^2} \quad (1.8)$$

where SS means “sum of square” and \bar{y} is the mean response. The parameter ranges from 0 to 1: a value close to 1 indicates a good fit between data and model. However, a high value of R^2 did not imply the adequacy of the regression model, since increasing the number of predictors variables always R^2 increases, despite whether they were significant or not. The used statistical models were composed by different terms encompassing significant variables and interactions variables to quantify the impact of each factor on the responses. Statistical insignificant variables were therefore detected by checking their confidence interval and were deleted from the model coefficients following the hierarchical procedure. The final purpose was to improve the adequacy of the model [35]. The predictive ability of the model was verified by the parameter Q^2 , which estimates the precision of additional predictions. In other words, it is the capacity of the model of explaining the availability of new predicted observations, and it is defined as (1.9):

$$Q^2 = \frac{PRESS}{SS_{tot}} \quad (1.9)$$

where $PRESS$ is the prediction residuals sum of square that is computed through the generalized cross-validation method [35]. Q^2 ranges from 0 to 1 and high values indicate the adequacy of the model. Nevertheless, a third parameter was required to claim the adequacy of the model to the data. Lack-of-fit occurred when the regression function was not linear and, therefore, more appropriate equations should be used. Anyway, the initial assumption of normal distribution had to be checked as skewed distributions could also cause deviations. The presence of significative lack-of-fit indicated that the model could be not appropriate to describe the experiment. The parameter is computed by using the p-value from the Fisher test between the pure error (PE) and the lack-of-fit (LOF). SS_{PE} (1.11) was model-independent because it was computed as the difference between each measured value (y_{ij}) and its means in replicates (\bar{y}_i) (1.10):

$$\bar{y}_i = \frac{1}{n_i} \sum_{j=1}^{n_i} y_{ij} \quad (1.10)$$

where, n_i is the number of replicates.

$$SS_{PE} = \sum_{i=1}^m \sum_{j=1}^{n_i} (y_{ij} - \bar{y}_i)^2 \quad (1.11)$$

On the other hand, SS_{LOF} was defined as the difference between each replicant mean value and the fit value in the same condition (\hat{y}_i) (1.12):

$$SS_{LOF} = \sum_{i=1}^m n_i (\bar{y}_i - \hat{y}_i)^2 \quad (1.12)$$

The degrees of freedom (DoF) of the pure error was $(n - m)$, where n was number of total observations and m the number of level of the variables. On the contrary, the DoF of the lack of fit was $(m - p)$, where p was the number of parameters in the model. The Fisher test of lack of fit was computed as (1.13):

$$F_0 = \frac{SS_{LOF}(n-m)}{SS_{PE}(m-p)} \quad (1.13)$$

Afterwards, F_0 was compared with the tabulated $F_{\alpha, m-p, n-m}$ and the p-value was evaluated. If the p-value was lower than the fixed value of 0.05, then model was afflicted by a significant lack of fit.

In the results chapter, the evaluated effects of the statistic models were reported. They were computed as the double of the MLR equation coefficients. Moreover, they were listed with their 95% confidence interval. The direction and the amplitude of the effects allowed to conclude how factors impact on response and whether they are crucial to define the results. For instance, an effect with a positive value increased the response. Moreover, the statistical significance of a factor is due to the width of its confidence value. In detail, the factor was considered insignificant if the interval had an absolute value larger than its own effect.

In the section 4.1.1 the complete statistical evaluation was reported in order to show the “modus operandis” during the analysis. All statistical analysis was carried out by following the procedure previously described.

4 Results

4.1 Cryoprotection of L-arginine-based formulations and comparison with sucrose

The freeze-concentration step was claimed as an important source of stress during the freeze-drying process [3] and sub-zero storage. The purpose of this section was to compare a wide used cryoprotectant such as sucrose, and its combination with a surfactant (PS80), with L-arginine salts, thus evaluating whether any advantage was gained by using the amino acid salts instead of sucrose as stabilizer in lyophilization. The second aim was to prove which salt provided the most effective protection at different levels of pH and how the acidity influenced the protein aggregation. A series of repeated freeze-thawing cycles was used to enhance the antibody self-combination in order to point out the effects of the excipients and to make a screening of the formulations.

4.1.1 Impact of the number of freeze-thawing cycles on the protein agglomeration in sucrose-based formulations

The following experiments highlighted how the number of freeze-thawing cycles impacted on the number of protein agglomerates in sucrose formulations. Moreover, the additional effect of a surfactant (PS80), in combination with sucrose, was investigated.

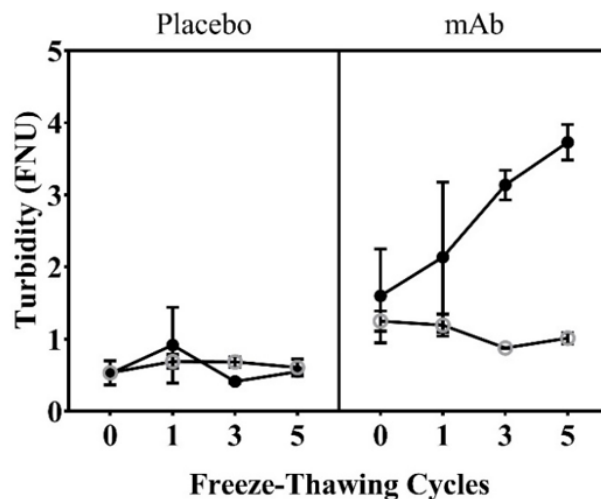


Figure 4.1 Turbidity of (●) Sucrose, and (⊖) Sucrose with PS80 ($n = 3$, mean \pm s.d.).

Figure 4.1 illustrates how the turbidity of sucrose, and sucrose with surfactant (PS80), solutions changed by increasing the number of the repeated freeze-thawing cycles (FT) in placebo and protein (mAb) containing formulations. Both placebo formulations showed an approximately constant value of turbidity throughout the entire process, at around 0.5 NFU. On the contrary, mAb solution containing only sucrose showed a linear increment of turbidity. The initial turbidity value was 1.6 ± 0.6 FNU and after five freeze-thawing cycles it rose more than twice the initial value (3.7 ± 0.2 FNU). On the other hand, mAb formulation containing PS80 showed an approximately constant turbidity (1.1 NFU), although a mild decrease was observed throughout the repetitions. Both mAb formulations highlighted higher values of turbidity than placebo across all the repeated cycles.

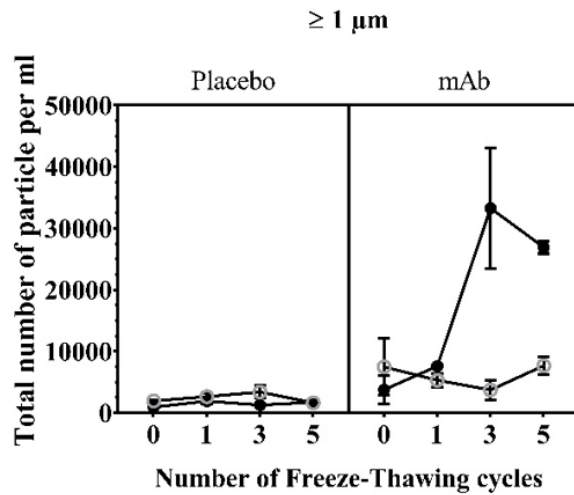


Figure 4.2 Particle counting measurements of (●) Sucrose, and (⊖) Sucrose with PS80 ($n = 3$, mean \pm s.d.) by light obscuration. The graphs show the total number of particles $\geq 1 \mu\text{m}$.

The turbidimetric observations were confirmed by particle counting analysis, that was carried out in order to have more detailed results (Figure 4.2 and Figure 4.3). Figure 4.2 shows the total number of particles per milliliter with a diameter larger than $1 \mu\text{m}$. It reflects the turbidimetric results, where approximately the same number of particles (2000 #/ml) was counted in both placebo solutions. Anyway, the placebo containing PS80 had always a few hundred particles more than sucrose. Protein formulations highlighted other analogies with turbidimetric results. The particle number observed in sucrose mAb solution increased with FT (Figure 4.1). Anyway, a peak of agglomerates after 3 FT was observed. However, the value increased more than six times after 5 cycles, and it passed from $4000 \pm 2000 \text{ #/ml}$ to $26900 \pm 900 \text{ #/ml}$. On the other hand, the PS80 inhibited the agglomeration process and its observations remained approximately constant ($8000 \pm 1000 \text{ #/ml}$).

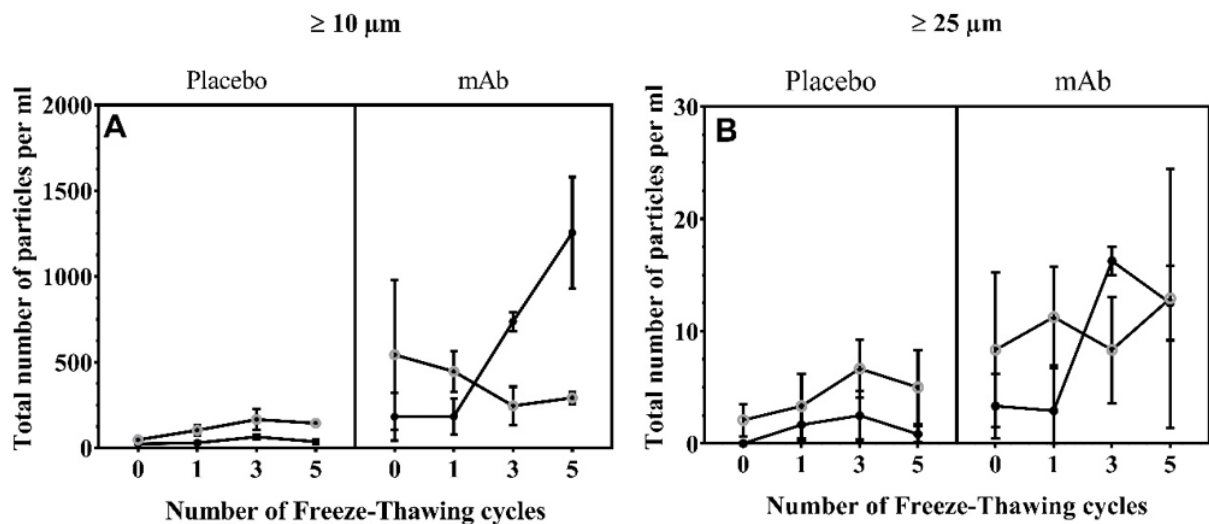


Figure 4.3 Particle counting measurements of (●) Sucrose, and (⊖) Sucrose with PS80 ($n = 3$, mean \pm s.d.) by light obscuration. The graphs show the total number of particles $\geq 10 \mu\text{m}$ (A) and $\geq 25 \mu\text{m}$ (B).

Same trends were shown in number of particles equal or larger than $10 \mu\text{m}$ (Figure 4.3-A), although the mAb sucrose formulation did not had a peak of particles after 3 FT. The number of particles larger than $25 \mu\text{m}$ (Figure 4.3-B) highlighted weak precision among data due to the high standard

deviation. However, placebo formulation containing PS80 had a larger number of particles than sucrose and the same characteristic was observed in mAb solution until 3 FT.

The turbidimetric and particle counting results provided similar results; therefore, a statistical analysis was carried out to confirm the evidence with mathematical significance. Full design of experiments with multilevel factors was used as described in the section 3.12.1. In the next paragraph, an example of how it was used in order to obtain an accurate model.

All turbidimetric measurements were tabled as responses and used to compute the linear regression model (LRM) with full interactions among factors. The normal distribution hypothesis was checked by plotting the normal probability plot (Figure 4.4). The assumption required to have the data plot as a straight line, with more emphasis on the central values than on the extremes [35]. Moreover, possible outliers are recognized as their residuals stand outside the significant interval of ± 4 the standard deviations (σ). Figure 4.4 highlighted a deviation from the dashed line in both tails and, therefore, it was necessary to transform the data with a suitable transformation to normalize them.

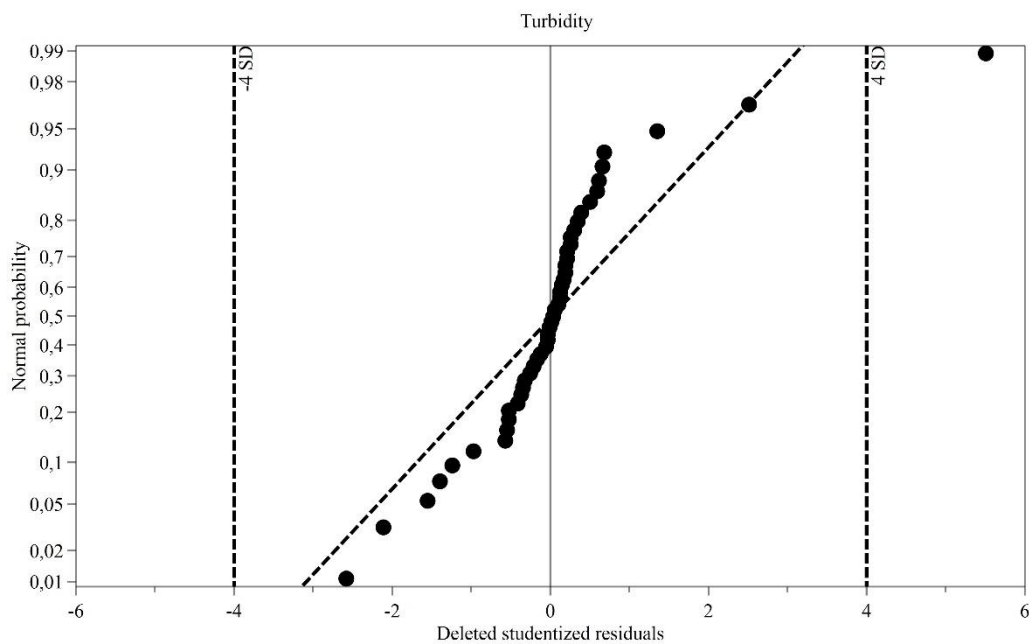


Figure 4.4 Normal probability plot of turbidimetric measurements. (●) Probability.

Due to the skewness of Figure 4.4 it was decided to normalize the data with a logarithmic transformation. The Figure 4.5 showed the transformed data on a normal probability plot. The defected tails were removed, and outliers were not detected. A higher concentration of points was detected in the center of the plot, although a mild asymmetry was observed between tails. Anyway, the assumption of normal distribution was considered proved.

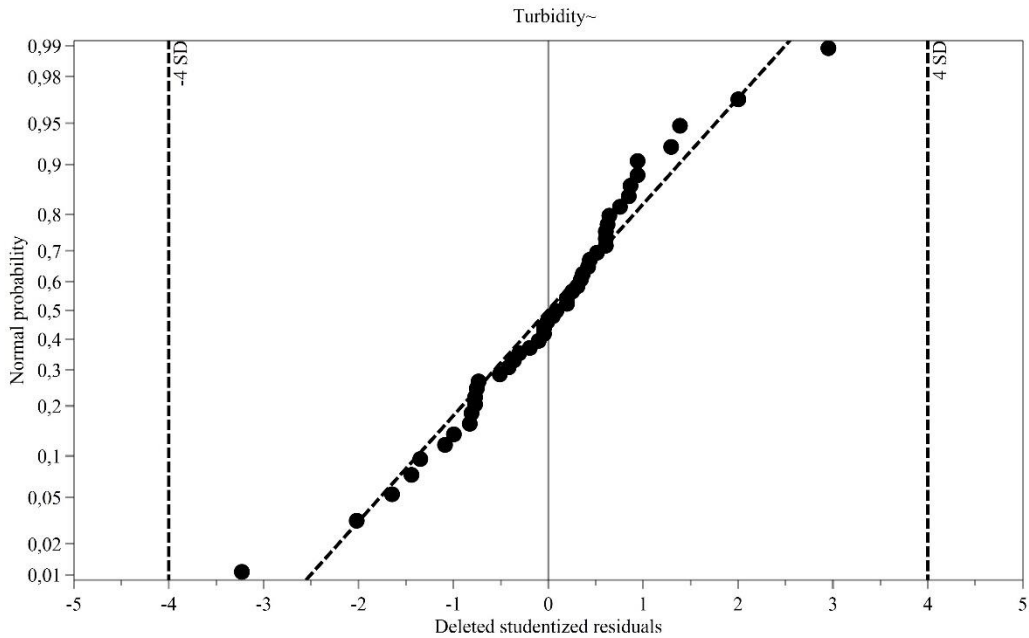


Figure 4.5 Normal probability plot of transformed turbidimetric measurements by using a logarithmic transformation. (●) Probability.

The responses of transformed turbidimetric observations generated a model with high fitting in response ($R^2 = 0.915$) and precision of predictions ($Q^2 = 0.878$); moreover, “lack of fit” was not observed as the model error did not differ significantly from the pure error or replicate error (p -value = 0.122). Figure 4.6 reports all variables considered in developing the turbidity model. The effects were evaluated as the double of the model parameters (as shown in Section 3.12.3) and they were plotted in descending order. A positive effect promoted the increase of turbidity, whereas a negative value had the opposite impact.

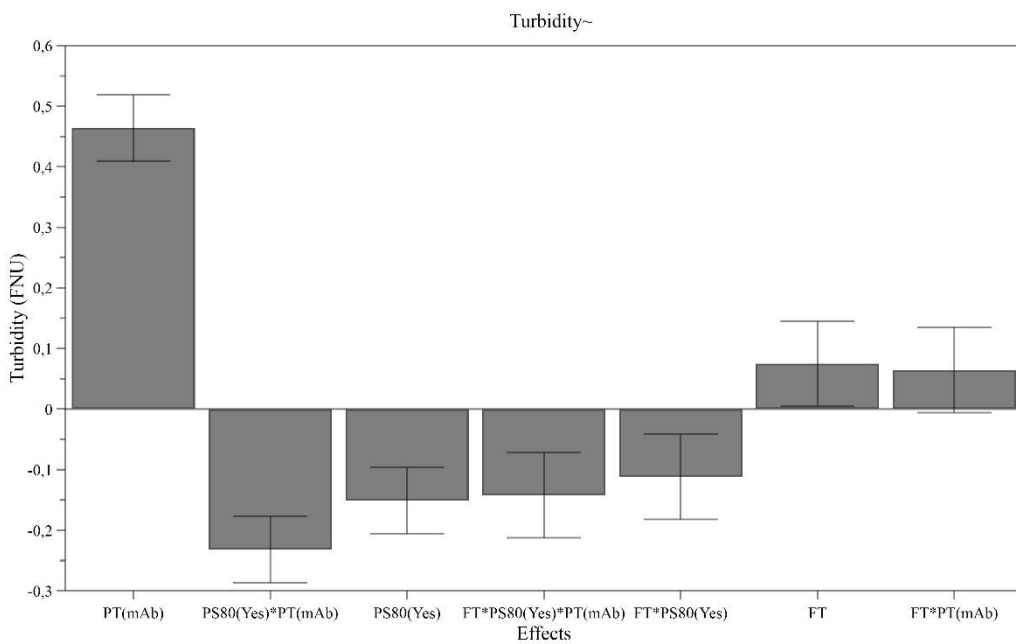


Figure 4.6 Effect plot of transformed turbidimetric measurements of sucrose-based formulations.

The major cause of turbidity was the presence of antibody (PT(mAb) = 0.464 ± 0.05 NFU); nevertheless, the technological process of freeze-thawing (FT) caused an increase of the signal (FT = 0.07 ± 0.07 NFU) as well. Anyway, the synergic interaction of FT with PT provided a statistically insignificant effect (FT·PT(mAb) = 0.064 ± 0.07 NFU), though it could not be deleted from the model due to the significant ternary antagonist combination with the surfactant (FT·PT(mAb)·PS80(Yes) = - 0.14 ± 0.07 NFU). The PS80 provided an effective decrease in turbidity due to its antagonism interactions with both FT and PT beside the negative value of the main effect (PS80(Yes) = - 0.15 ± 0.05 NFU). Especially, PS80 decreased the measurements in protein formulation (PT(mAb)·PS80(Yes) = - 0.23 ± 0.05 NFU). The significant enhancement in turbidity was due to the antibody, although the process caused a significant and weak increase. On the other hand, the effectiveness of PS80 was proved as a cause of lower observations than in sucrose formulations.

To confirm the similarity in turbidimetric and particle counting results it was necessary to develop a statistical analysis and a model in at least one of the three measured diameters in light obscuration. Initially, LRM models with all interactions were assumed, and the normal distribution assumptions were checked as it was described previously. It was necessary to normalize the data by logarithmic transformations due to the skewed initial distributions. Summaries of fit in models are reported in Table 4.1. The three diameters were compared in term of R², Q², “lack-of-fit” and reproducibility, in order to evaluate the adequacy of each model and the possibility of comparison with the turbidity results.

Table 4.1 Statistical parameters of models using light obscuration responses.

| Light obscuration diameters | R ² | Q ² | Lack-of-fit ^a (p-value) | Reproducibility |
|-----------------------------|----------------|----------------|------------------------------------|-----------------|
| ≥ 1 μm | 0.813 | 0.722 | 0.005 | 0.859 |
| ≥ 10 μm | 0.862 | 0.787 | 0.069 | 0.867 |
| ≥ 25 μm | 0.553 | 0.325 | 0.222 | 0.515 |

^a α = 0.05

The largest diameter (≥ 25 μm) highlighted a weak model with an extremely low precision in prediction and reproducibility, although the absence of lack-of-fit (p = 0.222). On the contrary, the particles larger than 1 μm showed a rather good (Q² = 0.722) and reproducible model, but they provided a p-value lower than 0.05, therefore probably LRM model was not suitable for the data (Section 3.12.3). The best model was provided for the 10 μm particles, since the extremely high statistical parameters; anyway, it could suffer by a weak lack-of-fit.

Figure 4.7 illustrates the light obscuration effects for particles larger than 10 μm. The following model considered the main effects and their interactions as the turbidimetric one. Moreover, comparable results were obtained in both cases. The antibody was confirmed being the main cause of particles aggregation (PT(mAb) = 0.7 ± 0.1 NFU), whereas the process enhanced its impact compared to the turbidity and it became the third effect as absolute value (FT = 0.3 ± 0.2 NFU). On the other hand, the surfactant showed a significative positive effect, in contrast with the previous result (PS80(Yes) = 0.2 ± 0.1 NFU). Anyway, all interactions involving PS80 were in antagonism: thus, they had similarities with turbidity. Moreover, the binary interaction between protein and process was statistically insignificant (FT·PT(mAb) = - 0.006 ± 0.2 NFU).

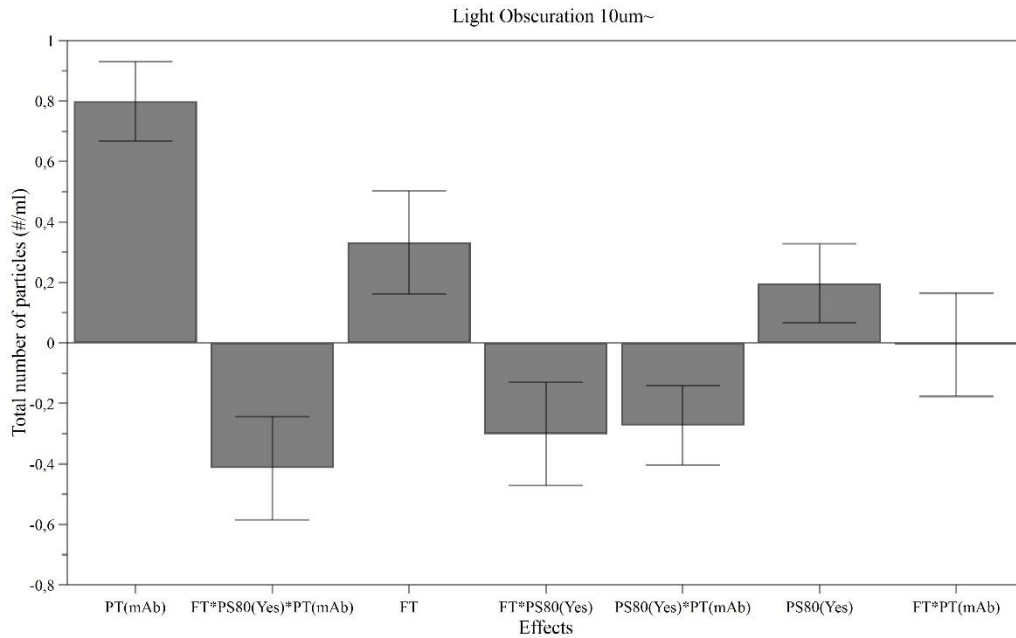


Figure 4.7 Effect plot of transformed total number of particles measurements $\geq 10 \mu\text{m}$ of sucrose-based formulations.

It was proved that turbidity and light obscuration give comparable results as their causes impacted the observations in the same way, and the PS80 main effect was the only exception. The main cause of particles aggregation in solutions was the antibody, although freeze-thawing cycles provided an increase in the measured values. The results highlighted that most particles in formulations were protein agglomerates due to wide differences between placebo and protein solutions throughout the entire process. The freeze-thawing repetitions enhanced the responses in both turbidity and particle counting, but remarkable results were just obtained in the total number of particles larger than $1 \mu\text{m}$ and $10 \mu\text{m}$. Therefore, the growth in number of agglomerates was confirmed with more freeze-thawing cycles. Furthermore, combination effects of PS80 with either FT or PT decreased all experiments responses. There were thus straightforward evidences of surfactant cryoprotection against to protein agglomeration. PS80 stabilized protein in both liquid solutions and during freeze-concentration step.

4.1.2 Protein stability of sucrose-based formulations

Previous investigations proved the enhancement of protein agglomeration by the repeated freeze-thawing cycles in sucrose-based formulation. The following experiment aimed to evidence how the protein formulations changed by five repeated freeze-thawing cycles. The investigation differed from the previous one as the amount of solution used during the turbidity measurements was reduced from 2.0 ml to 1.5 ml and the protein concentration was mildly increased, from 2.9 mg/ml to approximately 3.2 mg/ml. This protein concentration was fixed as the benchmark that was used in all the remaining investigations of the work. This test was carried out to confirm the previous conclusions about the sucrose-based formulations, although the turbidity and the particles counting would exhibit higher values due to the increase in protein concentration and the decrease in samples volume.

Turbidity measurements followed the expectations (Figure 4.8). In placebo solutions it approximately remained constant throughout the process at a value of 1.3 FNU. On the other hand, rather crucial differences were observed in protein formulations. Sucrose formulation showed a turbidity of 2.7 ± 0.2 FNU before the process (FT0), whereas it significantly increased to 11 ± 7 FNU in FT5. The addition of surfactant (PS80) blocked the enhancement that was caused by the process as its turbidity rose from 1.57 ± 0.07 FNU to 1.9 ± 0.3 FNU. These results were comparable to the previous investigation, although the turbidity was lower due to the higher samples volume and the lower protein concentration.

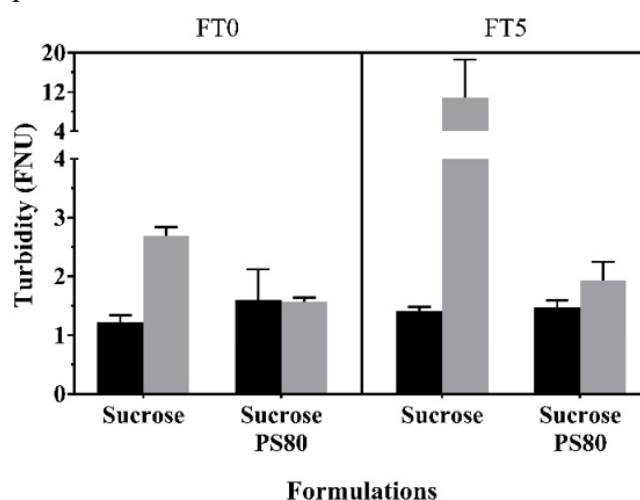


Figure 4.8 Turbidity of (■) placebo, and (▒) protein formulations in sucrose-based formulations (FT0) before and (FT5) after five freeze-thawing cycles ($n = 4$, mean \pm s.d.).

The particles counting shown in Figure 4.9 had many similarities with the turbidity results. Placebos caused a few thousands of particles, regardless of their conditions (FT0 or FT5). Nevertheless, solutions containing PS80 caused the formation of more particles than just sucrose; moreover, comparable behaviors were observed in Figure 4.9 of the previous section. Protein formulation contrasted with placebos and, therefore, sucrose formulations exhibited the same trend that was described in the turbidimetric experiment. A number of particles of 13000 ± 4000 #/ml in FT0 was obtained for the sucrose formulation, whereas it increased to 50000 ± 20000 #/ml after the process (FT5). On the contrary, PS80 approximately kept this value constant 7000 #/ml. Protein results were in accordance with the turbidimetric ones; moreover, placebo and protein containing PS80 were rather different from each others.

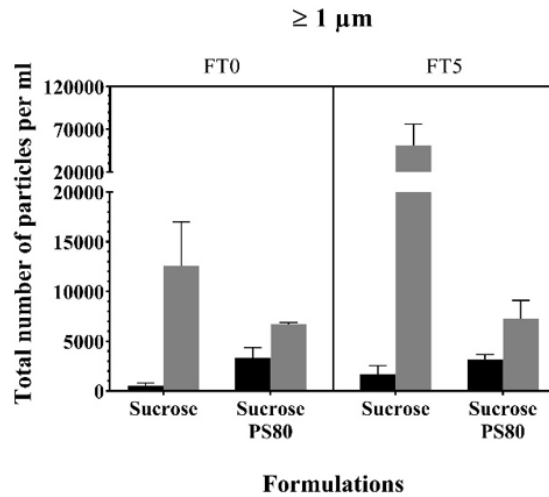


Figure 4.9 Total number of particles per milliliter larger than $1 \mu\text{m}$ (■) placebo, and (▒) protein formulations in sucrose-based formulations (FT0) before and (FT5) after five freeze-thawing cycles ($n = 4$, mean \pm s.d.).

Figure 4.10 showed the particle counting for diameters larger than $10 \mu\text{m}$ and $25 \mu\text{m}$. Sucrose solutions showed a number of particles lower than $50 \text{ \#}/\text{ml}$ (Figure 4.10 - l.h.s.) and absence of the largest ones in the initial conditions (FT0). On the contrary, the placebo containing PS80 showed a relevant number of particles in both cases, which was equal or even larger than that in the protein formulation at FT0. The process increased the number of particles larger than $10 \mu\text{m}$ in protein sucrose formulation, as it increased from $300 \pm 200 \text{ \#}/\text{ml}$ to $5000 \pm 5000 \text{ \#}/\text{ml}$ for particles. Protein formulation containing surfactant contrasted with the previous results and it kept an approximately constant value for particles larger than $25 \mu\text{m}$, whereas it caused an increase in those with a diameter larger than $10 \mu\text{m}$.

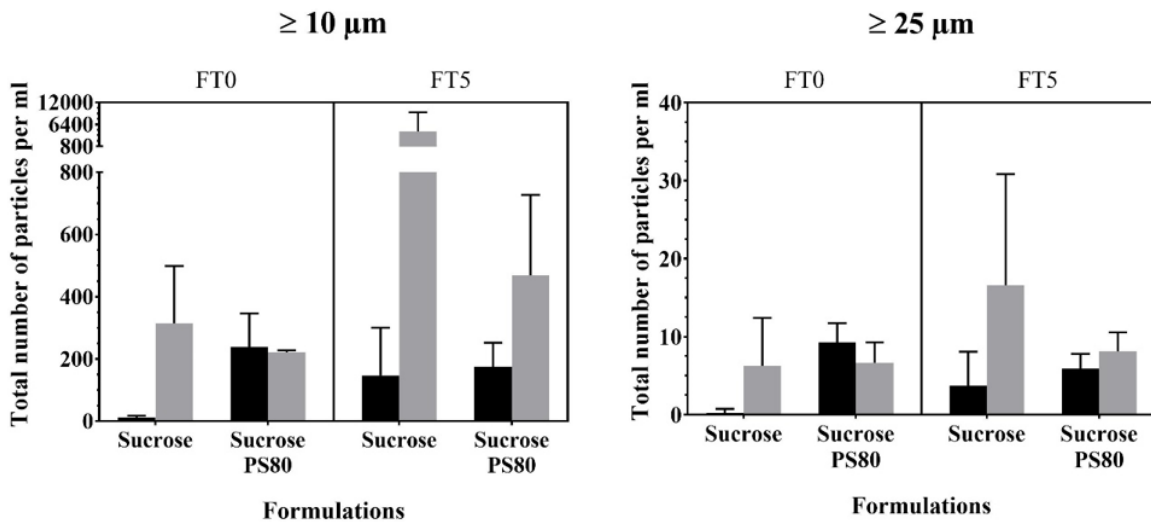


Figure 4.10 Total number of particles per milliliter larger than $10 \mu\text{m}$ (l.h.s.) and $25 \mu\text{m}$ (r.h.d.) for (■) placebo and (▒) protein formulations in sucrose-based formulations (FT0) before and (FT5) after five freeze-thawing cycles ($n = 4$, mean \pm s.d.).


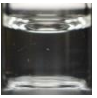


















The described experiments showed comparable results to the previous experiments, although the number of particles, especially those larger than $1 \mu\text{m}$ and the turbidity, were significantly higher than before.

4.1.3 Protein stability at pH 7 in L-arginine-based formulations at different counterions

The experiment aimed to prove how the change of the amino acid counterion impacted on the cryoprotection of the protein, especially on antibody agglomerates at a fixed pH. Moreover, the final purpose of the section was to identify which formulations had the most promising ability to stabilize the antibody. The investigation was performed in L-arginine-based formulations at pH 7, which were titrated with five different acids, then processed through five repetitions of freeze-thawing cycle. Similar experiments were performed at other two pH values to evaluate whether the pH changes impacted or not on liquid protein stabilization and cryoprotection abilities of the counterions.

The solutions appearances are shown in Table 4.2. Placebos showed a rather clear and bright solutions throughout the investigation, although a few visible particles were observed inside each sample. On the contrary, protein formulations (mAb) generally changed their appearances after the freeze-thawing processes (FT5), by becoming more turbid, with countless small visible particles. Anyway, the solutions clearness of mAb at FT5 quite depended on the employed acid. A relevant increase of the number of visible particles was observed with phosphate (P), citrate (C) and lactobionate (L), whereas chloride (H) and succinate (S) did not resulted in any modification of their appearances. Therefore, close values of turbidity were expected in all placebos solutions, and distinguishable differences between mAb in both FT0 and FT5 conditions.

Table 4.2 Visual inspection of L-arginine-based formulations at pH 7. Citric acid (C), Hydrochloric acid (H), Phosphoric Acid (P) and Succinic Acid (S) were used as counterions. Both placebo and protein solutions (mAb) were investigated. All solutions were photographed before (FT0) and after 5 freeze-thawing cycles (FT5).

| | <i>Placebo</i> | | | | | <i>mAb</i> | | | | |
|------------|---|---|---|---|---|---|--|---|---|---|
| <i>Ion</i> | C | H | L | P | S | C | H | L | P | S |
| <i>FT0</i> |  |  |  |  |  |  |  |  |  |  |
| <i>FT5</i> |  |  |  |  |  |  |  |  |  |  |

The turbidimetric measurements are illustrated in Figure 4.11. The visual inspection about the similarity among placebos was confirmed as they resulted in a turbidity of around 1 FNU, except for the C in FT5. In this specific condition, the solution was rather different from all the others, since it gained by FT5 a value around twice higher than the initial one (FT0). Nevertheless, the placebos showed comparable values to that obtained for sucrose solution (Figure 4.8). A substantial gap among protein formulations and the corresponding placebo solution at either FT0 or FT5 conditions was noticed, although C in FT5 was an exception. The turbidity that was measured in protein formulations depended on the employed acid. Similar measurements of around 2.5 FNU at FT0 encompassed S, P, and H, whereas C and L showed a higher turbidity, which ranged from 3.5 FNU to 4 FNU. The first three aforementioned ions caused a similar value of turbidity compared with sucrose formulation (Figure 4.8). FT5 did not cause a significant yield in every protein formulations as C, H, and S kept their turbidity approximately constant throughout the entire process. Nevertheless, a consistent increase was achieved by both L and P in FT5. Their turbidity increased of a few units until it reached a mean value of 6.5 NFU. These results provided lower values than those obtained with sucrose formulation, where the turbidity enhanced to 11 ± 7 FNU

(Figure 4.8). However, the PS80 combining with sucrose kept the lowest value of turbidity regardless of the arginine formulations.

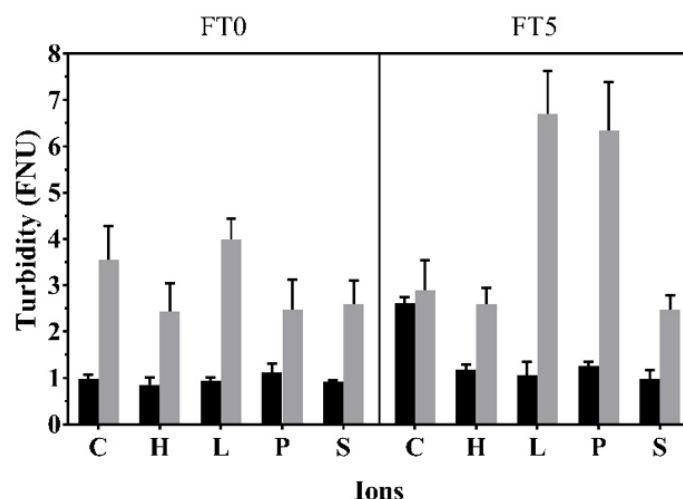


Figure 4.11 Turbidity of (■) placebo, and (■) protein formulations in arginine-based formulations at pH 7 (FT0) before and (FT5) after five freeze-thawing cycles. The investigated acids were (C) citric, (H) hydrochloride, (L) lactobionic, (P) phosphoric and (S) succinic (n = 4, mean ± s.d.).

The particle counting was carried out to confirm turbidimetric results and to provide more details about the protein agglomerates. The total number of particles with a diameter larger than 1 μm (Figure 4.12) resulted in similar conclusions with respect to those obtained from the turbidimetric analysis. In detail, all placebos contained negligible observations, of a just few thousands of particles, if they were compared with the protein formulations. Similar particles number was achieved with sucrose formulations (Figure 4.9). Distinguishable formulations, depending on the using counterion, were measured in the initial condition (FT0). The largest number of particles was counted in formulations containing either L ($31000 \pm 6000 \text{ \#}/\text{ml}$) or C. On the contrary, the other ions approximately showed a number of particles of $15000 \text{ \#}/\text{ml}$, which was half of that obtained from L. Sucrose formulations caused a similar number of particles at the same condition (Figure 4.9). The freeze-thawing processes (FT5) did not significantly enhance the protein observations in arginine-based formulations, except for the P. In this case, the number of particles drastically increased until it reached $70000 \pm 30000 \text{ \#}/\text{ml}$. H and S kept their low values throughout the process and, therefore, they were recognized as the most promising counterions in formulations and they provided significantly better results than sucrose formulation. However, the surfactant confirmed to result in the lowest number of particles (Figure 4.9).

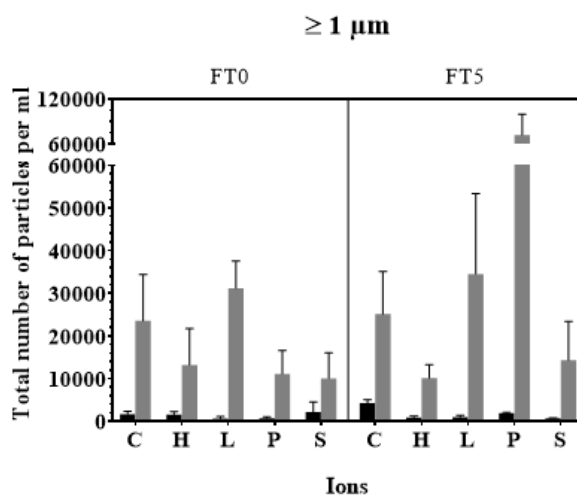


Figure 4.12 Total number of particles per milliliter larger than 1 μm (■) placebo, and (▒) protein formulations in arginine-based formulations at pH 7 (FT0) before and (FT5) after five freeze-thawing cycles. The investigated acids were (C) citric, (H) hydrochloride, (L) lactobionic, (P) phosphoric and (S) succinic (n = 4, mean ± s.d.).

Figure 4.13 illustrates the light obscuration observations for particles larger than 10 μm and 25 μm. The results at 10 μm partially disagrees with the previous experiments. Placebo solutions provided around 100 #/ml particles before the process (FT0), but they yielded approximately one hundred of particles by FT5. Anyway, those values did not contrast with sucrose-based placebos (Figure 4.10). The remarkable difference between placebos and protein arginine-based formulations was now diminished and it was not significant in every pair of formulations, for instance, in products containing either S or H at FT0. Nevertheless, L showed the highest number of particles in FT0, as previously observed, but it drastically increased after the freeze-thawing (FT5), since it resulted in the largest number. On the contrary, P, that was the protein formulation with more particles in Figure 4.12, provided a mild increase, and it exhibits even less particles than S in FT5. S greatly increased its number of particles in FT5 and, therefore, it contrasted with the previous results. On the other hand, H resulted in the lowest number of particles, and it confirmed its trend, which was described before. By the way, all arginine-based formulations showed less particles than sucrose-based one, as shown in Figure 4.10.

The particle counting for a diameter larger than 25 μm showed similar results with respect to the previous diameters. However, the differences between formulations were not significant in most of the cases. Placebos had less particles than protein formulations, but their values increased throughout the process. C and L caused the higher particles numbers in FT0 as it was observed in the previous experiments. Moreover, L drastically increased its value to 59 #/ml, whereas the other acids showed on average of 10 #/ml.

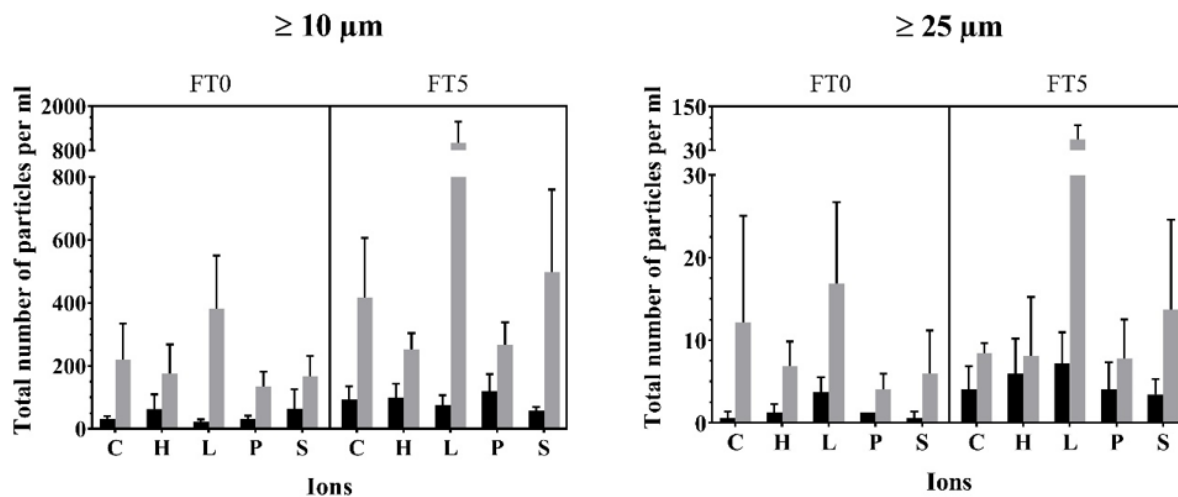


Figure 4.13 Total number of particles per milliliter larger than (l.h.s.) 10 μm and (r.h.s.) 25 μm (■) placebo, and (■) protein formulations in arginine-based formulations at pH 7 (FT0) before and (FT5) after five freeze-thawing cycles. The investigated acids were (C) citric, (H) hydrochloride, (L) lactobionic, (P) phosphoric and (S) succinic ($n = 4$, mean \pm s.d.).

Turbidity and light obscuration carried out distinctive features. Placebos exhibits approximately constant values throughout the freeze-thawing process, whereas protein formulations caused an enhancement of both turbidity and number of particles as in sucrose-based formulations. The response of every experiment changed basing on the arginine counterion. P showed the highest number of particles larger than 1 μm , whereas L overtook it in both particles number larger than 10 μm and 25 μm , although L and P caused comparable turbidities in FT5. The freeze-thawing process did not impact significantly on the turbidity of the other formulations; nevertheless, distinguishable results were obtained, especially in Figure 4.12, where H and S resulted in the lowest number of particles. These results were not completely confirmed in Figure 4.13 as S showed in both measurements a rather high response. Therefore, H was recognized as the most promising counterion in arginine formulation. Moreover, H and S highlighted less turbidity and number of particles than sucrose formulation, however the surfactant combined with sucrose caused the lower results in both turbidity and particles counting.

A statistical analysis was performed in order to confirm the results and to quantify the impact of every factor in the design of experiment. All data were previously transformed with a logarithmic transformation to verify the assumption of the normal distribution. Statistical parameters of the models that were based on the different responses are reported in Table 4.3. The turbidimetric statistical model carried out a satisfactory fitting of the data and rather precise capacity of prediction due to the high value of R^2 and Q^2 . Nevertheless, it was affected by a significant lack-of-fit and probably the data were not suitable for a liner regression model. The statistical parameters changed with the reference diameter in particle counting. The goodness of fitting, the accuracy of the predictions and the reproducibility of the measurements decreased with the particles diameters. Moreover, the absence of lack-of-fit in all models of particles counting suggested to illustrate the most precise and good one as all models were coherent to each other. Therefore, the particle counting for particle larger than 1 μm was shown and described.

Table 4.3 Statistical parameters of models using turbidity and light obscuration responses in arginine-based formulations at pH 7.

| Responses | R ² | Q ² | Lack-of-fit ^a (p-value) | Reproducibility |
|-----------------------|----------------|----------------|---------------------------------------|-----------------|
| Turbidity | 0.853 | 0.801 | <0.001 | 0.909 |
| ≥ 1 μm | 0.894 | 0.839 | 0.053 | 0.883 |
| ≥ 10 μm | 0.781 | 0.652 | 0.572 | 0.725 |
| ≥ 25 μm | 0.671 | 0.485 | 0.198 | 0.607 |
| ^a α = 0.05 | | | | |

The impact of each main factor and their interactions on the response were analyzed and quantified through the effect plot (**Figure 4.14**). The presence of the antibody inside the formulation was recognized as the main cause of particles formation in the observations (PT(mAb)). The interaction between the antibody and the process (PT(mAb)·FT(FT5)) was insignificant and, therefore, it was deleted from the model. Nevertheless, the freeze-thawing cycles impacted with a mild enhancement in the number of particles (FT(FT5)). Both main factors were in accordance with the statistical analysis performed on sucrose-based formulations (Figure 4.7). The kind of acid used in the formulation did not always impact significantly on the response. H and S has a negative significant main effect, whereas L and P had an insignificant and positive impact compared to C. Both interactions of H and S with process and antibody were in antagonism, but S was insignificant in combination with the protein (IO(S)·PT(mAb)). Therefore, H was detected as the most impactful ion with stabilizing abilities. This result was in accordance with the previous descriptions of the light obscuration results (Figure 4.12 and Figure 4.13). On the other hand, P showed the weakest protection, as it exhibited the most synergic effect in combination with the process (IO(P)·FT(FT5)), although L caused a comparable synergy with the protein (IO(S)·PT(mAb)).

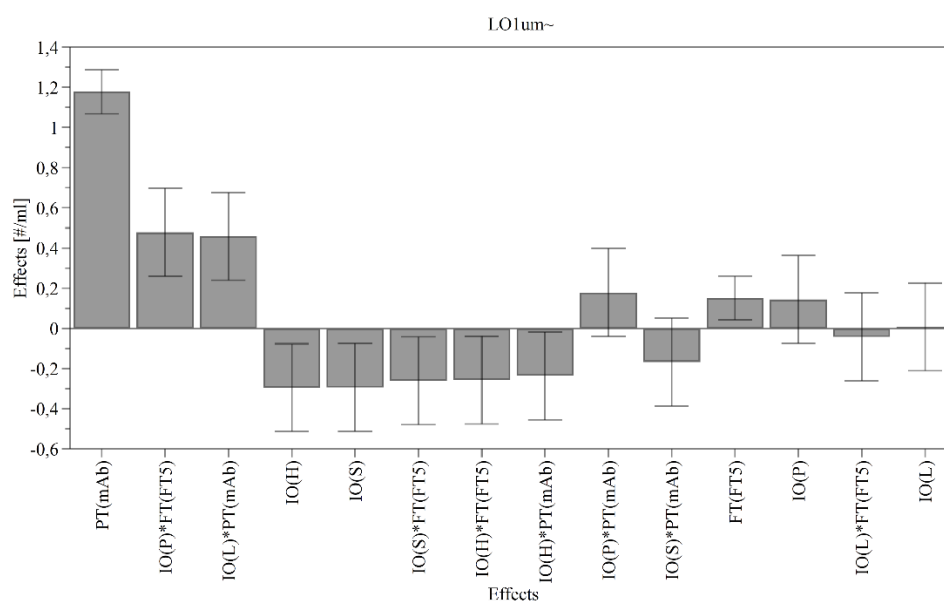













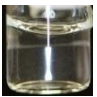




Figure 4.14 Effects plot of transformed total number of particles measurements $\geq 1 \mu\text{m}$ of arginine-based formulations at pH 7.

4.1.4 Protein stability at pH 6 in L-arginine-based formulations at different counterions

The previous investigation about the cryoprotection abilities of different counterions in arginine-based formulations was repeated likewise but at a lower value of pH. The aim was to demonstrate how the solution acidity changed the antibody agglomeration throughout the freeze-thawing process and whether significant differences were obtained, compared with the investigations at higher pH. Moreover, it was highlighted which acid provided the best stabilization abilities, and whether that was in accordance with the previous experiments or not. The experiments in this section were performed at pH 6 for all investigated acids before and after the repeated freeze-thawing process.

The formulations appearances changed, based on the composition of the solutions, although a few visible particles were detected in each sample (Table 4.4). The visual inspections highlighted significant changes in antibody (mAb) formulations throughout the process of freeze-thawing (FT5). A significant increase in visible agglomerates was shown in both phosphate (P) and citrate (C). Anyway, chloride (H), lactobionate (L) and succinate (S) mild changed in appearance with smaller visible particles. On the contrary, the appearance in placebos did not show any increases in particles. Placebo and mAb were not distinguishable in the initial solutions (FT0) due to the comparable appearances. Similar considerations were obtained at the previous pH, although it was not possible to claim which formulations contained the largest number of visible particles by using the visual inspection.

Table 4.4 Visual inspection of L-arginine-based formulations at pH 6. (C) Citric acid, (H) Hydrochloric acid, (L) Lactobionic acid, (P) Phosphoric acid and Succinic acid (S) were used as counterions. Both placebo and (mAb) protein solutions were investigated. All solutions were photographed (FT0) before and (FT5) after 5 freeze-thawing cycles.

| | <i>Placebo</i> | | | | | <i>mAb</i> | | | | |
|------------|---|---|---|---|---|---|--|---|---|---|
| <i>Ion</i> | C | H | L | P | S | C | H | L | P | S |
| <i>FT0</i> |  |  |  |  |  |  |  |  |  |  |
| <i>FT5</i> | n.d. | n.d. |  | n.d. | n.d. |  |  |  |  |  |

n.d. = not detected.

Figure 4.15 illustrates the turbidity results for all the investigated formulations at pH 6. Placebos did not result in remarkable differences through the process, as their turbidities remained approximately constant. Moreover, the kind of acid did not provide any distinguishable peaks in placebo solution, whereas they had approximately the same values, which fluctuated around 1.0 FNU. Similar results were obtained with the previous pH and in sucrose-based formulations (Figure 4.8 and Figure 4.11). All protein formulations resulted into similar turbidity values before the process (FT0), regardless of the used counterions. Anyway, the lowest turbidity was caused by the S with 2.3 ± 0.2 FNU. The previous pH also highlighted indistinguishable initial turbidities of around 2.5 FNU in all protein formulations, except for L and P (Figure 4.11). The repeated cycles of freeze-thawing (FT5) caused a significant increase in turbidity for C, H, and especially in P. P provided the largest increase as it moved from 2.9 ± 0.4 FNU to 5.5 ± 0.3 FNU, which was almost twice the value it had at the beginning. On the other hand, S and L were not significantly changed during the process and the value of S even decreased compared to the previous observations in FT0. L protein turbidity was in contrast with the measurement performed at pH 7 (Figure 4.11) as it did

not significantly increase by FT5 but it remained with a turbidity of 3.1 ± 0.9 FNU. On the other hand, C rather increased until 3.8 ± 0.5 FNU by FT5 and, therefore, it differed from the previous pH at the same conditions, where lower turbidity was observed (2.9 ± 0.7 FNU). Similar trends were observed for all the other ions. The comparison between pH evidenced a possible decrease of turbidity at pH 6 in all ions.

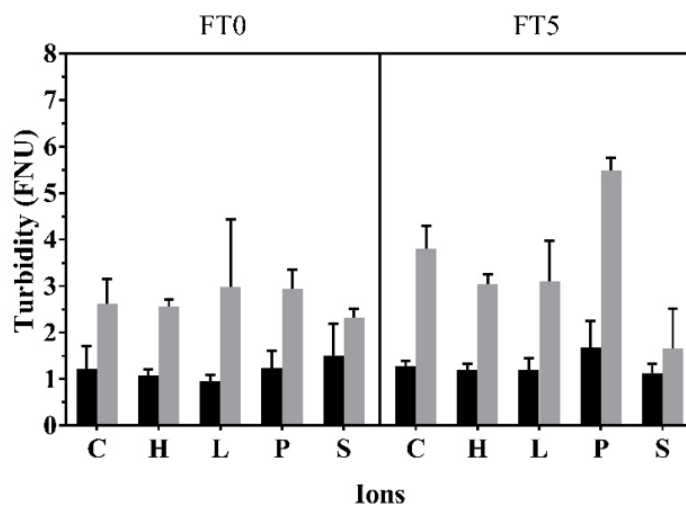


Figure 4.15 Turbidity of (■) placebo, and (▒) protein formulations in arginine-based formulations at pH 6 (FT0) before and (FT5) after five freeze-thawing cycles. The investigated acids were (C) citric, (H) hydrochloride, (L) lactobionic, (P) phosphoric and (S) succinic ($n = 4$ or 3 , mean \pm s.d.).

The turbidimetric evidences were compared with light obscuration observations. Figure 4.16 illustrates the total number of particles with a diameter larger than $1 \mu\text{m}$. Every placebo provided only a few thousands of particles ($< 5000 \text{ \#/ml}$) and their values did not depend on the process. This result was in accordance with pH 7 and sucrose-based formulations (Figure 4.12 and Figure 4.9). However, P highlighted a significant increase in placebo and, therefore the number of particles yielded by FT5 was more than twice the one in the beginning ($4700 \pm 3000 \text{ \#/ml}$). Anyway, the turbidity observations did not highlight this enhancement in P, whereas they were comparable to the previous considerations. On the contrary, some protein formulations encompass C, H and P were greatly affected by the process, since the larger number of particles in FT5 compared to FT0. Nevertheless, both S and L provided the lowest number of particles in protein solutions after the freeze-thawing process (FT5). P caused the largest change as it passed from $12000 \pm 4000 \text{ \#/ml}$ to $77000 \pm 7000 \text{ \#/ml}$, whereas C and H had approximately the same values of 40000 \#/ml . Those evidences were comparable to the turbidimetric ones, although the turbidity of L was similar to H and C. Both S and L proved to have less particles than sucrose in protein formulations after 5 freeze-thawing cycles. The number of particles in the initial condition (FT0) were mildly decreased compared to the formulations at pH 7, especially C was halved the previous value (Figure 4.12). However, both results at FT5 were rather different as H drastically increased by the process in Figure 4.16 but it approximately kept a constant value throughout the freeze-thawing cycles at pH 7. Moreover, L significantly decreased its number of particles towards more acidic formulations, although S resulted into a small number of particles and P was observed being above 70000 \#/ml particles at the both pH values.

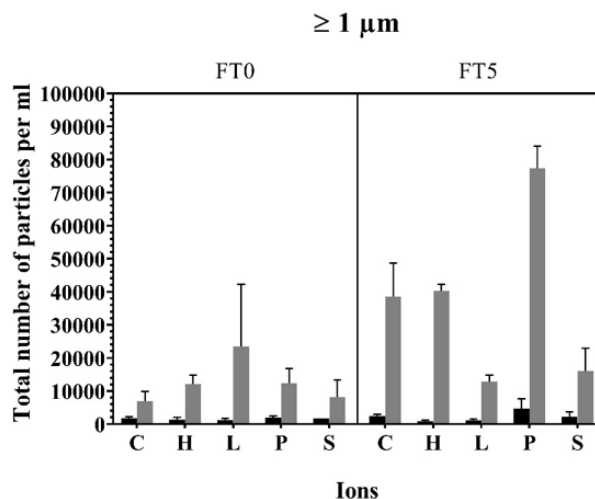


Figure 4.16 Total number of particles per milliliter larger than 1 μm (■) placebo, and (▒) protein formulations in arginine-based formulations at pH 6 (FT0) before and (FT5) after five freeze-thawing cycles. The investigated acids were (C) citric, (H) hydrochloride, (L) lactobionic, (P) phosphoric and (S) succinic (n = 4 or 3, mean ± s.d.).

The total number of particles larger than 10 μm and 25 μm give different results from the previous diameter and turbidity (Figure 4.17). Placebo and protein formulations were easily distinguished in the 10 μm diagram. The number of particles in placebo solutions was approximately constant throughout the process (150 #/ml), and only P yielded particles by FT5. This was analogous to Figure 4.16, where significant differences were only obtained for protein formulations. Similar results were showed at pH 7 for all placebos (Figure 4.13). Not significant differences among counterions were observed in FT0, although L and S had the lowest mean values. Significant increases caused by the process (FT5) were detected in C, P, and S, whereas both H and L kept their values constant (400 #/ml). This partially disagrees with 1 μm particles as H caused an important production of agglomerates, whereas the lowest number of particles were observed in S protein formulation. The number of particles in protein formulations at pH 7 were approximately smaller than the one obtained from pH 6 at the same condition, except for L (Figure 4.13). Thus, L drastically reduced its value from 1000 ± 600 #/ml to 300 ± 100 #/ml.

Placebo solutions caused less particles with a diameter ≥ 25 μm than the protein one (Figure 4.17). Anyway, the differences were not rather clear, especially in FT0. Moreover, P placebo solution in FT5 produced more particles than the protein one. L produced the lowest number of particles in FT5, anyway its value was comparable to H and S. Anyway, similar results were observed at pH 7 (Figure 4.13).

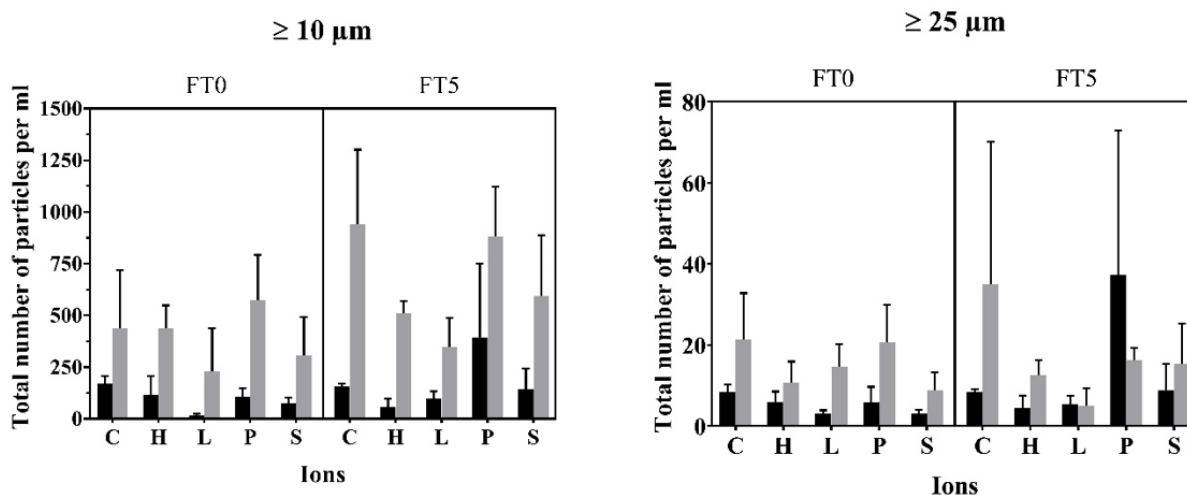


Figure 4.17 Total number of particles per milliliter larger than (l.h.s.) 10 μm and (r.h.s.) 25 μm (■) placebo, and (▒) protein formulations in arginine-based formulations at pH 6 (FT0) before and (FT5) after five freeze-thawing cycles. The investigated acids were (C) citric, (H) hydrochloride, (L) lactobionic, (P) phosphoric and (S) succinic (n=4/3, mean \pm s.d.).

The statistical analysis was performed to quantify the qualitative results, which were previously reported. In order to satisfy the normal distribution assumption, all measurements were transformed with a logarithmic transformation. Afterwards, the normal probability plot was checked, and possible outliers were excluded from the evaluation. A full interactions model was analyzed for all responses. Table 4.5 illustrates the four statistical parameters that allowed to quantify the adequacy of each model. The turbidity response made a quite good and valid model, due to the high R^2 and the absence of lack-of-fit (p-value greater than $\alpha = 0.05$). However, its reproducibility and precision of predictions were lower than both values evaluated in light obscuration at 1 μm . All parameters (R^2 , Q^2 , lack-of-fit, and reproducibility) of light obscurations responses decreased with larger diameters and, therefore, it was considered only the most precise and valid model. Similar trend was obtained in Table 4.4 for the previous analysis at pH 7. The particle counting in diameter larger than 1 μm provided the best predictions ($Q^2 = 0.887$) and fitting with data ($R^2 = 0.934$), and an extremely reproducible model with absence of lack-of-fit.

Table 4.5 Statistical parameters of models using turbidity and light obscuration responses in arginine-based formulations at pH 6.

| Responses | R^2 | Q^2 | Lack-of-fit ^a (p-value) | Reproducibility |
|---|-------|-------|---------------------------------------|-----------------|
| Turbidity | 0.837 | 0.734 | 0.372 | 0.798 |
| $\geq 1 \mu\text{m}$ | 0.934 | 0.887 | 0.199 | 0.918 |
| $\geq 10 \mu\text{m}$ | 0.828 | 0.696 | 0.057 | 0.794 |
| $\geq 25 \mu\text{m}$ | 0.531 | 0.223 | 0.037 | 0.470 |
| ^a $\alpha = 0.05$ | | | | |

The effects plot of transformed number of particles larger than 1 μm (Figure 4.18) showed several insignificant main effects and interactions. The presence of antibody (PT(mAb) = 0.99 ± 0.09 #/ml) in formulation was the most significant cause of particles. That result was in accordance with the

previous analysis that was performed at pH 7 and sucrose-based formulations (Figure 4.14 and Figure 4.7) for sucrose solutions, where the antibody was the most impactful effect. Moreover, it was confirmed that the repeated freeze-thawing cycles (FT(FT5) = 0.26 ± 0.09 #/ml) increased significantly the number of particles. On the other hand, the synergic interaction between the process and the antibody (FT(FT5)·PT(mAb)) was statistically significant, whereas according to both previous investigations it was insignificant. The change of acid in formulations showed different results, depending on the kind of arginine counterion. P, compared to C, caused more particles formation in both placebo and protein formulations due to its positive main effect; moreover, the synergic interaction with FT(FT5) was another significative cause of yield in particles number. On the contrary, both H and S had an insignificant main effects and interaction with FT(FT5), but H caused a synergic interaction with the PT(mAb). Therefore, significative differences between C and H were only detected in protein formulations (IO(H)·PT(mAb) = 0.3 ± 0.2 #/ml). Moreover, S was in antagonism with the protein (IO(S)·PT(mAb) = -0.2 ± 0.2 #/ml) and, therefore, it decreased the number of particles in protein formulations compared to C. A negative main effect and interaction with FT(FT5) was observed with the L counterion. Both negative effects suggested a smaller number of particles in L formulations compared to C, especially after the process.

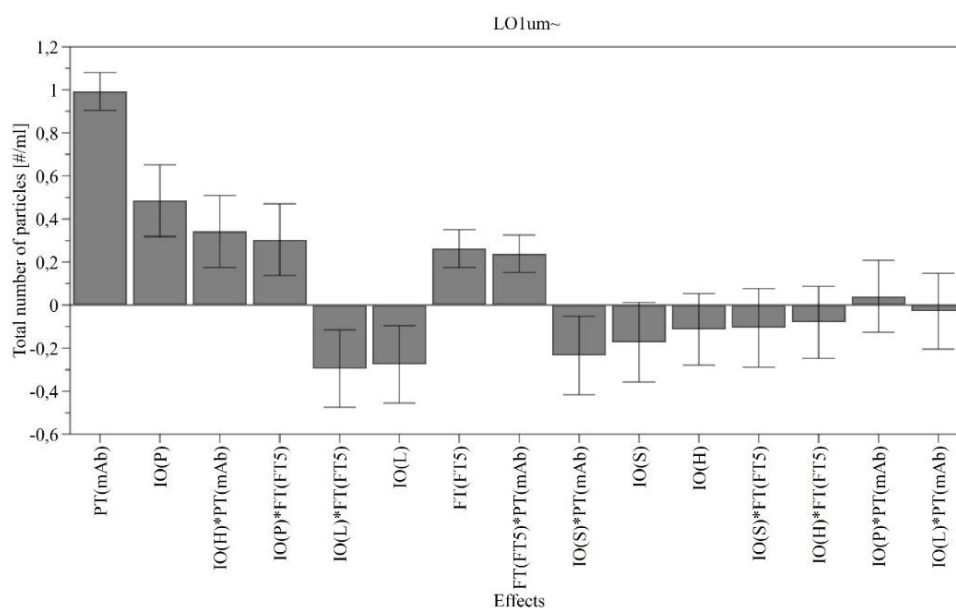


Figure 4.18 Effects plot of transformed total number of particles measurements $\geq 1 \mu\text{m}$ of arginine-based formulations at pH 6.

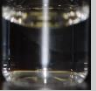


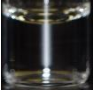

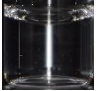






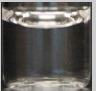
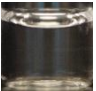
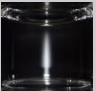





The protein and the process were thus the two main causes of yield in particle numbers, in accordance with the previous analysis. Different counterions impacted in diverse ways on the response. P impacted similarly in both pH due to its synergic interaction with the process, although the main effect was insignificant at pH 7. On the contrary, both significant antagonist interaction and main effect of L at pH 6 were completely in contrast with the previous pH, where the only one significant effect was in synergy. H highlighted different behaviors depending on the pH also, since its synergic interaction with the protein at pH 6 was in contrast with the negative effects at pH 7. Nevertheless, S carried out antagonist interactions and main effects for both pHs. In conclusion, the most relevant benefits at pH 7 were gained by using H, whereas L was proved being the best choice at pH 6 due to its two negative effects. Anyway, S was not deeply influenced by the pH changes and it could be also a possible choice.

4.1.5 Protein stability at pH 5 in L-arginine-based formulations at different counterions

It was previously proved a mild dependence of protein agglomeration on the pH. The following experiments was aimed to investigate whether a further enhance in solution acidity provided an advantage or not against protein stabilization throughout the repeated freeze-thawing cycles. In the previous sections some contradictory results were highlighted in both L and H ions. Therefore, the aim was either to confirm the previous conclusions or identify a different likely cryoprotectant for the lowest pH. In this section the acidity of the solutions was fixed by titrating the formulations until pH 5, and the investigation consisted on observations before and after the five freeze-thawing cycles.

All solutions appearances changed throughout the process depending on their compositions (Table 4.6), although a few visible particles were always observed in every sample. The visual inspections showed significant changes in formulations containing either citrate (C) or phosphate (P) as counterions. Comparable results were obtained at the previous pHs. The freeze-thawing cycles especially changed the appearances of protein solutions. On the other hand, succinic acid (S) and hydrochloric acid (H) did not show any change during the process; moreover, it was not possible to distinguish protein formulations from the placebo one. A mild increase of visible particles in lactobionic acid (L) formulations was caused by the process.

Table 4.6 Visual inspection of L-arginine-based formulations at pH 5. (C) Citric acid, (H) Hydrochloric acid, (L) Lactobionic acid, (P) Phosphoric acid and Succinic acid (S) were used as counterions. Both placebo and (mAb) protein solutions were investigated. All solutions were photographed (FT0) before and (FT5) after 5 freeze-thawing cycles.

| | <i>Placebo</i> | | | | | <i>mAb</i> | | | | |
|------------|---|---|---|---|---|---|--|---|---|---|
| <i>Ion</i> | C | H | L | P | S | C | H | L | P | S |
| <i>FT0</i> |  |  |  |  |  |  |  |  |  |  |
| <i>FT5</i> |  |  |  |  |  |  |  |  |  |  |

The turbidimetric measurements highlighted rather similar features with respect to the previous pHs (Figure 4.19). Placebo and antibody formulations were easily distinguishable in both initial solutions (FT0) and after the repeated freeze-thawing cycles (FT5). All placebo solutions showed an approximately constant value of 1.0 NFU, and FT5 did not cause any increase. This behavior was similar to that obtained at pH 6 and 7, where the turbidity of those placebo solutions fluctuated around the same value (Figure 4.15). On the contrary, all protein formulations showed a higher turbidity in FT0 compared with both pHs. The P, and C caused significant higher values than other counterions, whereas S, L, and H gave comparable results. FT5 emphasized the gap between placebos and protein formulations and all of them increased their turbidity, although significative increases were just obtained with P and C. For instance, P grown up from 6 ± 1 NFU to 14 ± 1 NFU. This evidence was in accordance to the previous investigation, where P and C showed the most turbid protein formulations at FT5 (Figure 4.15). Similar turbidities were obtained for H and L, whereas the S provided the lowest value (3.4 ± 0.6 NFU). Nevertheless, every protein formulation at pH 5 was more turbid than pH 6 in FT5 conditions. This evidenced that the pH was probably an important variable in protein stabilization, due to the wide range of results obtained across different pHs.

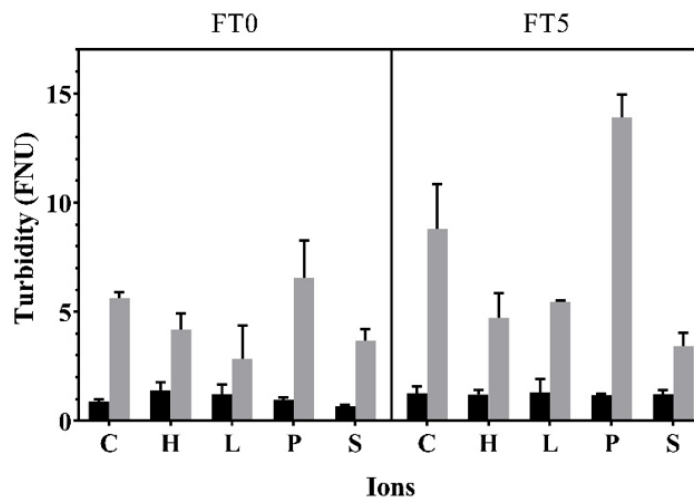


Figure 4.19 Turbidity of (■) placebo, and (▒) protein formulations in arginine-based formulations at pH 5 (FT0) before and (FT5) after five freeze-thawing cycles. The investigated acids were (C) citric, (H) hydrochloride, (L) lactobionic, (P) phosphoric and (S) succinic (n=4, mean \pm s.d.).

Figure 4.20 confirmed the turbidimetric evidences. The total number of particle larger than $1 \mu\text{m}$ was drastically higher in protein formulations than in placebo solutions. In all placebos, FT5 was not a cause of particles increase. The solutions approximately showed the same value of a few thousands of particles. Moreover, a significant gap with protein formulations was noticed. These evidences were in accordance with Figure 4.19, and even more remarkable than before. Similar results for placebos were obtained in the previous investigations (Figure 4.12 and Figure 4.16). On the other hand, all acids provided similar number of particles during FT0 and, therefore, P and C did not differ from other ions. The number of particles at pH 5 at FT0 was mildly higher than with the previous pHs. Nevertheless, S caused the lowest observation ($20000 \pm 2000 \text{ \#/ml}$), although it remained twice the values that was measured before. The freeze-thawing cycles (FT5) caused an increase in all protein formulations, especially in P. It drastically rose up its particles number and it reached $1.2 \cdot 10^6 \pm 1 \cdot 10^5 \text{ \#/ml}$ particles. Nevertheless, C formulation yielded approximately three times the number of particles that was observed in the FT0 ($105000 \pm 11000 \text{ \#/ml}$), whereas both H and L showed approximately 50000 \#/ml . Anyway, S still provided the lowest number of particles, although it grown up to $38000 \pm 8000 \text{ \#/ml}$ in FT5. Comparable trends were obtained through the turbidimetric measurements (Figure 4.19), but some differences were observed with respect to the previous pHs. After the process (FT5), protein formulations of C and H at pH 6 showed similar number of particles of 40000 \#/ml (Figure 4.16). However, the same formulations at pH 5 were rather different, although both formulations provided more particles than the past experiment. C drastically increased, more than H at the lowest pH. Furthermore, L was comparable to S at pH 6, whereas it was higher and similar to H at pH 5. Anyway, in both experiments of turbidity and particle counting S caused the lowest observation.

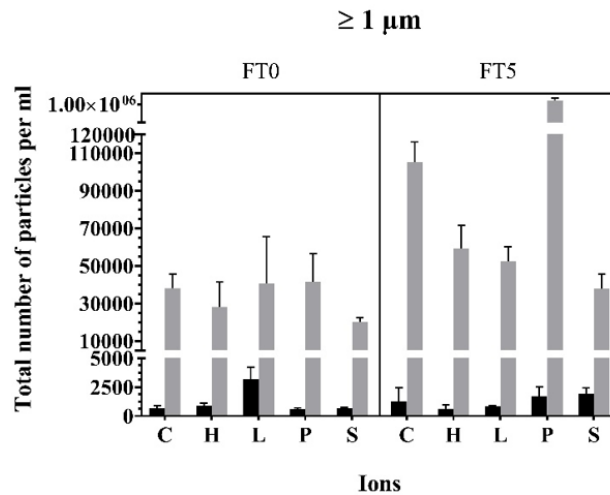


Figure 4.20 Total number of particles per milliliter larger than 1 μm (■) placebo, and (▒) protein formulations in arginine-based formulations at pH 5 (FT0) before and (FT5) after five freeze-thawing cycles. The investigated acids were (C) citric, (H) hydrochloride, (L) lactobionic, (P) phosphoric and (S) succinic ($n=4$, mean \pm s.d.).

The total number of particles larger than 10 μm gave similar consideration than before, although all differences were less remarkable (Figure 4.21). For instance, L protein formulation after the process was relatively high and it contrasted with Figure 4.20, where its value was significantly lower than C. Nevertheless, P provided the largest number of particles in FT5, and C caused the second highest particles number below P. Protein solution in the initial condition (FT0) were indistinguishable to each other; however, it was confirmed the lowest observation of S in FT5 400 ± 200 #/ml. That value was comparable to that shown in Figure 4.17 at the same conditions. On the contrary, all the other ions yielded clearly their observations in FT5 at the lower pH. Anyway, differences between placebos and protein formulations were quite significant. Moreover, the placebo solutions were not modified throughout the process.

Similar differences between protein and placebo were detected with the light obscuration of particles larger than 25 μm (Figure 4.21), although the number of particles was afflicted by large standard deviations in protein formulations. P significantly highlighted the highest number of particles in FT5, whereas S caused the smallest measurements. The results were rather similar to the pH 7 (Figure 4.17), although the observations rather increased by decreasing the pH.

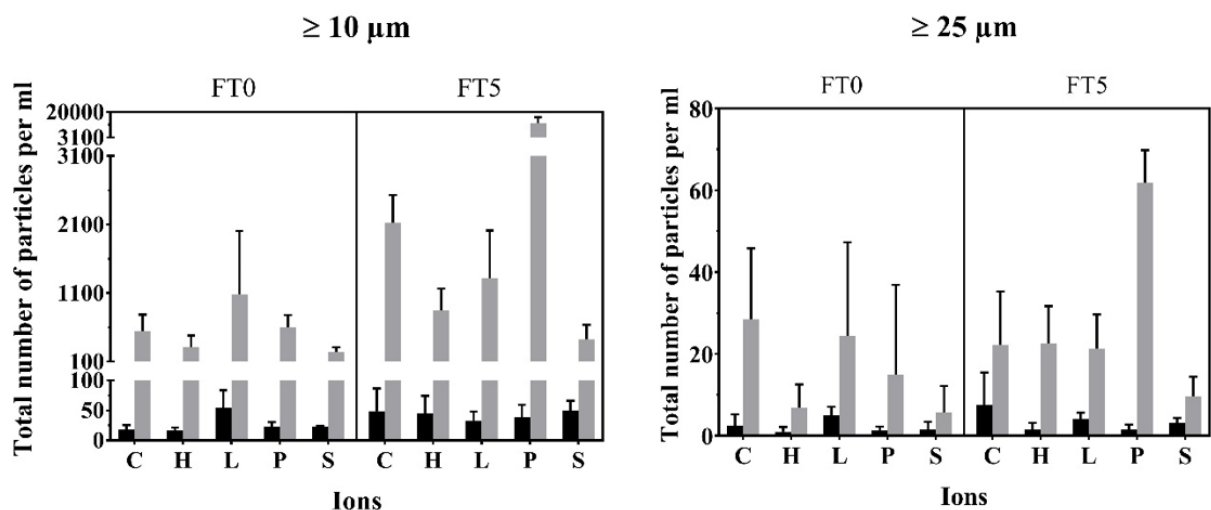


Figure 4.21 Total number of particles per milliliter larger than (l.h.s.) 10 μm and (r.h.s.) 25 μm (■) placebo, and (■) protein formulations in arginine-based formulations at pH 5 (FT0) before and (FT5) after five freeze-thawing cycles. The investigated acids were (C) citric, (H) hydrochloride, (L) lactobionic, (P) phosphoric and (S) succinic ($n=4/3$, mean \pm s.d.).

The ANOVA statistical analysis was carried out to quantify more accurately the results. The data were transformed with a logarithmic transformation to get the normal distribution. The Table 4.7 showed the computed statistical parameters necessary to evaluate the goodness of each statistical analysis. It was not possible to avoid the model lack-of-fit in every experiment, although the models were highly precise and reproducible due to the closeness of R^2 and Q^2 to 1 in turbidity and particle counting up to 10 μm . The lack-of-fit was probably caused by the inadequacy of the statistical model (LRM) to fit the data. Therefore, the statistical analysis was neither completed nor described.

Table 4.7 Statistical parameters of models using turbidity and light obscuration responses in arginine-based formulations at pH 5.

| Responses | R^2 | Q^2 | Lack-of-fit ^a (p-value) | Reproducibility |
|--------------------------------------|-------|-------|---------------------------------------|-----------------|
| Turbidity | 0.909 | 0.877 | 0.002 | 0.922 |
| ≥ 1 μm | 0.967 | 0.947 | <0.001 | 0.972 |
| ≥ 10 μm | 0.927 | 0.884 | 0.012 | 0.922 |
| ≥ 25 μm | 0.669 | 0.483 | 0.095 | 0.624 |
| ^a $\alpha = 0.05$ | | | | |

It was proved that protein agglomeration was enhanced by the lower pH of the formulations, due to the qualitatively higher results that were obtained through turbidimetric and particle counting up to 10 μm . Protein formulations containing either C or P were especially susceptible to the acidic shift and they especially enhanced their turbidity and number of particles. On the contrary, S carried out the lowest responses in both measurements, but its results remained significantly high compared to the previous pH.

4.2 Lyophilization of L-arginine-based formulations and investigation on lyoprotection abilities

Physical and chemical requirements must be satisfied in lyophilized biopharmaceuticals. The cryoprotection abilities of the formulations is necessary to obtain stable products and to avoid protein denaturation throughout the process, although other characteristics are necessary to produce suitable formulations for lyophilization. For instance, a formulation must have an enough high T_g to avoid the cake collapse during the drying step in order to provide an elegance cake appearance with the absence of breakages and major defects. Elegant cakes are necessary to minimize the residual moisture inside the products, which enhances protein denaturation reactions in the dried state and decreases the T_g . A relatively high T_g is wished to keep intact the glassy state inside the product during long-term storage and, possibly, to increase the storage temperature. Moreover, a nice cake appearance generally provides shorter reconstitution time than a collapsed one. The drying stresses occur afterwards the freezing step and, as it was previously described, the stabilizations mechanism differs from the freezing one; therefore, suitable cryoprotectants are not consequentially good lyoprotectants.

The aim of the section was to investigate whether the previously analyzed arginine formulations were actually suitable for lyophilization or not. A test cycle of lyophilization (Figure 4.22) was proposed and used on all formulations. Afterwards, the physical characteristics, namely residual moisture, glass transition temperature, and reconstitution time of the lyophilized cakes, were measured. Moreover, the x-ray diffraction was used to highlight possible crystalline states, which were identified by the modulated DSC. Turbidity and particle counting were performed on reconstituted formulations to investigate how the lyoprotection changes by different acids and whether the results were comparable or not with the freeze-thawed one.

The cycle of lyophilization was performed over 68 hours (Figure 4.22). After the freezing step the temperature was kept at -50°C for 90 minutes, then the vacuum was produced in the chamber. Unfortunately, the pressure did not reach easily the setpoint due to a short block of the vacuum system, and the products remained at the minimum temperature for 20 minutes more. The low temperature of -50°C prevented any possible degradations processes. During the primary drying the imposed shelf temperature was imposed at -20°C , whereas the monitored temperature increased since it overtook the shelf temperature. This unusual behavior was probably caused by the radiations on the products from outside. Anyway, secondary drying was performed correctly to reduce the residual moisture inside the cake.

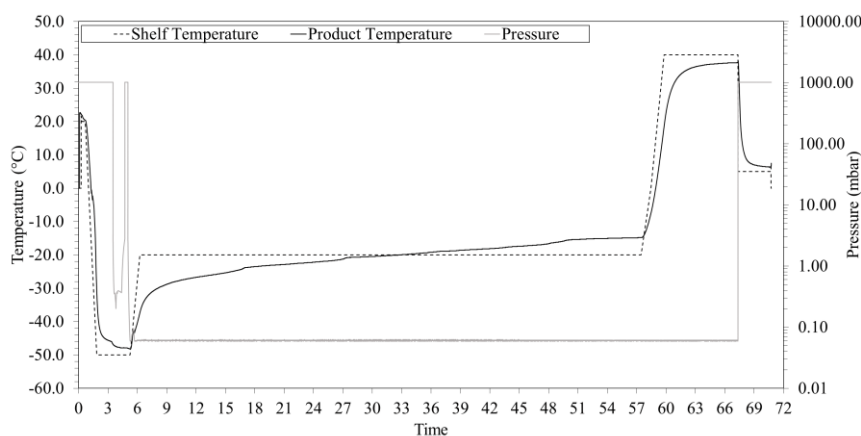
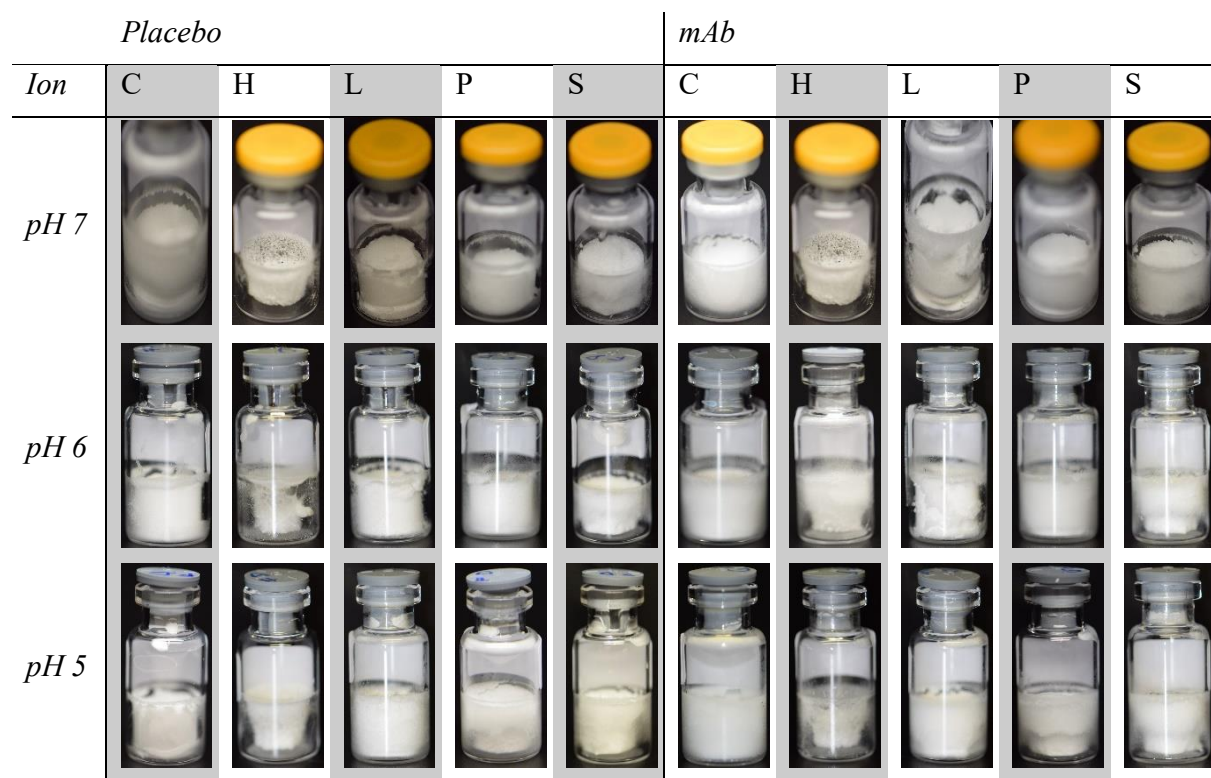


Figure 4.22 Freeze-drying cycle diagram. In the primary drying the shelf temperature was set at -20°C , whereas during the secondary drying was $+40^{\circ}\text{C}$. The chamber pressure under the process was 0.06 mbar. The temperature was monitored by three thermocouples, the average value was reported in the figure.

4.2.1 Physical characteristics of lyophilized arginine formulations

All physical characteristics of the lyophilized cakes were analyzed in this section in order to prove whether the formulations were suitable for the process or not. All formulations were processed with the same freeze-drying cycle and the results were compared to each other. First of all, an accurate inspection of the cakes was performed in order to detect either collapsed products or minor defects in cakes. The modulated DSC measured the T_g of the powders and the presence of possible crystalline states. Moreover, the residual moisture was obtained by the Karl Fisher titration and the reconstitution time was timed until all visible particles were solubilized. Higher residual moisture and lower T_g were expected in collapsed cakes than in elegant ones, although significance differences could be observed in all formulations. It was investigated which ions provided the most elegant structures and whether the change in pH impacted on the cakes characteristics or not. Table 4.8 illustrates the visual inspection for all lyophilized cakes composed by arginine-based formulations. Some cakes collapsed during the process, and probably their product temperature reached and trespassed the T_g ' of the formulation. On the other hand, other products provided elegant cakes, although a persisted shrinkage was observed. The shrinkage is a loss in volume of the product, which pulls away the cake from the vial walls. This defect is not directly associated with collapse, although it could be its first manifestation of that [9]. Approximately every vial showed a lyophilized ring around the neck of the container, which was probably caused by a remaining amount of solution on the vial walls during the loading operations [9], such as pipetting fails. These minor defects were considered acceptable [9]. Placebo did not differ significantly from protein cakes and they were affected by similar defects, although protein citrate (C) cakes were visibly more compact than placebo, especially at pH 5. Moreover, C provided a uniformed texture of the structures, especially in protein formulations. The pH caused relevant differences in both phosphate (P) formulations at pH 5 as a begin of collapse from the bottom of the vial was observed, whereas at pH 7 the cakes were uniform, with elegant appearances. On the contrary, in formulations containing lactobionic acid (L) it was observed a more uniform structure in placebo than protein cakes. A possible onset of collapse was detected in L protein formulation at pH 5 and 6, whereas at pH 7 a few major breakages appeared. Both succinate (S) formulations did not change their appearance with respect to the pH, but they showed a partially collapsed cake, especially at the bottom of the vials; moreover, protein and placebo cakes were indistinguishable to each other. Similar behavior with pH was detected for chloride (H), although a completely collapsed cake was observed for every formulation due to the presence of a fine-grained texture of the cakes instead of a uniform, and consistent structure of the products.

Table 4.8 Visual inspection of lyophilized cakes of L-arginine-based formulations at pH 5, 6, and 7. (C) Citric acid, (H) Hydrochloric acid, (L) Lactobionic acid, (P) Phosphoric acid and Succinic acid (S) were used as counterions. Both placebo and (mAb) protein solutions were investigated.



It was expected a decrease in T_g , and an enhancement in residual moisture, as a consequence of the cake collapse, especially in H, S and a mild influence in L. The collapsed cakes cause more resistance to the vapor flow and, therefore, a higher residual moisture remains inside the structure. A higher percentage of moisture caused also a drop in T_g . As consequence, a long term-storage has to be performed at lower temperatures to avoid an excessive molecular mobility. The residual moisture (RM) was measured by Karl-Fisher titration. The results are shown in Figure 4.23 and Figure 4.24. Previous papers proved a dependence of the residual moisture on the arginine concentration and on the used counterion [19,23,24]. A typical value for arginine-based formulations varied around a few units, although it typically stayed below 3.5% [19].

The placebos showed a wide range of RM depending on both pH and employed acid (Figure 4.23). Generally, the RM increased with lower acidity, but significant enhancements were observed only in some formulations. The fully collapsed cakes of H provided the highest RM, with a value of around 3% at pH 5 and 6 as it was previously expected, although it decreased to $2.1 \pm 0.1\%$ at pH 7. This result especially contrasted with the other partially collapsed cakes, which contained S and significantly increased their RM with the higher pH, since they reached $3.3 \pm 0.5\%$ at pH 7. Anyway, both C and P kept their values of RM approximately constant with pH 5 and 6, whereas a significant increase was observed at pH 7. Those results mildly contrasted with the cakes appearances, because it was expected a higher value of RM at the highest acidity due to the onset of collapse that was observed in the pictures. Nevertheless, L appearances were in accordance with the RM and the lowest value was provided at pH 5. The not collapsed cakes encompassed C, L, and P caused on average a RM equal to 1.5%.

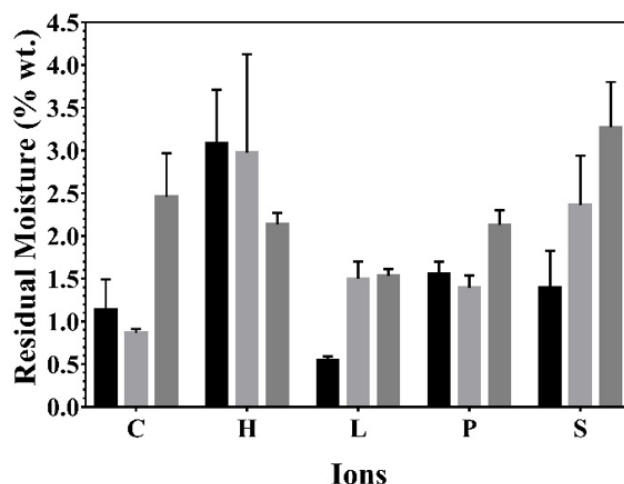


Figure 4.23 Residual moisture in placebo lyophilized cakes of L-arginine-based formulations at (■) pH 5, (▒) pH 6, and (░) pH 7. The investigated acids were (C) citric, (H) hydrochloride, (L) lactobionic, (P) phosphoric and (S) succinic (n = 3, mean ± s.d.).

The protein cakes usually yielded a lower RM than placebos (Figure 4.24), but this difference was apparently not relevant. Contrarily, S protein products was mildly lower than the first placebo at the same pH. On the other hand, H decreased its value to an average of 2.3%, which was lower than in Figure 4.23. Protein formulations containing either P or C caused an increase in RM with higher pH. Anyway, C highlighted on average the lowest value of RM (1%), whereas P was similar to L. The elegance appearances of C protein formulations were in accordance with the RM results, but it was expected a decreased of RM for P formulations due to the more elegant cakes obtained at higher pH. The pH increased the RM of L formulations as well, although it highlighted a peak of $1.7 \pm 0.5\%$ at pH 6.

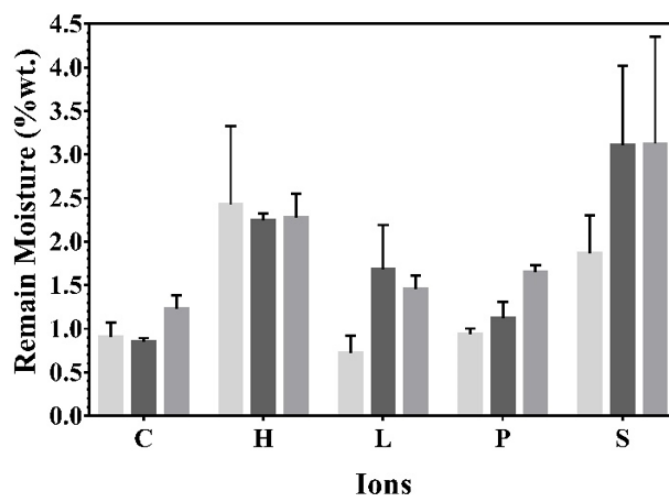


Figure 4.24 Residual moisture in protein lyophilized cakes of L-arginine-based formulations at (░) pH 5, (■) pH 6, and (▒) pH 7. The investigated acids were (C) citric, (H) hydrochloride, (L) lactobionic, (P) phosphoric and (S) succinic (n = 3, mean ± s.d.).

Every lyophilized cake was characterized by T_g , which was composition dependent and, therefore it depended on the pH, and on the employed counterion. Moreover, a lower value it will carried out

from collapsed products. The Figure 4.25, and Figure 4.26 illustrated how the T_g changed in both placebos and protein formulations containing arginine and different counterions.

Significant differences between collapsed and elegant cakes were easily recognized in Figure 4.25, as both collapsed H and S highlighted lower values of T_g compared with the other ions, although P at pH 5 ($66.3 \pm 0.9^\circ\text{C}$) was similar to S. Anyway, some species of placebos significantly differed by changing the pH, whereas H kept its T_g approximately constant on the average of 46°C . On opposite, S ranged between $62 \pm 3^\circ\text{C}$ and $72 \pm 9^\circ\text{C}$, but its changes were not enough distinguishable to each other. Moreover, it was observed the persistent presence of a recrystallization peak on the modulated DSC thermograph (figures not shown) for both collapsed ions and, therefore, possible crystalline structures could be established in the products. Nevertheless, this contrasted with the other ions, which were completely amorphous. The results were in accordance with the expectations, as the collapsed cakes resulted, on average, in the highest value of RM (Figure 4.23), whereas their T_g was significantly decreased. On the other hand, the highest value of T_g was produced by C at pH 6 ($106.91 \pm 0.06^\circ\text{C}$), whereas all the other not collapsed cakes showed similar values, which were around 90°C , except for both L ($100 \pm 2^\circ\text{C}$) and P at pH 5. Moreover, it was observed that both peaks in T_g for C and L occurred with the lowest value of RM. This confirmed the reversed correlation between the two measurements, although in P formulations a mild increase of RM caused a significant enhancement in T_g .

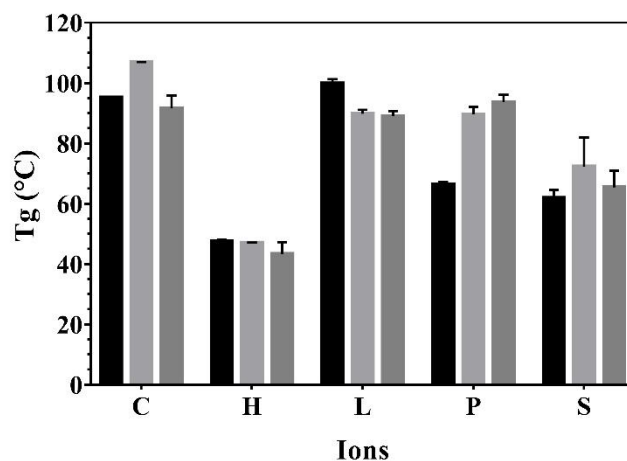


Figure 4.25 Glass transition temperature in placebo lyophilized cakes of L-arginine-based formulations at (■) pH 5, (■) pH 6, and (■) pH 7. The investigated acids were (C) citric, (H) hydrochloride, (L) lactobionic, (P) phosphoric and (S) succinic ($n = 3$ or 2 , mean \pm s.d.).

The protein formulations showed similar trends for T_g (Figure 4.26), but with higher values compared with the placebos one (Figure 4.25); therefore, they were in accordance with the expected and previously described correlation between the T_g and the RM. Both collapsed formulations of H and S highlighted significant lower T_g than in presence of the elegant cakes. For instance, H varied from $58 \pm 1^\circ\text{C}$ to $51.0 \pm 0.2^\circ\text{C}$ with the increase of pH and, therefore it was significantly higher than the placebos average (46°C). Nevertheless, this contrasted with S, which showed similar and even mild lower T_g in protein formulations than the placebo. The increase of T_g in H protein formulations was correlated with a decrease of RM (Figure 4.24). On the other hand, the lower value of T_g in S protein products than placebo was supported by a higher concentration of RM. The modulated DSC thermographs of both ions illustrated a recrystallization peak as it was observed for placebo formulations. Further investigations with x-rays diffraction were therefore provided in order to confirm whether the presence of a crystalline structure affected the products or not (Figure 4.27). The elegant cakes containing either C, L, or P produced an extremely high T_g as it was

observed with the previous placebos (Figure 4.25), although their values were partially higher than before. The increase caused by the antibody depended on the formulations and also on both pH and acid. It was proved that the antibody usually decreased the RM in protein formulation meanwhile it enhanced the T_g .

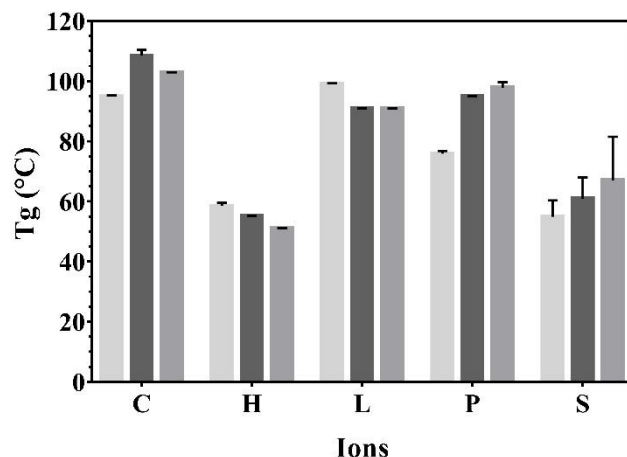


Figure 4.26 Glass transition temperature in protein lyophilized cakes of L-arginine-based formulations at (□) pH 5, (■) pH 6, and (▒) pH 7. The investigated acids were (C) citric, (H) hydrochloride, (L) lactobionic, (P) phosphoric and (S) succinic ($n = 3$ or 2 , mean \pm s.d.).

The possible crystalline structures of the collapsed cakes containing either S or H required a confirmation by using the x-rays diffraction. The experiment was performed for each investigated ion at pH 7, but it was not repeated at every pH. The results are shown in Figure 4.27. Any clear pattern was not highlighted in the diffractogram; therefore, it was proved the complete absence of crystalline structure inside all samples. Anyway, this contrasted with the previous measurements on the modulated DSC, where it was observed a recrystallization peak on the thermographs, with the S and H formulations. The pH did not impact on the results as every sample showed a similar peak. It can be supposed that the crystallization process was due to temperatures higher than ambient temperature or a prolonged time in contact with wet air.

Mattern et al. proved an exothermic peak of crystallization (T_c) for L-arginine solution at 61°C , and they obtained a diffractogram with superimposed crystalline peaks on the characteristic amorphous halo [19]. The amino acid was therefore partially crystalline in the freeze-drying conditions, whereas a mixture with a third portion of phosphoric acid produced a fully amorphous product. They proved that heating the basic amino acid sample above its T_c produced a conversion to an entire crystalline structure. On the other hand, the addition of phosphoric acid inhibited the spontaneous process. The similarity in results between the pure amino acid and its salts that were composed by either hydrochloride or succinic acid proved the fully transformation from the amorphous state to the crystalline structure above the characteristic T_c . Nevertheless, the observations of completely amorphous structures of arginine salts at ambient temperature were also consistent with results by Stärtzel et al. [23] who found a fully amorphous halo in all diffractograms of arginine compounds.

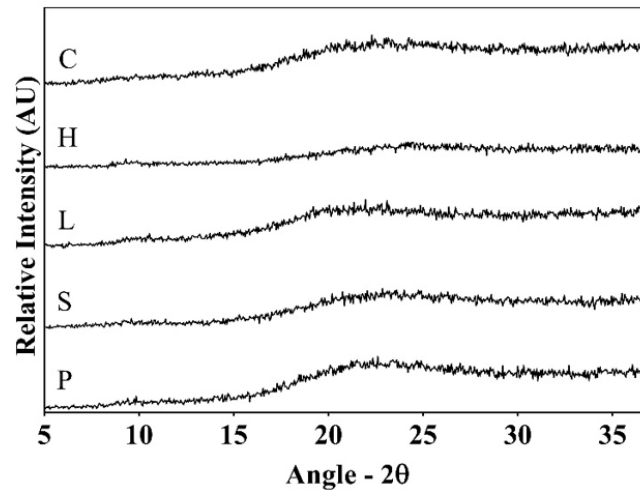


Figure 4.27 X-rays diffraction patterns in protein lyophilized cakes of protein L-arginine-based formulations at pH 7. The investigated acids were (C) citric, (H) hydrochloride, (L) lactobionic, (P) phosphoric and (S) succinic.

Lyophilized cakes were reconstituted with a volume of 1.5 ml of high purify water (HPW). The reconstitution time was monitored by a chronometer until visible particles of cake were not completely dissolved. The reconstitution is a fundamental step for freeze-dried products as the pharmaceuticals return to their previous liquid state, with all solubilized solutes inside the formulations. Table 4.9 illustrates all the monitored reconstitutions time of the formulations. The experiment failed during the recording of some samples and, therefore, they appeared as not detected (n.d.). Anyway, placebos carried out at rather short times, less than one minutes in every sample, and the pH influenced the reconstitution as the time increased with higher values of pH. On the other hand, the antibody formulations showed significant longer time of reconstitution compared with placebos. Nevertheless, every cake was completely solubilized in around two minutes. Protein samples were more difficult to solubilize because they produced a compact superficial layer of foam, which was probably caused by the protein, and it obstructed the solutes solubilization. Moreover, they did not highlight any dependence of the reconstitution from both pH and the employed counterion. A reconstitution time of a few minutes was considered acceptable for each sample, although at the end of the process the formulation was not completely clear and many small air bobbles were still present in the solution.

Table 4.9 Reconstitution time expressed in second of lyophilized cakes of L-arginine-based formulations at pH 5, 6, and 7. (C) Citric acid, (H) Hydrochloric acid, (L) Lactobionic acid, (P) Phosphoric acid and Succinic acid (S) were used as counterions. Both placebo and (mAb) protein solutions were investigated (n = 3, mean \pm s.d.).

| Ion | Placebo | | | | | mAb | | | | |
|------|------------|-------------|------------|------------|-------------|--------------|--------------|--------------|------------|-------------|
| | C | H | L | P | S | C | H | L | P | S |
| pH 7 | 51 \pm 8 | 36 \pm 2 | 55 \pm 1 | 50 \pm 4 | 44 \pm 2 | 85 \pm 3 | 61 \pm 7 | 132 \pm 9 | 91 \pm 1 | 78 \pm 4 |
| pH 6 | n.d. | 23 \pm 0 | 48 \pm 7 | n.d. | 12 \pm 11 | 120 \pm 30 | 141 \pm 17 | 135 \pm 1 | n.d. | 46 \pm 1 |
| pH 5 | n.d. | 19 \pm 10 | n.d. | 34 \pm 8 | 34 \pm 19 | 54 \pm 2 | 46 \pm 13 | 108 \pm 13 | 42 \pm 4 | 45 \pm 11 |

The lyophilization cycles produced collapsed cakes in formulations containing either H or S, as it was proved by the visual inspections of the products (Table 4.8). Therefore, it was investigated how the T_g' changed in different formulations in order to understand whether product temperature reached T_g' during the drying step of the process. The Figure 4.28 illustrates the tendency of every formulation in changing their T_g' by different pHs and compositions. The employed acid

characterized the T_g' in every formulation. Both collapsed products highlighted significant lower T_g' than the other ions. It was measured an approximately constant value in H formulations of -46°C at different pH, whereas the S showed a rather higher temperature of around -37.5°C . P and L significantly changed their T_g' as a function of the pH, and this contrasted with the other ions, where the characteristic remained approximately constant at different acidity. P increased its temperature of more than 3°C in the investigated range, whereas a peak at pH 6 was observed in protein formulations containing L. The increase of T_g' in P was in accordance with the visual inspections as the cakes appeared more elegant at higher pH. Moreover, it was observed that generally protein formulations showed a higher T_g' than the placebo one, although this difference dropped by decreasing the temperature. For example, C produced a difference between formulations at pH 5 of 2.4°C , whereas H did not cause any significant differences between protein and placebo.

The results were also consistent with Izutsu et al. [21] who found a dependence between the thermal properties (T_g' and T_g) and the number of carboxyl group of the employed acid in basic amino acid based formulation. They proved that the T_g' increased with either di- or tricarboxylic acids; moreover, the results were higher than those of individual solute solutions. On the contrary, the combinations of amino acid with a monocarboxylic acid showed a T_g' between those of the singular solutions. The investigated C and P were tricarboxylic acid and, therefore, they significantly increased T_g' of the arginine solutions (Figure 4.28). Moreover, it was observed a lower T_g' by combining arginine with S, which was a dicarboxylic acid. The lowest values were obtained with H and it showed a similar value of T_g' to the one reported by Izutsu et al. [22]. However, L contrasted with the expectations and produced the highest T_g' of the investigation.

The low shelf temperature during and the high vacuum during the primary drying of the lyophilization cycle (Figure 4.22) did not avoid the collapse in H, and S products at every pH and a partial collapse of P at pH 5. The lowest measured temperature at the end was the freezing stage: it was on average of -48.2°C , which was just 2°C below the T_g' of H. The collapse could be prevented if the used pressure throughout the process was set to a lower value than the used one (0.06 mbar).

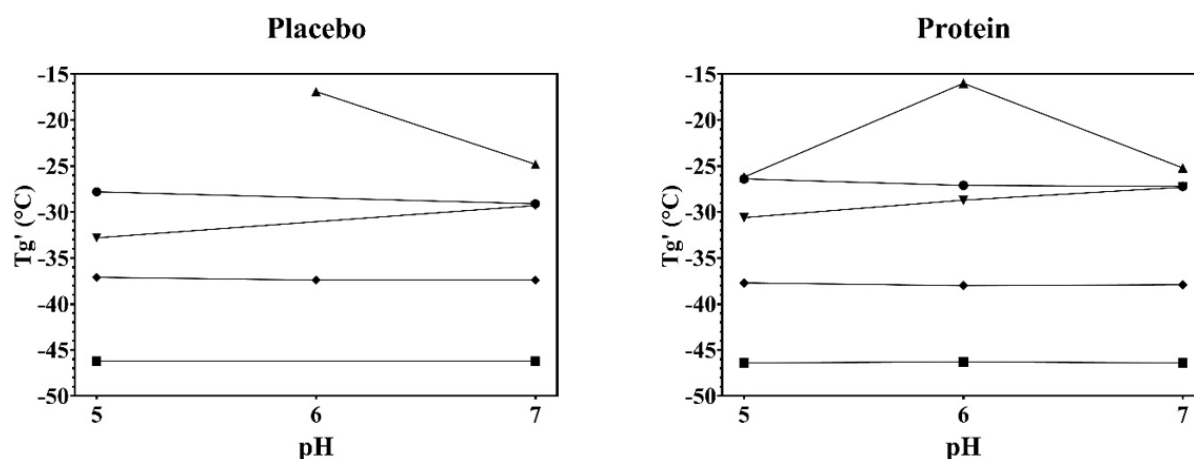


Figure 4.28 Glass transition temperature (T_g') in both (l.h.s.) placebo and (r.h.s.) protein of L-arginine-based formulations. The investigated acids were (●) citric, (■) hydrochloride, (▲) lactobionic, (▼) phosphoric and (◆) succinic ($n = 3$, mean \pm s.d.).

4.2.2 Protein stability at pH 7 in L-arginine-based formulations at different counterions

The protein stability investigation was necessary to highlight whether the products produced different results or not on protein agglomerates than the cryoprotection study. The cryoprotection mechanism (Section 1.2.1) was just the first part of the protein stabilization process required to obtain satisfied lyophilized products. There is the possibility that a cryoprotectant could not sustain the drying stress and, therefore it produced unsuitable cakes, which would provide an extremely high turbidity and number of particles inside the reconstituted formulation. The aim of this section was to highlight similarity and differences of lyophilized products with the freeze-thawed formulations and perhaps finding the best counterion for both processes. The investigation was performed at the three levels of pH to compare the impact of the acidity on the protein agglomeration phenomena. Moreover, the final condition of reconstituted products was compared with the initial measurement before the lyophilization cycle. The initial condition was therefore identical in the one described throughout the cryoprotection studies.

The following investigations were performed on reconstituted products with 1.5 ml of HPW. The clearness of each sample was checked before starting the measurements by waiting that all air bubbles were removed from the solution, in order to avoid errors during the experimental analysis.

The performed turbidimetric measurements on lyophilized, and then reconstituted, products were illustrated in Figure 4.29 and rather crucial differences were observed if they are compared with the freeze-thawing results at the same pH (Figure 4.11). Nevertheless, the important gap between the protein formulations and placebos was highlighted also after the freeze-drying (FD). On the other hand, the protein behaviors quite differed, depending on type of the studies. Both C and S significantly increased their values in contrast with the previous results. C yielded around one turbidimetric unit with the FD since it reached 3.8 ± 0.4 FNU, whereas it was significantly lower (2.8 ± 0.6 FNU) after the repeated freeze-thawing cycles (Figure 4.11). An even larger yield was observed for S, which increased to 5.075 ± 0.007 FNU and, therefore it showed around twice the previous experiment value. A dubious increase was observed in H, although it produced the lowest measurements in both investigations. Another mild difference between FD and FT5 was produced by L that increased its value of less than one turbidimetric unit. On the other hand, P drastically dropped its turbidity from 6 ± 1 FNU at FT5 to 4.0 ± 0.2 FNU after the FD.

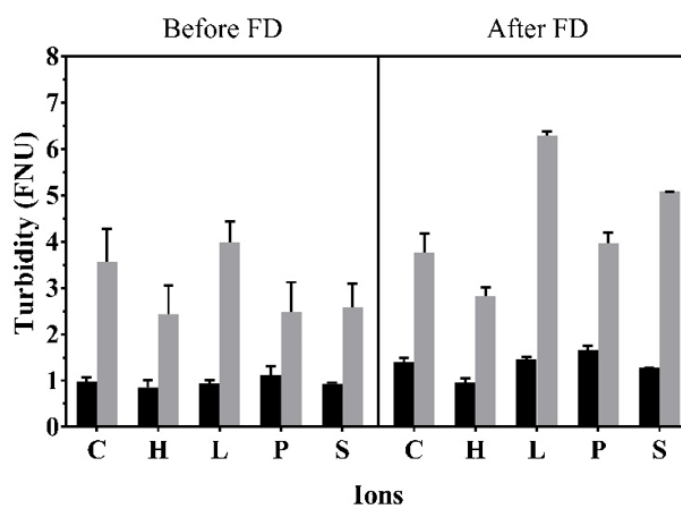


Figure 4.29 Turbidity of (■) placebo, and (▒) protein formulations in arginine-based formulations at pH 7 before and after the (FD) lyophilization cycle. The investigated acids were (C) citric, (H) hydrochloride, (L) lactobionic, (P) phosphoric and (S) succinic ($n = 4$ or 3 , mean \pm s.d.).

The particle counting confirmed the turbidimetric results (Figure 4.30), but some incongruences were observed in the comparison with the freeze-thawing investigation (Figure 4.12). C did not significantly increase its number of particles with the FD if compared to the FT5, but it mildly dropped from 25000 ± 10000 #/ml to 22000 ± 5000 #/ml. However, every other ion behaved as it was previously described when they were compared with Figure 4.12. L, especially, yielded a large number of particles as it produced the highest response in FD. The low value of turbidity for P corresponded to similar particles number with S, whereas it was the highest measurements in the freeze-thawing investigation. Anyway, the lowest observation was highlighted by the H and the result was in accordance with the previous turbidity. Each ion gained a specific number of particles compared to the initial conditions. Both P and S kept their similarity in measurements throughout the process and they increased of around the same number of particles, whereas C and H kept their initial values approximately constant. L showed the largest increase during the process, as it was expected from the previous description.

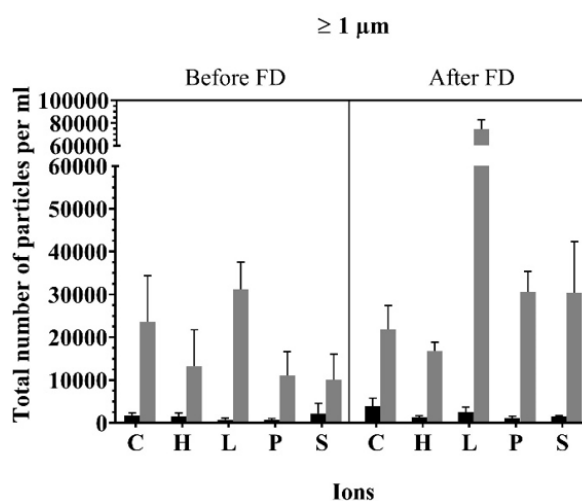


Figure 4.30 Total number of particles per milliliter larger than $1 \mu\text{m}$ (■) placebo, and (■) protein formulations in arginine-based formulations at pH 7 before and the (FD) lyophilization cycle. The investigated acids were (C) citric, (H) hydrochloride, (L) lactobionic, (P) phosphoric and (S) succinic ($n = 4$ or 3 , mean \pm s.d.).

The counting of particles larger than $10 \mu\text{m}$ was carried out to confirm the previous experiments, however Figure 4.31 did not proved similar conclusions. It was remarked the major differences between protein formulations and placebos, but all ions produced similar experimental responses after FD. The lyophilization significantly increased the number of particles in every protein formulation, whereas the placebos remained approximately a constant value. The protein observation produced a mean of around 500 #/ml, whereas almost all placebos were even lower than 100 #/ml. The processed formulations by FD yielded more particles than the numbers caused by the FT5 (Figure 4.13). Anyway, L caused a drop on particles number by passing from the freeze-thawing investigation to the FD, whereas all other ions produced more particles especially H and P. Nevertheless, both C and S did not gain a considerable number of particles, therefore they were considered constant.

The particles counting for diameters larger than $25 \mu\text{m}$ were not significant as the previous results with smaller diameters (Figure 4.31). The experiment measures of placebos did not always differ significantly as for diameter larger than $10 \mu\text{m}$. Moreover, it was not observed any important increase of particles by the FD and the expected increased on L protein formulations was not measured (Figure 4.13).

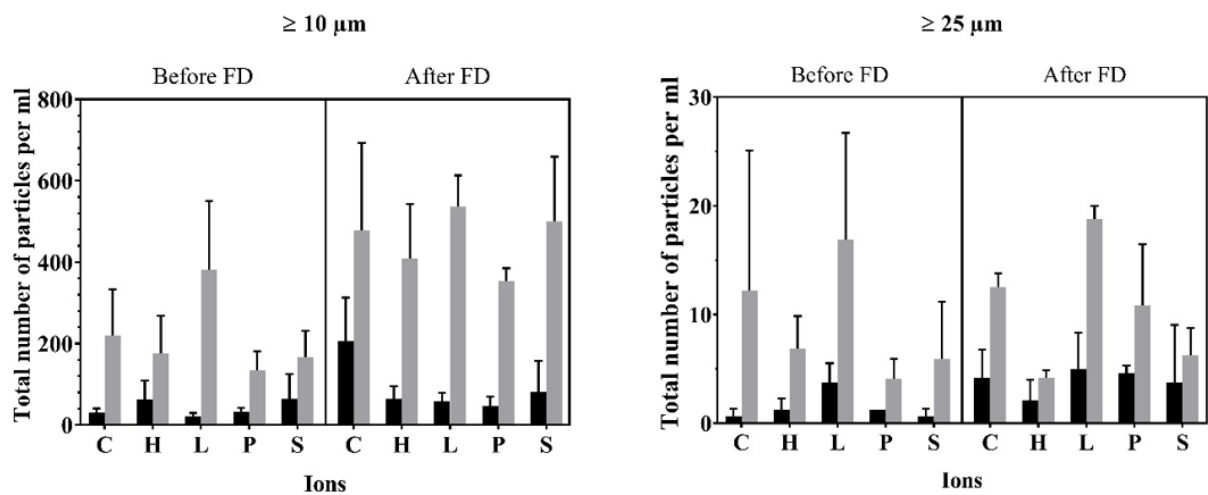


Figure 4.31 Total number of particles per milliliter larger than (l.h.s.) 10 μm and (r.h.s.) 25 μm (■) placebo, and (■) protein formulations in arginine-based formulations at pH 7 before and after the (FD) lyophilization cycle. The investigated acids were (C) citric, (H) hydrochloride, (L) lactobionic, (P) phosphoric and (S) succinic (n = 4 or 3, mean \pm s.d.).

The highlighted differences of turbidity and number of particles larger than 1 μm between the two processes concluded that the protein stability throughout the lyophilization in arginine-based formulations was deeply influenced by the employed acid. In general, the freeze-drying process provided additional drying stress to the formulations and, therefore, the reconstituted formulations were more turbid than the freeze-thawed one. Anyway, the P proved being a moderate stabilizer in lyophilization, although it was recognized as the weakest cryoprotectant after five repeated cycles of freeze-thawing. Moreover, H and S were recognized as the best cryoprotectants at pH 7 by the statistical analysis, but their results in lyophilization probably provided similar protein stabilization than C. On the other hand, L caused a weak protection against freezing stress, and it did not produce any remarkable protein stabilization in lyophilization either. The particle counting with larger diameters did not pointed out additional information about the characteristic behavior of each ion, but they confirmed the increases in experimental responses for protein formulations, which were reconstituted from lyophilized cakes.

The statistical analysis was performed to quantify the previous results and to ensure statistical relevance to the results. The normal distribution assumption was satisfied by transforming the data through a logarithmic transformation. Afterwards, the normal probability plot was checked and probable outliers were deleted and excluded from the evaluation. All experimental responses were fitted with a full interaction model and all statistical parameter to evaluate the adequacy of the model were reported in Table 4.10. The absence of lack-of-fit from each model highlighted the adequacy of them to describe the experiments, whereas the precision of further predictions (Q^2) and the reproducibility were extremely close to one for the turbidity, but they decreased with the particle counting. The goodness of the particle counting models was therefore dropped with higher diameters, as it was observed in the previous investigation (Table 4.3, Table 4.5, and Table 4.7). The effects plot for the light obscuration up to 1 μm was illustrated in the following paragraph to keep coherency with the previous investigation (Figure 4.32), although the turbidity carried out the greatest precision in prediction ($Q^2 = 0.921$) and the best fitting with the data ($R^2 = 0.951$). Therefore, it allowed to make comparisons between the freeze-thawing and the lyophilizing investigations.

Table 4.10 Statistical parameters of models using turbidity and light obscuration responses in arginine-based formulations at pH 7.

| Responses | R ² | Q ² | Lack-of-fit ^a (p-value) | Reproducibility |
|-----------------------|----------------|----------------|---------------------------------------|-----------------|
| Turbidity | 0.951 | 0.921 | 0.203 | 0.940 |
| ≥ 1 μm | 0.882 | 0.833 | 0.091 | 0.877 |
| ≥ 10 μm | 0.769 | 0.671 | 0.411 | 0.731 |
| ≥ 25 μm | 0.699 | 0.565 | 0.472 | 0.646 |
| ^a α = 0.05 | | | | |

The statistical model of particle counting larger than 1 μm produced many insignificant effects, and it did not include both interactions of ions with process (IO·FD(Yes)), and process with antibody (PT(mAb)·FD(Yes)) as well. All those effects were not significant and, therefore, the model was simplified by deleting the unnecessary elements. The first certain cause of particles was the antibody, due to its highest and positive main effect (PT(mAb) = 1.2 ± 0.1). Similar results were obtained in the analysis of the freeze-thawing results (Figure 4.14). The process of lyophilization impacted positively on the responses (FD(Yes) = 0.3 ± 0.1). Moreover, the differences between C and other ions were not important and significant, excluding the negative main effect for P (IO(P) = -0,29052 ± 0,2). That result contrasted with Figure 4.14, where only H and S produced significant and negative effects. On the other hand, the synergic interaction between L and the antibody was positive and important in both analysis (IO(L)·PT(mAb) = 0.5 ± 0.2). The results of P apparently contrasted with the Figure 4.30 as the use of C highlighted less particles than P after the FD. However, if the number of particles inside the protein formulations before and after the FD were summed together, C produced higher responses particles than P and, therefore, the usage of P generated a negative effect with a gain in protein stabilization.

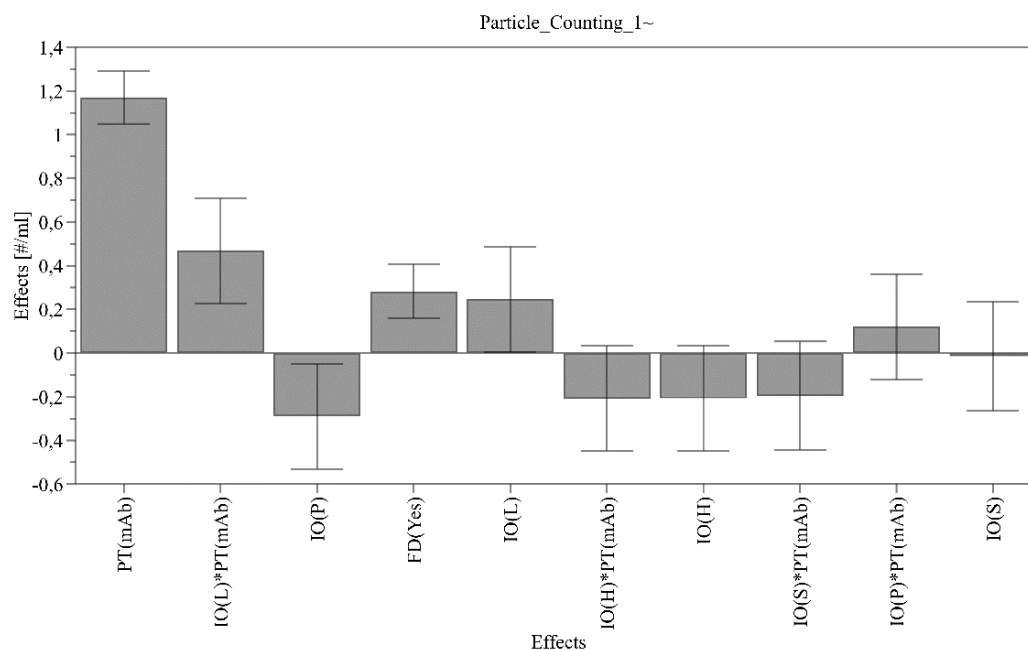


Figure 4.32 Effects plot of transformed total number of particles measurements ≥ 1 μm of arginine-based formulations at pH 7.

4.2.3 Protein stability at pH 6 in L-arginine-based formulations at different counterions

The investigation aimed to prove whether significant differences were obtained by changing the pH or not in protein agglomerates. The protein stabilization studies throughout freeze-thawing cycles evidenced a pH dependence on protection abilities of each used counterion. Their stabilization characteristics dropped with the increase in acidity from pH 6 to 5, although a significant and mild difference was also observed between pH 7 and 6. Moreover, a comparison of freeze-thawing results with reconstituted formulations was wished to prove whether each acid satisfied both requirements of good cryoprotectants and lyoprotectant for biopharmaceuticals. The final goal of this section was to identify the best protectants, which also provided elegant cakes appearances and satisfying physical characteristics in lyophilized products.

The turbidity measurements at pH 6 (Figure 4.33) showed some similarity with the results at the previous pH (Figure 4.29), but they differed in some features anyway. The most visible feature in Figure 4.33 was the substantial gap between protein formulations and placebos, which was also detected in all the other investigations. Thus, all placebos kept an approximately constant value throughout the process, of around 1.5 FNU, although C and P yielded a turbidity of 2 FNU after the FD process. The initial turbidity of protein products did not significantly differ with the ions and they were ranged from 2.3 ± 0.2 FNU to 3 ± 1 FNU. On the other hand, both C and L highlighted significant higher turbidity than the other ions at pH 7 in the same conditions (Figure 4.29). The FD enhanced all values of around 1 FNU at pH 6 but it did not cause any significant highlights among formulations as their turbidity varied between 3.3 ± 0.8 FNU to 4.273 ± 0.03 FNU. The L produced the highest turbidimetric measurements in both conditions, whereas the lowest values were carried out in the beginning by the S and after the process by H. That was in contrast with the results at pH 7, where both L and S produced an important increase throughout the process since they differed from the other formulations (Figure 4.29). Similar differences between FD and freeze-thawing results (FT5) were observed in both pH, as the FD caused a higher yield in turbidity than FT5 in all protein formulations, excluding both C and P at pH 6 (Figure 4.15). Therefore, P decreased significantly its process enhancement from FT5 to FD, whereas C measured approximately a similar value.

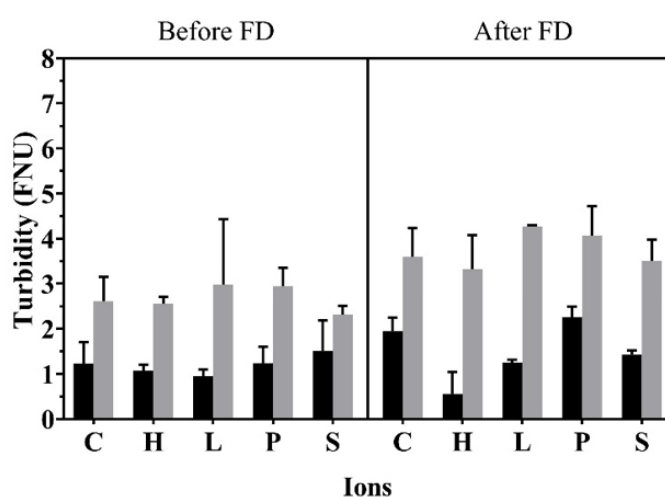


Figure 4.33 Turbidity of (■) placebo, and (▒) protein formulations in arginine-based formulations at pH 6 before and after the (FD) lyophilization cycle. The investigated acids were (C) citric, (H) hydrochloride, (L) lactobionic, (P) phosphoric and (S) succinic ($n = 4$ or 3 , mean \pm s.d.).

Turbidity and particle counting larger than $1 \mu\text{m}$ highlighted some similarities but they differed especially after FD (Figure 4.34). Anyway, the significant gap between protein and placebos was

easily observed, and placebos showed on average a few thousands of particles throughout the entire process. The number of particles in the initial condition differed to different ions. L produced the highest observation (23000 ± 18000 #/ml), whereas both C and S caused the lowest values of around 7000 #/ml. That differed from the similarity in turbidity among the protein formulations. The pH did not impact significantly on the experiment response as similar number of particles were observed at pH 7 but C highlighted a decrease with the major acidity. The FD yielded an important increase in particles number on each protein formulation, although C remained the products with the lowest observation (28000 ± 2000 #/ml). Similar measurement was caused by H, whereas L increased drastically to 52000 ± 5000 #/ml; moreover, both P and S produced a particles number of 37000 #/ml on average. Therefore, the particle counting carried out more distinguishable results than the turbidity. The comparison between the FD and the freeze-thawing results at pH 6 differed from the previous description at pH 7, as it was observed a significant decrease in number of particles for all formulations, except L and S. Those ions greatly increased their particles number due to the FD, whereas especially P dropped its values of a few ten thousand (Figure 4.16). On the other hand, the lyophilization performed at pH 7 caused a significant increase in number of particles on the lowest measurements, which were C and H but L was drastically dropped. Nevertheless, P and S produced similar number of particles after FD.

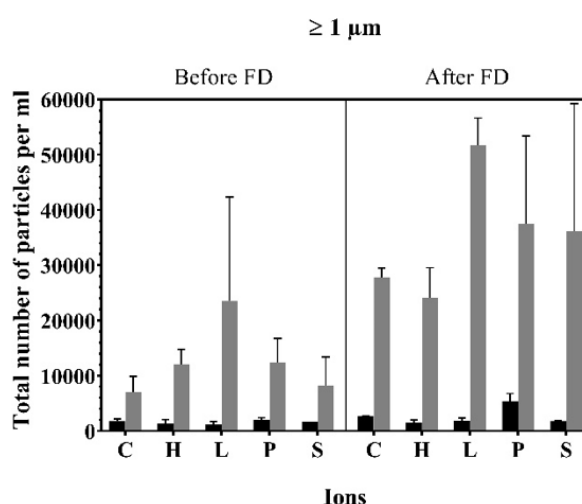


Figure 4.34 Total number of particles per milliliter larger than 1 μm (■) placebo, and (■) protein formulations in arginine-based formulations at pH 6 before and the (FD) lyophilization cycle. The investigated acids were (C) citric, (H) hydrochloride, (L) lactobionic, (P) phosphoric and (S) succinic (n = 4 or 3, mean ± s.d.).

The particles number with diameter larger than 10 μm and 25 μm are shown in Figure 4.35. The graphs provided less information about the differences between formulation, and they were in contrast with the results in Figure 4.34.

Nevertheless, it was observed the significant gap between protein formulations and placebos especially in diameters larger than 10 μm. The number of particles of placebos was approximately constant to 100 #/ml and any changes by the FD were significantly measured. On the other hand, both L and S protein samples produced the lowest responses in the initial conditions, and they differed from the approximately 500 #/ml particles produced in C, H, and P formulations. The cycle of lyophilization impacted with importance in only on C and P ions as it caused enhancements in the number of particles. That result contrasted with the previous one, where both ions produced similar and the lowest responses and L caused the highest one. In Figure 4.34 (l.h.s), H highlighted more than twice its initial values after the FD, whereas both P and S produced on average 500 #/ml and they did not significantly changed by the process. Moreover, similar behavior was observed in

L formulation as well but with a mild lower number of particles. The particle counting differed between pH 7 and 6 because the higher pH produced approximately less particles than pH 6.

The particle counting in diameter larger than 25 μm confirmed the remarkable difference between protein and placebo formulations, although the L remained the lowest measure and produced a value similar to the placebo one.

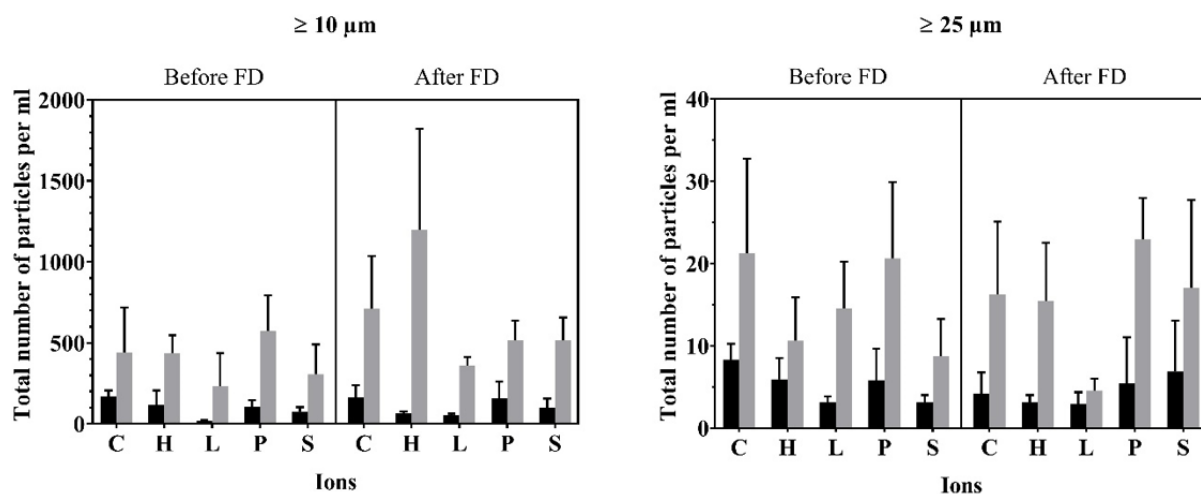


Figure 4.35 Total number of particles per milliliter larger than (l.h.s.) 10 μm and (l.h.s.) 25 μm (■) placebo, and (■) protein formulations in arginine-based formulations at pH 6 before and after the (FD) lyophilization cycle. The investigated acids were (C) citric, (H) hydrochloride, (L) lactobionic, (P) phosphoric and (S) succinic (n = 4 or 3, mean \pm s.d.).

The similarities in the turbidity and particle counting comparisons between lyophilization and freeze-thawing investigations at both pH highlighted the moderate P protection abilities against the drying stresses as lower measurements were produced. Nevertheless, the cryoprotection of S was not enough to stabilize the protein throughout the freeze-drying because the ion caused an increase in turbidimetric responses, and, therefore, a weak lyoprotection was observed. Anyway, its stabilization ability increased when the pH was shifted from 7 to 6 due to the lower observations. The drop in pH produced also an increase in protein protection with L due to the drop in particle counting measurements, whereas a significant increase in turbidity was measured in H formulations. On the other hand, C did not highlight any crucial differences between the pHs and its turbidity remained approximately constant and it also produced similar values during the freeze-thawing testes. Anyway, Figure 4.34 showed a significant increase in particle numbers at pH 6, therefore a better stabilization was proved at lower pH. Similar trends were highlighted in H formulations due to the lower value of the light obscuration response.

The statistical analysis was performed for all experimental responses. All data were transformed by a logarithmic transformation to fulfill the normal distribution assumption, and therefore fitted with a LRM. The normality of the distribution was checked by the normal probability plot and possible outliers were excluded from the evaluation. The Table 4.11 reported all statistical parameters that were computed from each response model to evaluate its adequacy to describe the experiments. All analysis were not affected by the lack-of-fit due to the higher values than 0.05, therefore all the models describe correctly the data. On the other hand, the highest precision in predictions (Q^2), fitting data (R^2) and reproducibility was achieved by the light obscuration at 1 μm due to its closest values to one of all parameters. It was observed a similarity with all the previous investigations about the decrease in light obscuration models of the statistical parameters with larger diameter. Anyway, the turbidity carried out a rather precise and reproducible model, but it was not as satisfying as the aforementioned one.

Table 4.11 Statistical parameters of models using turbidity and light obscuration responses in arginine-based formulations at pH 6.

| Responses | R ² | Q ² | Lack-of-fit ^a (p-value) | Reproducibility |
|-----------------------|----------------|----------------|---------------------------------------|-----------------|
| Turbidity | 0.858 | 0.767 | 0.097 | 0.836 |
| ≥ 1 μm | 0.863 | 0.863 | 0.086 | 0.903 |
| ≥ 10 μm | 0.792 | 0.706 | 0.336 | 0.802 |
| ≥ 25 μm | 0.500 | 0.365 | 0.426 | 0.452 |
| ^a α = 0.05 | | | | |

The evaluation of the impact of each factor on the response was conducted through the effect plot showed at Figure 4.36 Effects plot of transformed total number of particles measurements $\geq 1 \mu\text{m}$ of arginine-based formulations at pH 6., that was referred to the model produced by data of the particle counting larger than $1 \mu\text{m}$. The antibody was proved being the first cause of particles during the measurements ($\text{PT(mAb)} = 1.0 \pm 0.1$), as it was highlighted in all the previous analysis. That results confirmed the difference between protein formulations and placebos and it evidenced the significance of the gap. Both models were simplified by deleting the not significant integration of the process with either ions ($\text{IO} \cdot \text{FD(Yes)}$) or antibody ($\text{FD(Yes)} \cdot \text{PT(mAb)}$). The process of FD impacted by enhancing the response significantly with a positive main effect ($\text{FD(Yes)} = 0.3 \pm 0.1$) and, therefore analysis at both pH were rather similar (Figure 4.32). H and S ions did not produce significant differences when they were compared with C, either with their interactions with the protein. Moreover, L was defined sources of increased response as both its main positive effect and synergic interaction with the antibody were significant. On the other hand, P highlighted a positive main effect and it contrasted with Figure 4.32, where the ion produced a negative one. However, the antagonist interaction of P and protein partially canceled this gain ($\text{IO(P)} \cdot \text{PT(mAb)} = -0.2 \pm 0.2$).

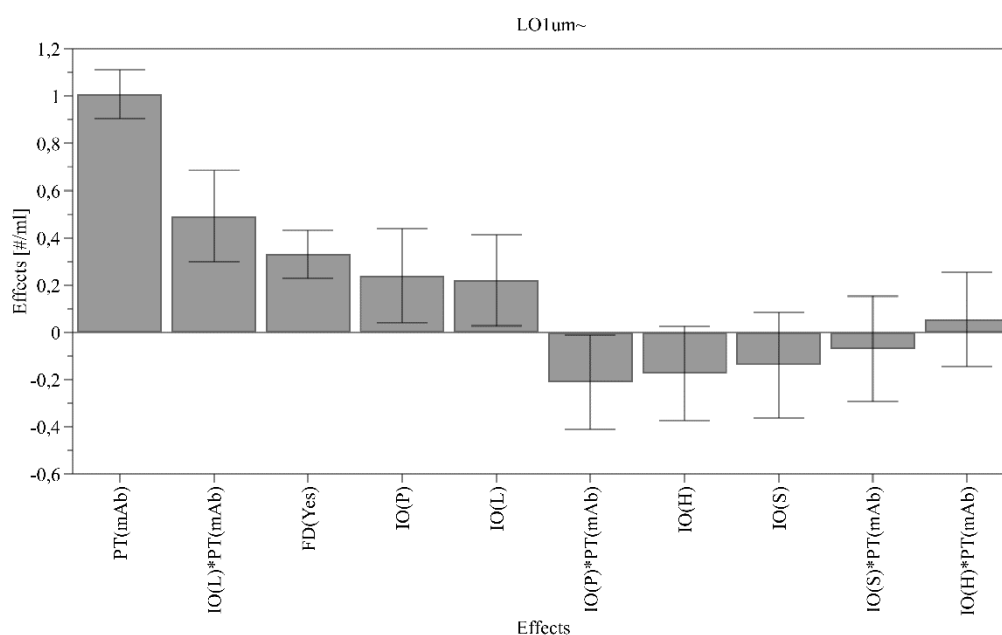


Figure 4.36 Effects plot of transformed total number of particles measurements $\geq 1 \mu\text{m}$ of arginine-based formulations at pH 6.

4.2.4 Protein stability at pH 5 in L-arginine-based formulations at different counterions

The previous sections highlighted quite different results from the freeze-thawing cycles one, although it was usually observed an increase in the observations caused by the lyophilization cycle in comparison with the cryoprotection investigation. The aim of this section was to investigate whether the observed destabilization throughout the repeated freeze-thawing cycles affected the lyophilized products as well. Anyway, it was expected an increase from the previous studies in both turbidity and particle number for every formulation at pH 5. Therefore, the pH probably significantly impacted the protein agglomeration and the ion with the best cryoprotection abilities was not necessary equal to the one that avoided agglomerates in lyophilization.

The turbidimetric measurements at pH 5 appeared higher than the previous pHs with a significative relevance (Figure 4.37). Placebo solutions were certainly lower than protein formulations in both initial conditions and after the FD process. Their values were measured at around 1.5 FNU and, therefore they behaved as in the previous investigations at different pHs. On the other hand, the protein formulations differed in turbidity from the beginning and P produced the highest value as it was described in Section 4.1.5. FD yielded the measures of every formulations depending on the used counterion. An extremely high turbidity was observed L formulations (97 ± 81 NFU), although it was drastically lower at the pH 6 (Figure 4.33). C highlighted a value of 7 ± 1 NFU, which significantly increased by the process (5.6 ± 0.3 NFU); moreover, a similar behave was observed for S formulation that yielded its turbidity from 3.6 ± 0.5 FNU to 6 ± 3 FNU. On the other hand, H and P were not affected by the process but rather they mildly decreased after the FD. Anyway, both ions carried out the lowest measurements of the experiment. All measured turbidity after FD at pH 5 significantly differed from both previous pHs, as they significantly enhanced with the increased acidity, especially C and L. The turbidimetric results in the freeze-thawing investigation at the same pH were approximately higher, except for L that highlighted an extremely lower value.

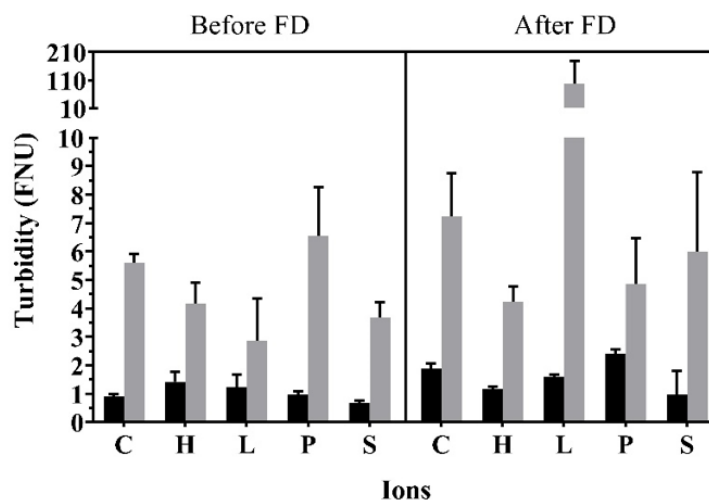


Figure 4.37 Turbidity of (■) placebo, and (▒) protein formulations in arginine-based formulations at pH 5 before and after the (FD) lyophilization cycle. The investigated acids were (C) citric, (H) hydrochloride, (L) lactobionic, (P) phosphoric and (S) succinic ($n = 4$ or 3 , mean \pm s.d.).

The light obscuration produced additional information in comparison with turbidity. The particle counting with diameter larger than $1 \mu\text{m}$ was showed in Figure 4.38. The difference between protein and placebos was easily observed in both before and after FD. Possible increases of a few thousands of particles impacted on all placebos during the process, although they remained significantly lower than placebo. The protein formulation before FD were not distinguishable to each other but a certain

lower value was observed for S formulation (20000 ± 2000 #/ml). On the other hand, the other ions were similar to each other, except for H that showed a mild lower measure. The process of FD enhanced all experiments responses depending on the investigated formulation but it caused a decrease in H. In accordance with the turbidity results (Figure 4.37), L highlighted the highest number of particles (400000 ± 200000 #/ml). C was observed being the second product for particle number (80000 ± 6000 #/ml), as it was previously observed in the turbidimetric measurements. The accordance between the two analysis techniques were observed in all the remaining ions as well. The decrease in pH caused an enhancement in every measurement especially in the reconstituted products. Major differences were observed between the freeze-thawing and the FD investigations at the same pH due to the increase in number of particles in all formulations with the cycle of lyophilization.

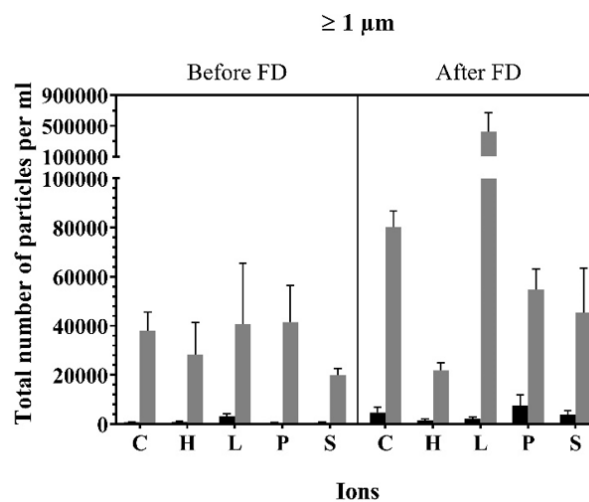


Figure 4.38 Total number of particles per milliliter larger than $1 \mu\text{m}$ (■) placebo, and (■) protein formulations in arginine-based formulations at pH 5 before and the (FD) lyophilization cycle. The investigated acids were (C) citric, (H) hydrochloride, (L) lactobionic, (P) phosphoric and (S) succinic ($n = 4$ or 3 , mean \pm s.d.).

The particle counting in larger diameter confirmed but with less significance the previous results (Figure 4.39). Rather different numbers of particles larger than $10 \mu\text{m}$ were measured in protein formulations and placebos. Placebos particles were approximately constant at both conditions, although an increase of around 100 #/ml was observed after FD. Similar trends were observed in protein formulations, although L was clearly higher compared to the other ions, especially after the FD. The process drastically enhanced the number of particles in L, which gained around seven times its initial number. On the other hand, C and P highlighted less particles after FD than before, and that was in contrast with the previous measurements (Figure 4.38). Anyway, a dubious increase was measured in both H and S, which remained around the initial number of particles. The results at pH 5 did not highlight any differences from the other two pHs because they carry out similar particle number larger than $10 \mu\text{m}$ but L was drastically higher than all the previous observations.

The particle counting larger than $25 \mu\text{m}$ was similar to the previous diameter, as they illustrated analogies on the trends of protein formulations. For instance, L drastically increased throughout the process and it produced the largest number of particles throughout the process. Anyway, the significant gap between placebos and protein formulations did not always appear, especially after FD. All measurements were approximately similar to the previous one, which were obtained at different pH, although L was significantly higher in (Figure 4.39).

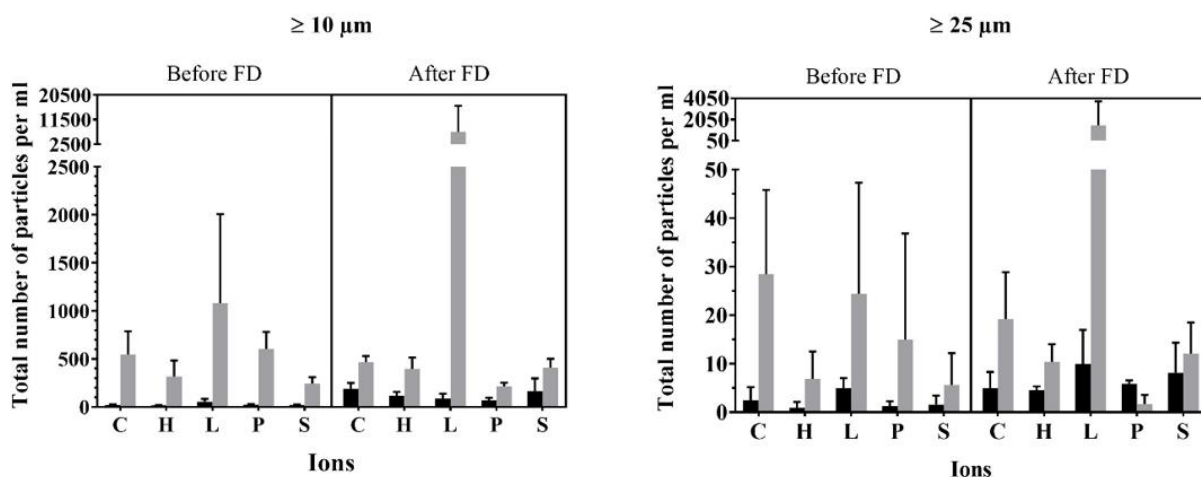


Figure 4.39 Total number of particles per milliliter larger than (l.h.s.) 10 μm and (l.h.s.) 25 μm (■) placebo, and (■) protein formulations in arginine-based formulations at pH 5 before and after the (FD) lyophilization cycle. The investigated acids were (C) citric, (H) hydrochloride, (L) lactobionic, (P) phosphoric and (S) succinic ($n=4/3$, mean \pm s.d.).

The statistical analysis was performed to quantify the impact of each factor of the design of the experiments on the experimental responses. The assumption of normal distribution in the data was verified by transforming the measurements with a logarithmic transformation. Afterwards, the results were checked by the normal probability plot and possible outliers were deleted from the evaluations. Table 4.12 reported all statistical parameters evaluated from every model. The most precise and reproducible model was provided from the particle counting $\geq 1 \mu\text{m}$, whereas the parameters decreased with larger diameter as it was observed in all the previous analysis. On the other hand, the lack-of-fit was verified in all cases and, therefore the models were not significantly adequate to describe the experiments. Consequentially, the statistical analysis neither completed nor described.

Table 4.12 Statistical parameters of models using turbidity and light obscuration responses in arginine-based formulations at pH 6.

| Responses | R ² | Q ² | Lack-of-fit ^a (p-value) | Reproducibility |
|---|----------------|----------------|---------------------------------------|-----------------|
| Turbidity | 0.801 | 0.865 | <0.001 | 0.898 |
| $\geq 1 \mu\text{m}$ | 0.915 | 0.876 | <0.001 | 0.960 |
| $\geq 10 \mu\text{m}$ | 0.870 | 0.774 | <0.001 | 0.855 |
| $\geq 25 \mu\text{m}$ | 0.583 | 0.236 | 0.025 | 0.519 |
| ^a $\alpha = 0.05$ | | | | |

The performed experiments at pH 5 proved significant increases in turbidity and particle counting for protein formulations after the lyophilization cycle. It was evidenced by those enhancements the impact of the solution acidity on the experimental responses and consequentially similarity between freeze-thawing results and FD results was observed. Although, the increases were even more significant throughout lyophilization. The statistical analysis did not perform suitable results to confirm the evidences that were highlighted in this section but it was possible to make some considerations about them. P did not carry out the highest responses and, therefore it was not reputed

the weakest protein stabilizer. Another significant change was produced by L, which showed relatively low measures on freeze-thawing investigation, whereas it highlighted the largest response with lyophilization. On the other hand, the lowest measurements in both investigations at pH 5 were caused by S. Moreover, both responses of C were rather high in comparison with the other ions, except to L.

5 Conclusions

The cryoprotection studies proved important results on the investigated formulations. In the first section the influence of the freeze-thawing cycles on the turbidity of the sucrose-based formulations and their total number of particles at three different diameters was highlighted. Sucrose is one of most employed protein stabilizers on liquid and lyophilized biopharmaceutical and, therefore, it was used as a reference to compare with arginine-based products. Surfactant, such as PS80, could be used with sugar in order to improve the protein protection ability. In the performed investigation, the enhancement of both analysis responses by the number of repeated freeze-thawing cycles was significant only in protein formulation containing sucrose and, therefore, the increase was a consequence of the protein agglomeration process. The presence of PS80 in small percentage with sucrose contrasted the denaturation due to the absence of any enhancements of turbidity and number of particles. The conclusions were confirmed by the significant effects, which were computed through a statistical analysis of the results. Moreover, it was highlighted the similarity of the turbidimetric and particle counting results as both techniques provided comparable trends in their effects plots. The antibody was recognized as main cause of responses enhancements, nevertheless the freeze-thawing cycles increased significantly the measured values.

Afterwards, the investigation was repeated with a higher concentration of antibody to point out the differences between placebos and protein formulations and a smaller volume. Equivalent conclusions were made in the new formulations.

The protection abilities of arginine-based biopharmaceutics against protein agglomeration was proved being influenced with statistical significance by the excipient, which was used as amino acid counter ion. pH and consequently the acid concentration inside the products was another source of antibody stabilization; nevertheless, the magnitude of its gain relied on the compound. The investigation was ranged between pH 7 and 5 and it evidenced how different counterions produced either comparable or distinct results between each other at three solutions acidities. In every formulation, statistically significant higher values of both turbidity and number of particles were highlighted in protein formulations than placebos, as it was previously obtained in the sucrose-based ones. It was therefore supported that the differences between the solutions were directly consequences of protein agglomerates. This evidence was confirmed through the highest positive effect in the statistical analysis, which were satisfactory performed at pH 7 and 6. The permanent lack-of-fit in each statistical model at pH 5 did not allow to use the evaluated effects in order to improve the significance of the results and, therefore, these conclusions were not supported by statistic. Another analogy with sucrose-based formulations was the impact of the freezing stresses on protein agglomeration that was detected by the enhancement of both measured variables. The importance of this increase was not easily pointed out in every analyzed formulation due to the apparently similarity of the results. However, statistical main effects were computed thus to remove any suspicions and to assert the enhancement in particles number throughout the process. The protein formulations containing citrate before the freeze-thawing process highlighted a minimum at pH 6 in turbidity and number of particles larger than 1 μm , whereas the results after the five repeated cycles were always increased with the major acidity in all analysis responses. Anyway, the biggest enhancements were caused in pH 5. Comparable trends of results were achieved with chloride as counterion, but both its measurements were lower than citrate especially for pH 7 and 5, although they caused approximately same values at pH 6. Nevertheless, the computed effects through the statistical model highlighted significant differences and they confirmed the increase in protein protections by using the hydrochloride acid instead of citric acid. Succinate showed comparable results to chloride due to its low values of turbidity and number of particles through the entire range of pH. However, the freeze-thawing process did not cause any significant increases in both succinate responses and, therefore the ions rather differed after the repeated cycles. Thus, chloride showed higher measurements than succinate at pH 6 and 5, whereas it was the lowest one

at pH 7. The statistical analysis confirmed the best abilities of chloride at pH 7 as it evidenced more significant and negative effects than succinate. On the other hand, the synergic interaction of chloride and protein at pH 6 contrasted with the antagonism of succinate and, therefore succinate was highlighted as a better protectant than chloride. On the opposite, lactobionic acid proved a maximum of protein stabilization at pH 6 due to the lowest measured turbidity and number of particles. That contrasted with the previous acids and probably the least concentration of arginine titrating with lactobionic acid it could be a cause of these differences, although the best chloride cryoprotection abilities carried out comparable results to the best one by using lactobionate. Phosphate was observed being the weakest stabilizer both before and after the process of freeze-thawing as it caused the largest number of particles and the higher turbidity compared with the other ions. The statistical analysis confirmed the evidences through positive main effects and synergic interactions with both protein and process. According to the statistical analysis and results, the pH changed the protein stabilization abilities of each formulations depending on the used acid, although the best protection against agglomeration was highlighted at pH 7 and 6, but by using different ions. Therefore, chloride was recognized as the best counterion at pH 7, whereas lactobionate provided comparable results with chloride but at pH 6. The most promising ions showed significant lower results than sucrose formulations, although the surfactant mixed with sucrose it provided the lowest turbidity and number of particles, which were ever measured.

The arginine formulations were processed with a test cycle of lyophilization to investigate their suitability to the process. The physical characteristics evaluated encompassed cake appearance, residual moisture, T_g , and reconstitution time were measured to determinate, which formulations produced the most satisfying results and to evidence possible correlations among the physical proprieties. The protein stability study was performed as well with turbidity and particle counting to analyse, how the process of protein agglomeration changed by the lyophilization and whether the additional stresses of drying and then reconstitution influenced the number of agglomerates.

The lyophilizing cycle was performed over 68 hours and the primary drying was the longest stage of the process. The cycle did not highlight any anomalies, which could produce undesirable results. However, the vacuum was not reached easily before the primary drying and it was interrupted for a short period of time and, therefore the product was kept at the minimum temperature for a little longer time than the protocol. Anyway, the low temperature prevented any possible degradation.

The cake inspections showed either partially or fully collapse of formulations containing the same counterion of arginine but at different pH. The presence of antibody at the identical concentration of the investigation on cryoprotection did not produce any improvements or defects on cakes in comparison with placebos. The acidity showed no impact, but in phosphate formulations a beginning of collapse was observed at pH 5. Every hydrochloride formulations produced a completely collapsed cakes with major defects such as loss structure and fine-grained texture. Similar defects were observed by using succinate acid as counterion, although they were less important than in the previous ion. On the other hand, phosphate products mildly improved its appearance by increasing the pH and, therefore they produced compact and elegant cakes. Lactobionic and citric acid provided elegance and compactness as well, although a minor defect of shrinkage from vial walls was visible in each sample but it was not recognized as an obvious beginning of collapse. The residual moisture rather depended on the used acid, and pH, but it did not apparently change between placebo and protein formulations. Although, placebos cakes claimed being more humid than protein one. Collapsed cakes containing either chloride or succinate carried out significantly higher residual moisture than the other ions; however, their placebo humidity approximately changed with significance with the pH. On the other hand, the not collapsed cakes lowered residual moisture than the collapsed one. The T_g ' significantly varied in different formulations, although the most relevant difference was observed between collapsed and elegant cakes due to the significantly higher T_g ' on the not collapsed products. Anyway, the pH mildly changed the product properties depending on the analyzed formulations, but a significant lower value was measured in phosphate formulations at pH 5 compared with the both remained pHs. The

amorphous phase of every protein cake at pH 7 was confirmed by the amorphous halo on the diffractogram, whereas modulated DSC thermographs of collapsed cakes showed recrystallization peaks at elevated temperatures. The absence of peaks in the diffractogram highlighted that the recrystallization observed in the thermographs was caused by either higher temperature of ambient [19]. The reconstitution times of the lyophilized products were considered acceptable in all formulations as they were timed at maximum at two minutes. The difference between protein formulations and placebos was the only one observed among the results because of the longest necessary time to reconstitute the products. The T_g' of every formulation was measured because of the collapse of both chloride, and succinate formulations during the lyophilization test cycle and to investigate whether the change in counterion, pH, presence of antibody impacted or not on the results. It resulted that the T_g' increased with the number of either hydroxy or carboxyl group in the used acids [21,22], except for lactobionic acid. The lactobionic showed the highest T_g' , although it had just one carboxyl group but many eight hydroxy groups. The pH did not significantly impact on T_g' but phosphate highlighted a relevant increase with lower acidity. Moreover, the presence of antibody enhanced T_g' compared to placebos, especially for citrate, and phosphate formulations. In conclusion, physical characteristics of lyophilized products changed by the counterion of arginine. It was proved that both multi carboxyl and hydroxy acids produced more suitable formulations for the process due to the increase T_g' with the number of those groups. The collapse could be avoided by decreasing the pressure during the primary drying (0.06 mbar) to drop the product temperature. Anyway, a formulation having extremely low T_g' was difficult to lyophilized, for instance H products.

Citric, phosphoric, and lactobionic acids were the more suitable acids to employ in arginine-based biopharmaceutics for lyophilization, due to their abilities to produced acceptable cakes appearance with low percentage of residual moisture, and a ranged T_g between approximately 90°C and 110°C. The pH did not largely impact on physical characteristics and, therefore it was not considered a crucial variable. Anyway, the formulation acidity carried out widely different results during the previous investigation on cryoprotection abilities and, therefore it became decisive in protein stability of reconstituted product as well.

The protein stability investigation after lyophilization produced quite different results compared to the cryoprotection. However, the crucial and statistically significant gap between the protein and placebos confirmed the antibody as major cause of enhancement in both turbidity and number of particles. The pH was proved being a crucial variable against protein agglomerations as it produced widely spread results across the investigated range from pH 7 to 5. It was especially observed an important increase in both experimental responses by decreasing the pH to 5. That was in accordance with the cryoprotection, where the pH 5 proved the weakest protein stabilization. On the other hand, the drop to pH 6 from pH 7 caused relevant increases only in citrate, and chloride ions, whereas it produced a drop by using lactobionic. The differences were significantly observed in number of particles larger than 1 μm but they were less relevant for turbidity and particles numbers at larger diameter. The statistical analysis was carried out with adequacy and, therefore absence of lack-of-fit at just pH 6 and 7. Analogous problem was affected the previous stability investigations, but the both computed models in the lyoprotection study were contrarily simplified of some insignificant interactions. The process did not produce any significant interactions with either ions or protein. On the other hand, the lyophilization process was recognized as a source of destabilization due to its positive main effect at both analyzed pH. The statistical analysis allowed to conclude with significance the investigation and to highlight the differences among ions. The analysis were rather similar, although they differed on stabilization abilities of phosphate formulations. Phosphate formulations showed a decrease in experimental responses related to the other ions in comparison with the cryoprotection investigation. The weakest lyoprotection was therefore showed from lactobionic formulations at every investigated pH, due to the highest numbers of particles larger than 1 μm and turbidities. That result was confirmed by the significant main effects and synergic interactions with the protein at pH 6 and 7. Contrarily, phosphate highlighted a significant stabilization at pH 7 due to a negative main effect. However, it produced

a mild destabilization in protein formulations at pH 6, which was caused by a higher positive main effect than the antagonist interaction with the protein. Phosphate was therefore suggested instead of the citrate at pH 7 but it should be avoided at lower pH. Chloride and succinate did not highlight any significant advantages compared to citrate stabilization abilities due to the low insignificant effects at both pH. Therefore, the protein stability investigations after lyophilization carried out rather different results compared to the previous freeze-thawing study.

In conclusion, the pH was demonstrated being an essential variable in protein stabilization against the agglomeration process during lyophilization. The best cryoprotection abilities in arginine-based formulations were achieved by employing as amino acid counterion either hydrochloride acid at pH 7 or lactobionic acid at pH 6. Their protection abilities were even better than sucrose formulations, but the addition of surfactant (PS80) at low concentration to the sugar carried out a better stabilization than with every arginine-based formulation. On the other hand, lactobionic acid showed the weakest protection throughout the lyophilization test cycle, although it produced satisfactory physical characteristic of cakes, such as elegant appearance and relatively high T_g . Its weak ability could be caused by the lower concentration of amino acid inside the formulations (3.6% w.t. instead of 5% w.t). Hydrochloric acid did not highlight any relevant advantage in protein protection compared to citric acid; moreover, it produced collapsed products due to the lowest T_g . The best counterion of arginine in lyophilized biopharmaceutics was phosphate at pH 7. It highlighted the best stabilization ability, although it was the weakest stabilizer during the freezing stress. Nevertheless, it produced elegant cakes at pH 7 with low residual moisture, short reconstitution time, and high T_g .

6 Outlook

Further investigations may focus on using the significant cryoprotection advantage of hydrochloridic acid combined with arginine at pH 7 in protein formulation. Due to the relatively low T_g' is therefore necessary to add a bulking agent, such as sucrose [23,24], in order to obtain not collapsed cakes. A higher T_g' is also necessary to reduce the process time by increasing the temperature of the shelf.

Lactobionic acid was another valid excipient for biopharmaceutics due to its high T_g' and relevant cryoprotection. However, its weak lyoprotection could be modified by increasing the concentration to 5% w.t. of arginine inside the formulation as the other formulations. The low solubility of this compound in water did not permit to obtain extremely high concentrations and, therefore it was not possible to reach high concentration of arginine during the titration.

References

1. Fissore, D. Freeze Drying of Pharmaceuticals. *Encycl. Pharm. Sci. Technol.* **2013**, 37–41.
2. Wagner, W.; Saul, A. P. International Equations for the Pressure Along the Melting Along the Sublimation Curve of Ordinary Water Substance. *J. Phys. Chem. Ref. Data* **1994**, *23*, 515–527.
3. Carpenter, J. Rational Design of Stable Lyophilized Protein Formulations Some Practical Advice. *Pharm. Res.* **1997**, *14*, 969–976.
4. Remmele, R. L.; Krishnan, S.; Callahan, W. J. Development of stable lyophilized protein drug products. *Curr Pharm Biotechnol* **2012**, *13*, 471–496.
5. Dalvi-Isfahan, M.; Hamdami, N.; Xanthakis, E.; Le-Bail, A. Review on the control of ice nucleation by ultrasound waves, electric and magnetic fields. *J. Food Eng.* **2017**, *195*.
6. Xu, M.; Chen, G.; Zhang, C.; Zhang, S. Study on the Unfrozen Water Quantity of Maximally Freeze-Concentrated Solutions for Multicomponent Lyoprotectants. *J. Pharm. Sci.* **2017**, *106*, 83–91.
7. Esfandiary, R.; Gattu, S. K.; Stewart, J. M.; Patel, S. M. Effect of Freezing on Lyophilization Process Performance and Drug Product Cake Appearance. *J. Pharm. Sci.* **2016**, *105*, 1427–1433.
8. Barresi, A. A.; Pisano, R.; Fissore, D.; Rasetto, V.; Velardi, S. A.; Vallan, A.; Parvis, M.; Galan, M. Monitoring of the primary drying of a lyophilization process in vials. *Chem. Eng. Process.* **2009**, *48*, 408–423.
9. Patel, S. M.; Nail, S. L.; Pikal, M. J.; Geidobler, R.; Winter, G.; Hawe, A.; Davagnino, J.; Rambhatla Gupta, S. Lyophilized Drug Product Cake Appearance: What Is Acceptable? *J. Pharm. Sci.* **2017**, *106*, 1706–1721.
10. Abrantes, C. G.; Duarte, D.; Reis, C. P. An Overview of Pharmaceutical Excipients: Safe or Not Safe? *J. Pharm. Sci.* **2016**, *105*, 2019–2026.
11. Franks, F. Freeze-drying of bioproducts: Putting principles into practice. *Eur. J. Pharm. Biopharm.* **1998**, *45*, 221–229.
12. Ohtake, S.; Kita, Y.; Arakawa, T. Interactions of formulation excipients with proteins in solution and in the dried state. *Adv. Drug Deliv. Rev.* **2011**, *63*, 1053–1073.
13. Arakawa, T.; Prestrelski, S. J.; Kenney, W. C.; Carpenter, J. F. Factors affecting short-term and long term stabilities of proteins. *Adv. Drug Deliv. Rev.* **1993**, *10*, 1–28.
14. Jorgensen, L.; Hostrup, S.; Moeller, E. H.; Grohgan, H. Recent trends in stabilising peptides and proteins in pharmaceutical formulation – considerations in the choice of excipients. *Expert Opin. Drug Deliv.* **2009**, *6*, 1219–1230.
15. Carpenter, J. F.; Manning, M. C. *Rational Design of Stable Protein Formulations*; Media, S. S., Ed.; New York, 2002.
16. Buera, M. P.; Roos, Y.; Levine, H.; Slade, L.; Corti, H. R.; Reid, D. S.; Auffret, T.; Angell, C. A. State diagrams for improving processing and storage of foods, biological materials, and pharmaceuticals (IUPAC Technical Report). *Pure Appl. Chem.* **2011**, *83*, 1567–1617.

17. Ruiz-Cabrera, M. A.; Rivera-Bautista, C.; Grajales-Lagunes, A.; González-García, R.; Schmidt, S. J. State diagrams for mixtures of low molecular weight carbohydrates. *J. Food Eng.* **2016**, *171*, 185–193.
18. Akers, M. J.; Milton, N.; Byrn, S. R.; Nail, S. L. Glycine Crystallization During Freezing: The Effects of Salt forms, pH, and Ionic Strength. *Pharm. Res.* **1995**, *12*, 1457–1461.
19. Mattern, M.; Winter, G.; Kohnert, U.; Lee, G. Formulation of Proteins in Vacuum-Dried Glasses. II. Process and Storage Stability in Sugar-Free Amino Acid Systems. *Pharm. Dev. Technol.* **1999**, *4*, 199–208.
20. Izutsu, K.; Yoshida, H.; Shibata, H.; Goda, Y. Amorphous – Amorphous Phase Separation of Freeze-Concentrated Protein and Amino Acid Excipients for Lyophilized Formulations. *Chem. Pharm. Bull.* **2016**, *64*, 1674–1680.
21. Izutsu, K.; Kadoya, S.; Yomota, C.; Kawanishi, T.; Yonemochi, E.; Terada, K. Freeze-drying of proteins in glass solids formed by basic amino acids and dicarboxylic acids. *Chem. Pharm. Bull. (Tokyo)*. **2009**, *57*, 43–8.
22. Izutsu, K. I.; Fujimaki, Y.; Kuwabara, A.; Aoyagi, N. Effect of counterions on the physical properties of L-arginine in frozen solutions and freeze-dried solids. *Int. J. Pharm.* **2005**, *301*, 161–169.
23. Stärtzel, H. Gieseler, M. Gieseler, A.M. Abdul-Fattah, M. Adler, H.C. Mahler, P. Goldbach, Freeze Drying of l -Arginine/Sucrose-Based Protein Formulations, Part I: Influence of Formulation and Arginine Counter Ion on the Critical Formulation Temperature, Product Performance and Protein Stability. *J. Pharm. Sci.* **2015**, *104*, 2345–2358.
24. Stärtzel, P.; Gieseler, H.; Gieseler, M.; Abdul-Fattah, A. M.; Adler, M.; Mahler, H. C.; Goldbach, P. Freeze-Drying of l -Arginine/Sucrose-Based Protein Formulations, Part 2: Optimization of Formulation Design and Freeze-Drying Process Conditions for an l -Arginine Chloride-Based Protein Formulation System. *J. Pharm. Sci.* **2015**, *104*, 4241–4256.
25. Hawe, A.; Schaubhut, F.; Geidobler, R.; Wiggernhorn, M.; Friess, W.; Rast, M.; De Muynck, C.; Winter, G. Pharmaceutical feasibility of sub-visible particle analysis in parenterals with reduced volume light obscuration methods. *Eur. J. Pharm. Biopharm.* **2013**, *85*, 1084–1087.
26. Houde, J. D.; Berkowitz, A. S. *Biophysical characterization of proteins in developing biopharmaceuticals*; 2015.
27. Maccarthy, P.; Klusman, R. W.; Rice, J. A. *Water Analysis*; 1989.
28. Gu, J. H.; Beekman, A.; Wu, T.; Piedmonte, D. M.; Baker, P.; Eschenberg, M.; Hale, M.; Goldenberg, M. Beyond glass transitions: Studying the highly viscous and elastic behavior of frozen protein formulations using low temperature rheology and its potential implications on protein stability. *Pharm. Res.* **2013**, *30*, 387–401.
29. Kumagai, H.; Nakamura, K.; Fujiwhara, J. DSC Measurement of Frozen Water in Liquid Foods. *Agric. Biol. Chem.* **1985**, *49*, 3097–3101.
30. Lueckel, B.; Bodmer, D.; Helk, B.; Leuenberger, H. Formulations of Sugars with Amino Acids or Mannitol–Influence of Concentration Ratio on the Properties of the Freeze-Concentrate and the Lyophilizate. *Pharm. Dev. Technol.* **1998**, *3*, 325–336.

31. Bisinella, R. Z. B.; Ribeiro, J. C. B.; de Oliveira, C. S.; Colman, T. A. D.; Schnitzler, E.; Masson, M. L. Some instrumental methods applied in food chemistry to characterise lactulose and lactobionic acid. *Food Chem.* **2017**, *220*, 295–298.
32. Grünke, S. The influence of conductivity on the Karl Fischer titration. *Food Chem.* **2003**, *82*, 99–105.
33. De Caro, C. A.; Aichert, A.; Walter, C. M. Efficient, precise and fast water determination by the Karl Fischer titration. *Food Control* **2001**, *12*, 431–436.
34. Epp, J. *X-Ray Diffraction (XRD) Techniques for Materials Characterization*; 2016.
35. Montgomery, D. C. *Montgomery - Design and Analysis of Experiments*, 2001.